Electronic Supplementary Material (ESI) for Chemical Science.

Supporting Information

One-pot chemical pyro- and tri-phosphorylation of peptides by diamidophosphate in water

Huacan Lin*, Luke J. Leman*, and Ramanarayanan Krishnamurthy*

Table of Contents

1. General experimental

All amino acids were purchased from AAPPTec, Oakwood Chemical, Advanced ChemTech, Novabiochem, Ambeed and Combi-Blocks. The peptide coupling reagents were purchased from Chem-Impex, Fluka and Sigma-Aldrich. Trifluoroacetic acid was purchased from VWR. Anhydrous N-methylpyrrolidone, dimethylformamide, dichloromethane and methanol were purchased from Sigma-Aldrich. Rink Amide MBHA resin and Wang resin were purchased from Novabiochem and CreoSalus. Diamidophosphate (DAP) was synthesized according to the reported procedure.[1] NMR were recorded at 298 K. ^{31}P-NMR spectra were acquired using a Bruker DPX-400. Chemical shifts (δ) were reported in parts per million (ppm).

Preparative reverse-phase HPLC was performed on a Waters Autopurification System equipped with Waters 2545 binary gradient module on a Waters HSS T3 C18 column (5 µm, 19 × 160 mm) using a mobile phase of 0.05% TFA in H_2O (Buffer A) and CH_3CN (Buffer B). Fractionation was monitored by a Waters single quadrupole mass spectrometer.

Preparative HPLC Method A:

This method employed a main segment of gradient of buffer B starting at 10% to 25% over 8 min at a flow rate of 30 ml/min. The purification of all phosphopeptides except RPA190, IC2C, Gcr1 and Nopp140 used this method.

Preparative HPLC Method B:

This method employed a main segment of gradient of buffer B starting at 5% to 20% over 8 min at a flow rate of 30 ml/min. The purification of RPA190, IC2C, Gcr1 and Nopp140 used this method.

Low-resolution LC-MS experiments were performed on an Agilent InfinityLab single quadrupole LC/MSD system coupled with an Agilent 1260 Infinity II. High-resolution LC-MS experiments were performed on an Agilent 6230 time-of-flight LC/MS system coupled with an Agilent 1260 Infinity II. Agilent 1260 Infinity II was equipped with either a reverse-phase column Agilent Poroshell 120 EC-C8 (2.7 µm, 4.6 × 50 mm) (Column I) or Agilent Zorbax 300SB-C8 (5.0

μm, 4.6 × 50 mm) (Column II). The binary gradients of Buffer A (0.1% formic acid in H_2O) and Buffer B (0.1% formic acid in CH_3CN) were employed for HPLC. Detail of analytical HPLC methods was described as below.

Analytical HPLC Method A:

This method employed a gradient of buffer B starting at 5% for 2 min, then 5% to 25% over 15 min, then 25% to 95% over 3 min at a flow rate of 0.5 ml/min in Column I. Elution was monitored by UV absorbance at 280 nm.

Analytical HPLC Method B:

This method employed a gradient of buffer B starting at 5% for 2 min, then 5% to 25% over 15 min, then 25% to 95% over 3 min at a flow rate of 0.5 ml/min in Column I. Elution was monitored by UV absorbance at 230 nm.

Analytical HPLC Method C:

This method employed a gradient of buffer B starting at 5% for 2 min, then 5% to 25% over 15 min, then 25% to 95% over 3 min at a flow rate of 0.5 ml/min in Column II. Elution was monitored by UV absorbance at 230 nm.

Analytical HPLC Method D:

This method employed a gradient of buffer B starting from 0% to 8% over 15 min, then 8% to 95% over 3 min at a flow rate of 0.5 ml/min in Column I. Elution was monitored by UV absorbance at 230 nm.

Analytical HPLC Method E:

This method employed a gradient of buffer B starting at 5% for 2 min, then 5% to 25% over 15 min, then 25% to 95% over 3 min at a flow rate of 0.5 ml/min in Column II. Elution was monitored by UV absorbance at 280 nm.

Analytical HPLC Method F:

This method employed a gradient of buffer B starting from 0% to 8% over 15 min, then 8% to 95% over 3 min at a flow rate of 0.5 ml/min in Column II. Elution was monitored by UV absorbance at 230 nm.

Anion exchange chromatography was performed with AKTA pure with UNICORN system control using 280 nm on a DNAPac™ PA100 column with a flow rate of 1 mL/min. Elution condition: Buffer A: 5 mM Tris base (pH 8.2), Buffer B: 5 mM Tris base, 330mM $NaClO_4$ (pH 8.2) with a linear gradient of Buffer B from 0% to 15% in 15 min.

Tandem MS/MS experiment (collision-induced dissociation) was performed on an Agilent G6538A Q-TOF mass spectrometer in the standard electrospray source. The peptide sample was diluted in a mixture of water and acetonitrile and directly injected into the mass spectrometer. The MS/MS spectrum was analyzed in Agilent MassHunter software.

2. Synthesis of phosphopeptide substrates

2.1 Solid-phase peptide synthesis (SPPS)

2.1.1 Synthesis of N- and C-terminus protected model phosphopeptides

Phosphopeptide synthesis (peptide **1**-**14**) were carried out by using standard Fmoc chemistry on an Advanced ChemTech Apex 396 peptide synthesizer. A typical synthesis was performed on 0.11 mmol scale using Rink Amide MBHA resin (loading capacity: 0.89 mmol/g) for phosphopeptides with C-terminal amides. Standard side chain protecting groups in amino acids included Ser(PO_3BzlH), Thr(PO_3BzlH), Tyr(PO_3BzlH), Ser(tBu), Thr(tBu), Trp(Boc), Asn(Trt), Gln(Trt), Lys(Boc), His(Trt), Arg(Pbf), Tyr(tBu), Asp(OtBu), Glu(OtBu) and Cys(Trt). General amino acid coupling was carried out using 1,3-diisopropylcarbodiimide (DIC) and ethyl 2-cyano-2-(hydroxyimino) acetate (Oxyma) in NMP for 75 min. Fmoc deprotection was achieved using 2 × 7 min treatments with 5% 4-methylpiperidine in DMF. Washing steps involved 6 × 1 min treatments with DMF. Acetylation on the N-terminus was achieved using a mixture of acetic anhydride: *N*,*N*-diisopropylethylamine (DIPEA): NMP (2:1:2, v/v/v) for 10 min. The crude peptides were cleaved from the resin with concomitant side chain deprotection by agitation in a solution of TFA: triisopropylsilane (TIS): water (95:2.5:2.5, v/v/v) for 4 h. A mixture of TFA: TIS: ethane-1,2-dithiol (EDT): water (94:1:2.5:2.5, v/v/v/v) was used instead for peptide sequence containing Cys residue. The resin was washed with TFA after cleavage. The combined TFA solutions were concentrated under N_2 stream to less than 3 ml. The crude peptides were precipitated by adding diethyl ether,

centrifuged, and washed three additional times with diethyl ether. Then the crude peptides were dissolved in water/acetonitrile and purified by preparative reverse-phase HPLC. Purified peptides were analyzed by LC-MS.

2.1.2 Synthesis of RPA190, IC2C, Gcr1 and EIF2S2 fragment phosphopeptides

Phosphopeptide synthesis (peptide **15**-**18**) were carried out by using standard Fmoc chemistry on an Advanced ChemTech Apex 396 peptide synthesizer. A typical synthesis was performed on 0.11 mmol scale using preloaded Fmoc-L-Leu-Wang resin (loading capacity: 0.64 mmol/g) and Fmoc-L-Glu(OtBu)-Wang resin (loading capacity: 0.50 mmol/g). Fmoc deprotection was achieved using 1 × 3 min and 1 × 4 min treatments with 5% 4-methylpiperidine in DMF. Amino acid coupling, washing, peptide cleavage and work-up were carried out as described above for the synthesis of peptide **1**-**14**. Purified peptides were analyzed by LC-MS.

2.1.3 Synthesis of Nopp140 fragment phosphopeptide

Phosphopeptide synthesis (peptide **52**) was carried out from the precursor peptide **51** by phosphitylation and subsequent oxidation on the resin.[2] Peptide **51** was synthesized by using standard Fmoc chemistry on an Advanced ChemTech Apex 396 peptide synthesizer. A typical synthesis for peptide **51** was performed on 0.11 mmol scale using preloaded Fmoc-Gly-Wang resin (loading capacity: 0.60 mmol/g). The serine residue (to be phosphorylated) was incorporated as the Fmoc-Ser-OH derivative and other serine residues were incorporated as the Fmoc-Ser(tBu)-OH derivative. The Boc-Lys(Boc)-OH was coupled as the N-terminal residue. Fmoc deprotection was achieved using 2 × 7 min treatments with 25% 4-methylpiperidine in DMF. Amino acid coupling, washing, peptide cleavage and work-up were carried out as described above for the synthesis of peptide **1**-**14**. After the completion of amino acid coupling, 5 mg resin was cleaved and the crude product was analyzed by LC-MS before the further phosphitylation and oxidation.

To obtain peptide **52**, the resultant Boc-Lys(Boc)-Lys(Boc)-Val-Lys(Boc)-Lys(Boc)-Glu(OtBu)-Thr(tBu)-Ser(tBu)-Ser(tBu)-Ser(tBu)-Asp(OtBu)-Ser(tBu)-Ser-Glu(OtBu)-Asp(OtBu)-Ser(tBu)-Ser(tBu)-Glu(OtBu)-Glu(OtBu)-Glu(OtBu)-Asp(OtBu)- Lys(Boc)-Ala-Gln(Trt)-Gly-Wang resin was dried under vacuum and added into a mixture of $(BnO)_2PN$*i*-Pr_2 (20 equiv.) and 1*H*-tetrazole (50 equiv.) in 4 ml anhydrous DMF (DMF was dried with molecular sieve prior to use) and stirred for 1 h in a nitrogen atmosphere. The resin was washed with DCM (DCM was dried with molecular sieve prior to use) for three times. Then the resin was added in 3 ml DCM and mCPBA (20 equiv.) in 1 ml DCM solution was added and the mixture was shaken for 30 min. The peptide cleavage and work-up were carried out as described above for the synthesis of peptide **1**-**14**. Purified peptide was analyzed by LC-MS.

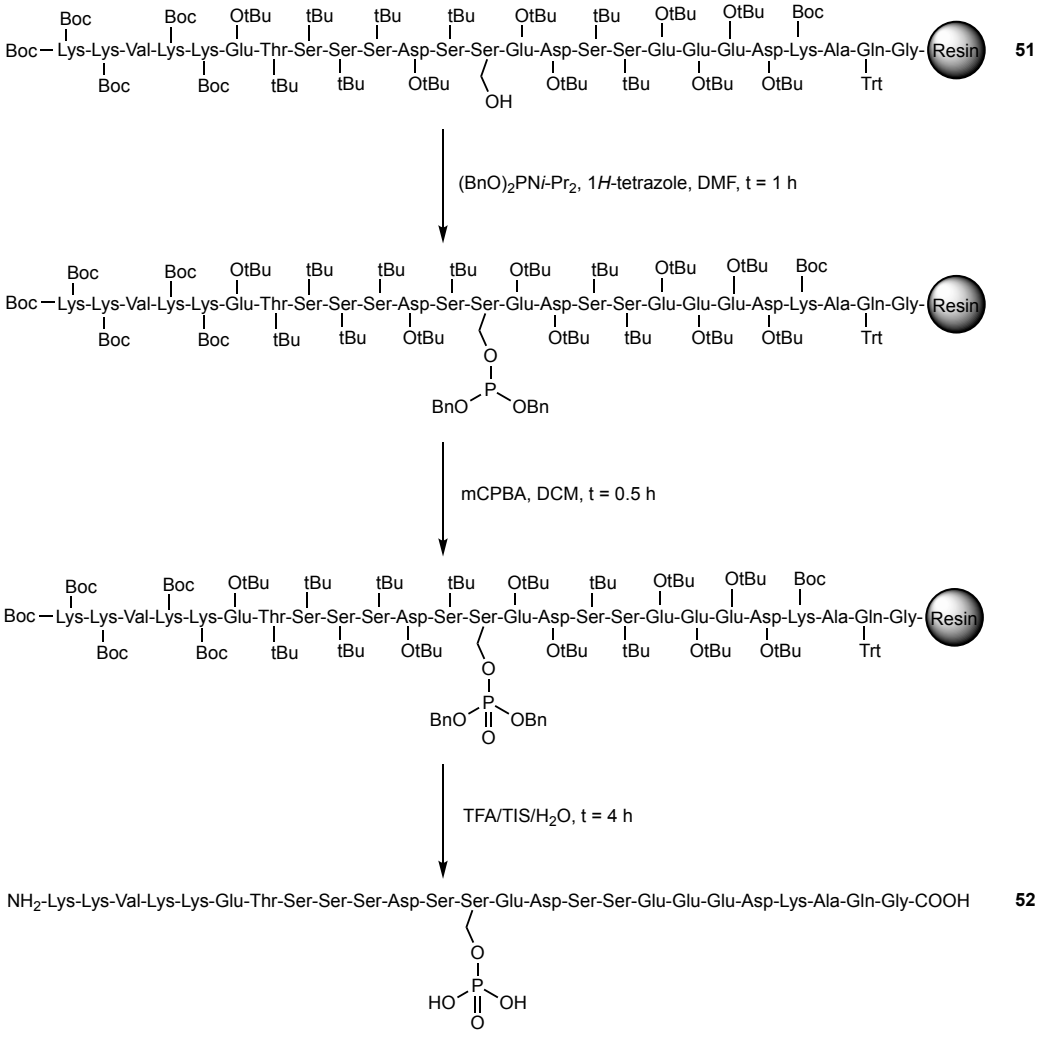

Figure S1. Synthesis of Nopp140 fragment phosphopeptide **52** from the precursor peptide **51** via two-step phosphitylation and oxidation on resin.

2.2 Liquid chromatography-mass spectrometry (LC-MS)

Synthesis and analytical data for model phosphopeptide **1**

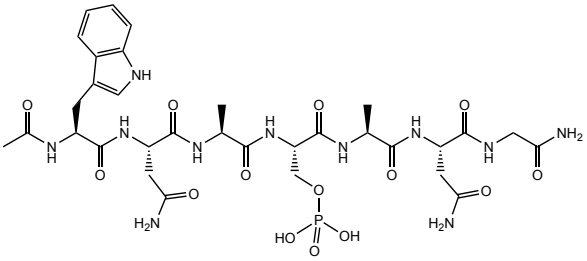

Phosphopeptide **1** was synthesized on the Fmoc-Rink amide resin (0.11 mmol). The crude peptide was purified by preparative reverse-phase HPLC and obtained as a lyophilized solid (30 mg, 0.036 mmol, 33%).

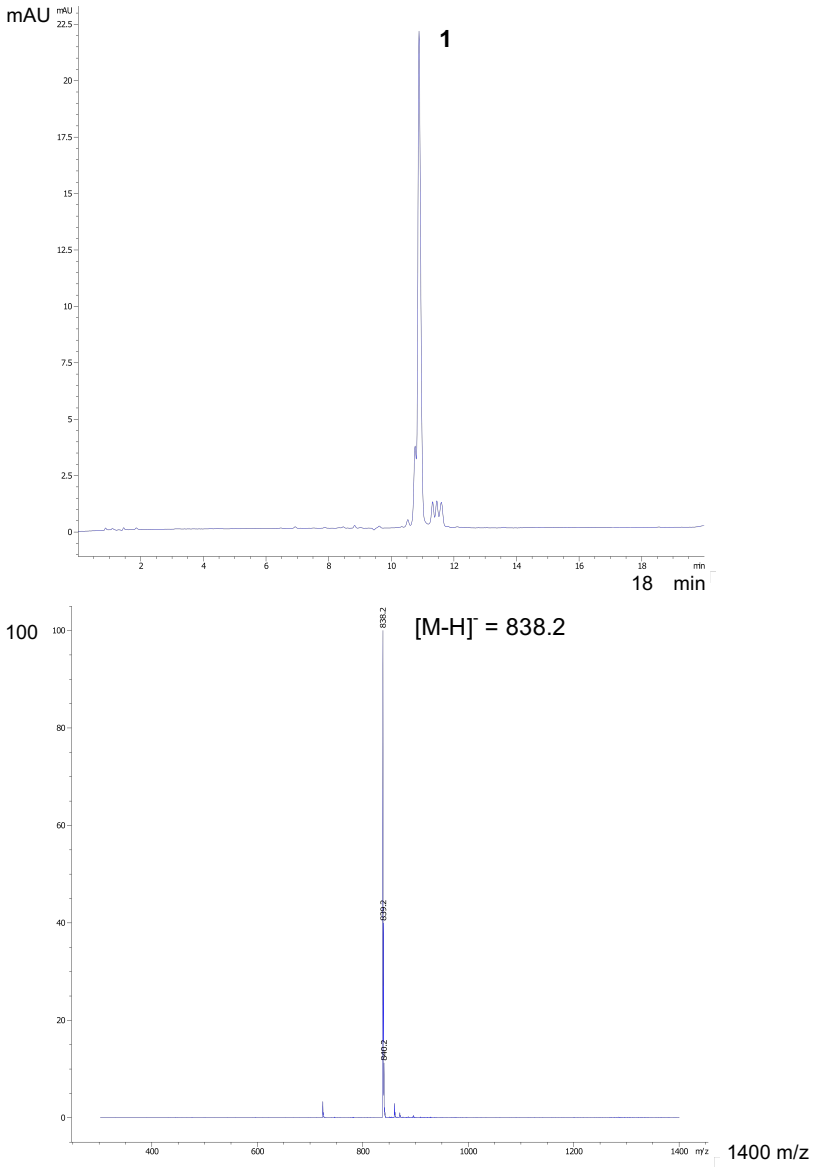

Figure S2. Analytical HPLC-MS spectra of pure phosphopeptide **1** in Method A. Calculated mass $[M-H]^-$: 838.3, observed mass $[M-H]^-$: 838.2.

Synthesis and analytical data for model phosphopeptide **2**

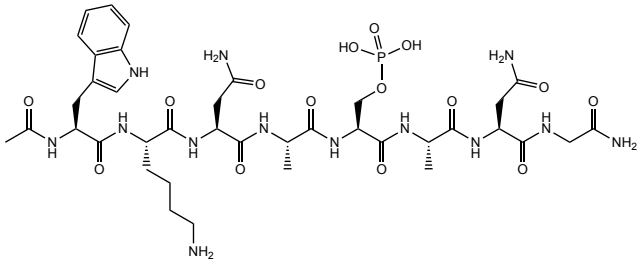

Phosphopeptide **2** was synthesized on the Fmoc-Rink amide resin (0.11 mmol). The crude peptide was purified by preparative reverse-phase HPLC and obtained as a lyophilized solid (25 mg, 0.026 mmol, 24%).

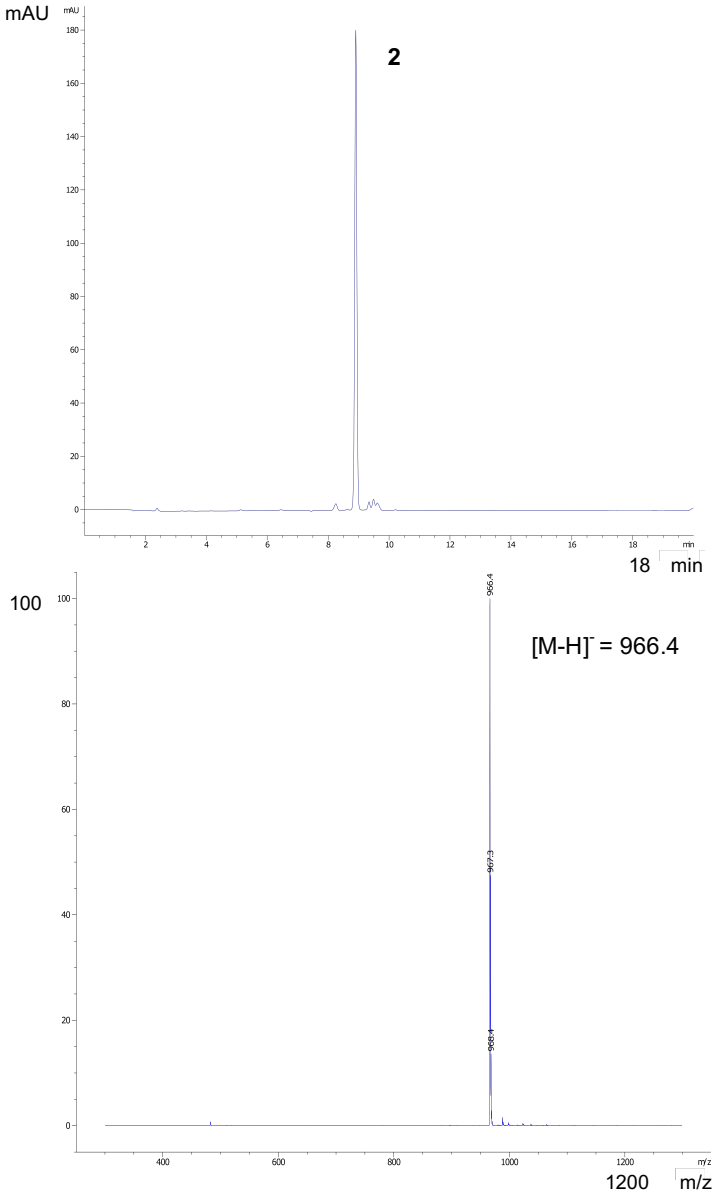

Figure S3. Analytical HPLC-MS spectra of pure phosphopeptide **2** in Method A. Calculated mass $[M-H]^-$: 966.4, observed mass $[M-H]^-$: 966.4.

Synthesis and analytical data for model phosphopeptide **3**

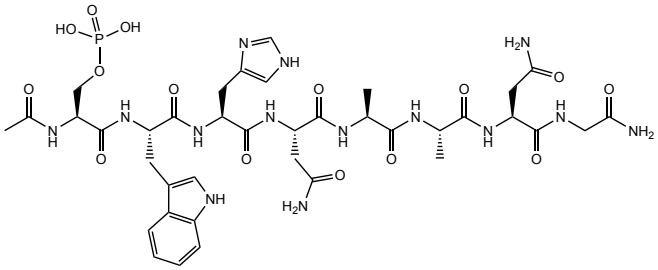

Phosphopeptide **3** was synthesized on the Fmoc-Rink amide resin (0.11 mmol). The crude peptide was purified by preparative reverse-phase HPLC and obtained as a lyophilized solid (43 mg, 0.044 mmol, 40%).

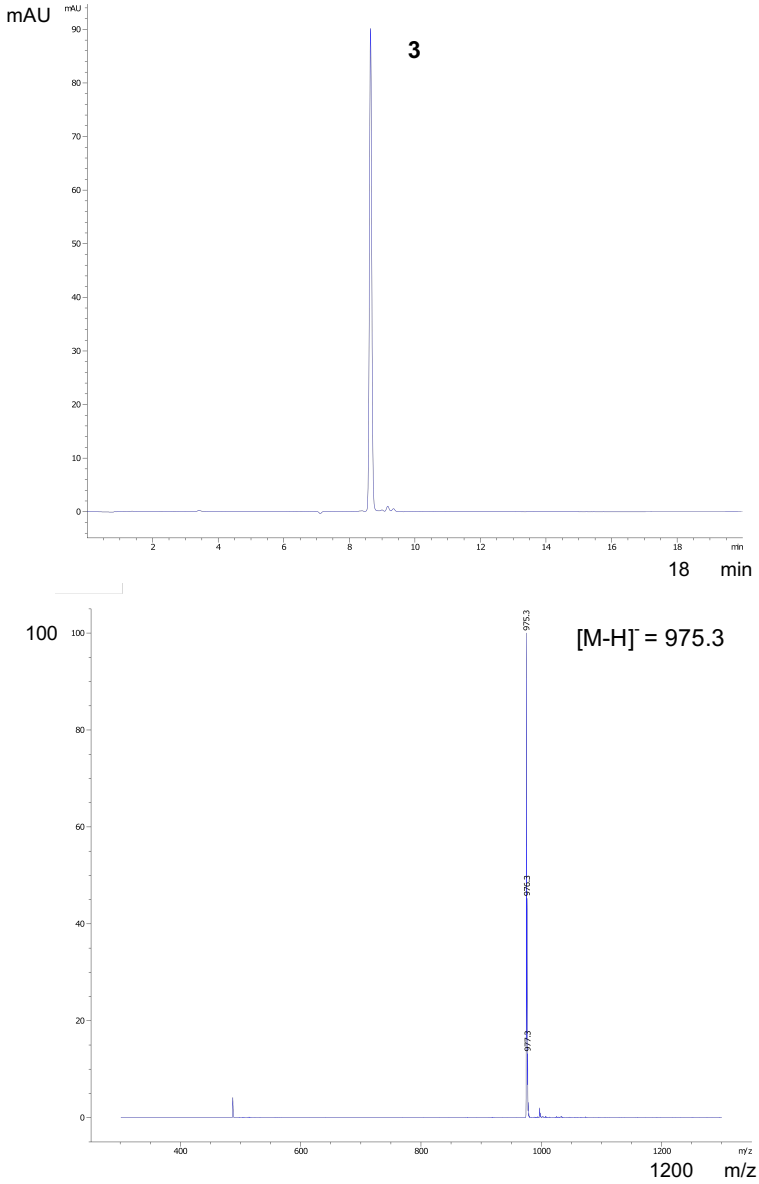

Figure S4. Analytical HPLC-MS spectra of pure phosphopeptide **3** in Method A. Calculated mass $[M-H]^-$: 975.3, observed mass $[M-H]^-$: 975.3.

Synthesis and analytical data for model peptide **4**

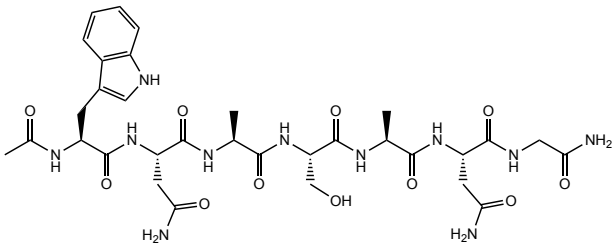

Peptide **4** was synthesized on the Fmoc-Rink amide resin (0.11 mmol). The crude peptide was purified by preparative reverse-phase HPLC and obtained as a lyophilized solid (22 mg, 0.029 mmol, 26%).

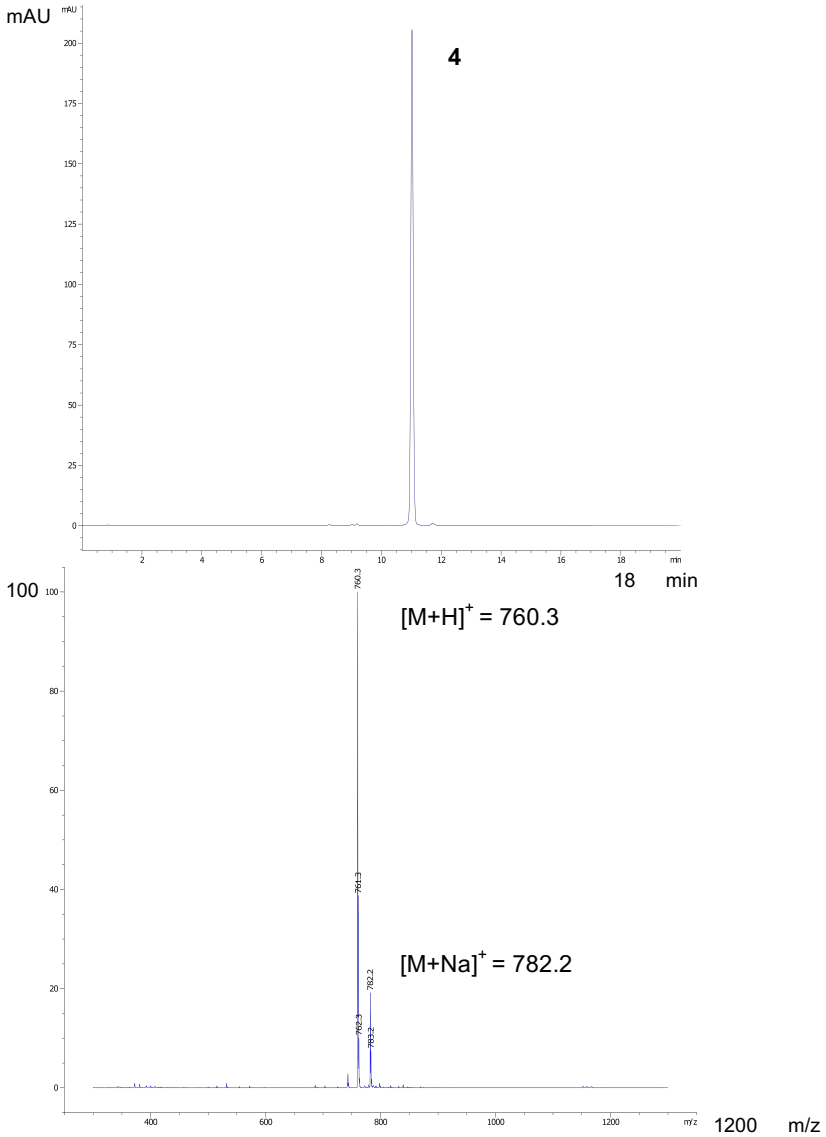

Figure S5. Analytical HPLC-MS spectra of pure peptide **4** in Method A. Calculated mass $[M+H]^+$: 760.3, observed mass $[M+H]^+$: 760.3; Calculated mass $[M+Na]^+$: 782.3, observed mass $[M+Na]^+$: 782.2.

Synthesis and analytical data for model phosphopeptide **5**

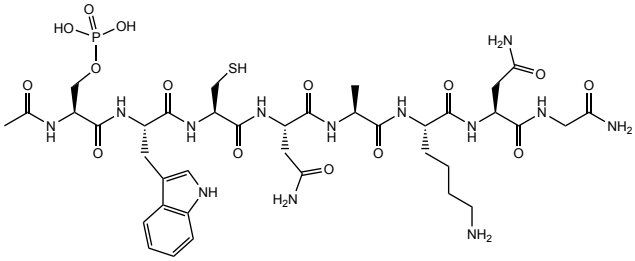

Phosphopeptide **5** was synthesized on the Fmoc-Rink amide resin (0.11 mmol). The crude peptide was purified by preparative reverse-phase HPLC and obtained as a lyophilized solid (21 mg, 0.021 mmol, 19%).

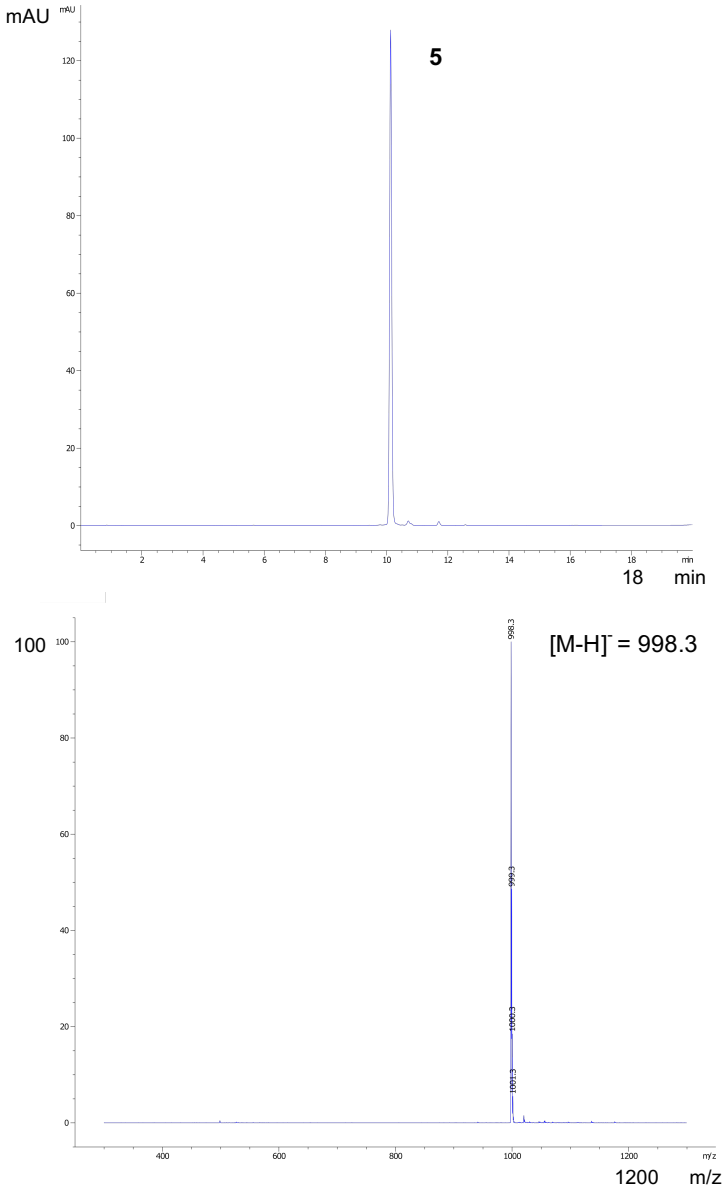

Figure S6. Analytical HPLC-MS spectra of pure phosphopeptide **5** in Method A. Calculated mass $[M-H]^-$: 998.4, observed mass $[M-H]^-$: 998.3.

Synthesis and analytical data for model peptide **6**

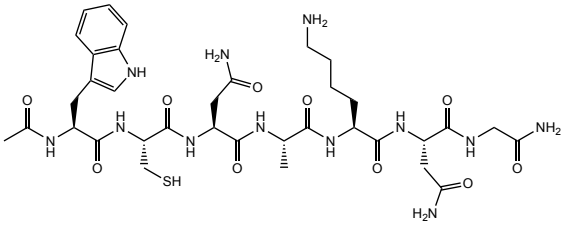

Peptide **6** was synthesized on the Fmoc-Rink amide resin (0.11 mmol). The crude peptide was purified by preparative reverse-phase HPLC and obtained as a lyophilized solid (45 mg, 0.054 mmol, 49%).

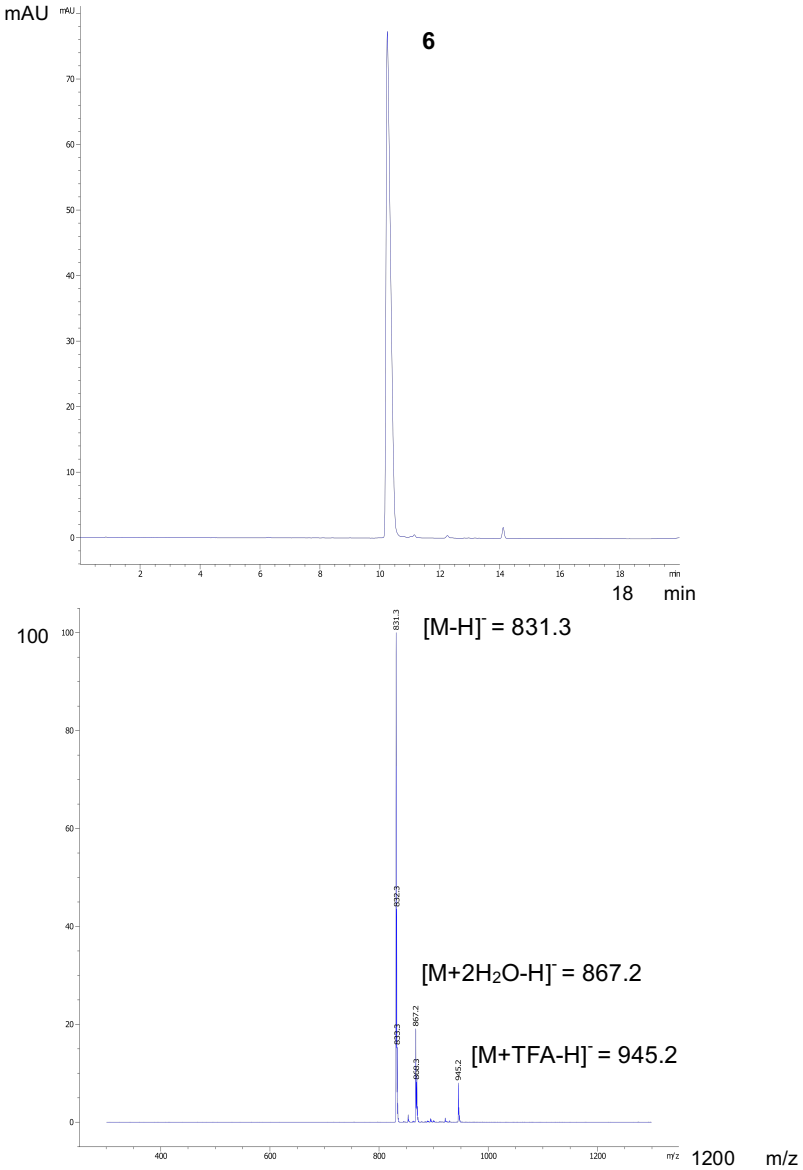

Figure S7. Analytical HPLC-MS spectra of pure peptide **6** in Method A. Calculated mass $[M-H]^-$: 831.4, observed mass $[M-H]^-$: 831.3; Calculated mass $[M+2H_2O-H]^-$: 867.4, observed mass $[M+2H_2O-H]^-$: 867.2; Calculated mass $[M+TFA-H]^-$: 945.4, observed mass $[M+TFA-H]^-$: 945.2.

Synthesis and analytical data for model phosphopeptide **7**

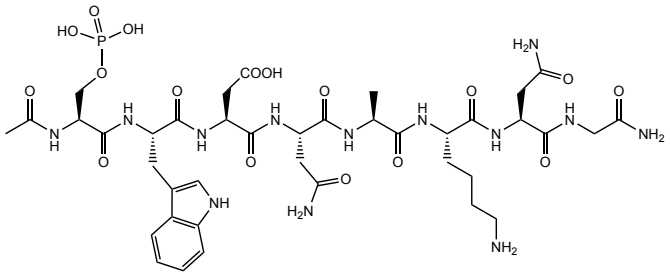

Phosphopeptide **7** was synthesized on the Fmoc-Rink amide resin (0.11 mmol). The crude peptide was purified by preparative reverse-phase HPLC and obtained as a lyophilized solid (62 mg, 0.061 mmol, 55%).

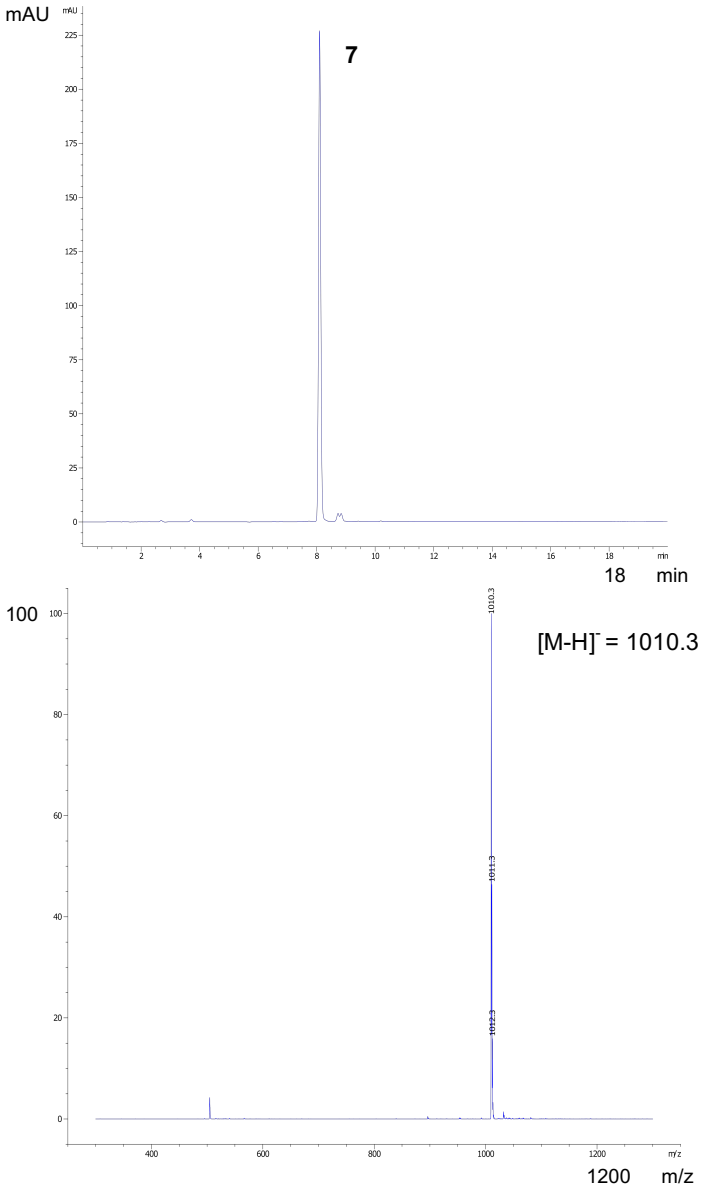

Figure S8. Analytical HPLC-MS spectra of pure phosphopeptide **7** in Method A. Calculated mass $[M-H]^-$: 1010.4, observed mass $[M-H]^-$: 1010.3.

Synthesis and analytical data for model phosphopeptide **8**

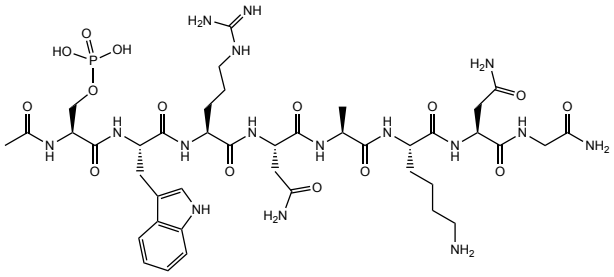

Phosphopeptide **8** was synthesized on the Fmoc-Rink amide resin (0.11 mmol). The crude peptide was purified by preparative reverse-phase HPLC and obtained as a lyophilized solid (55 mg, 0.052 mmol, 47%).

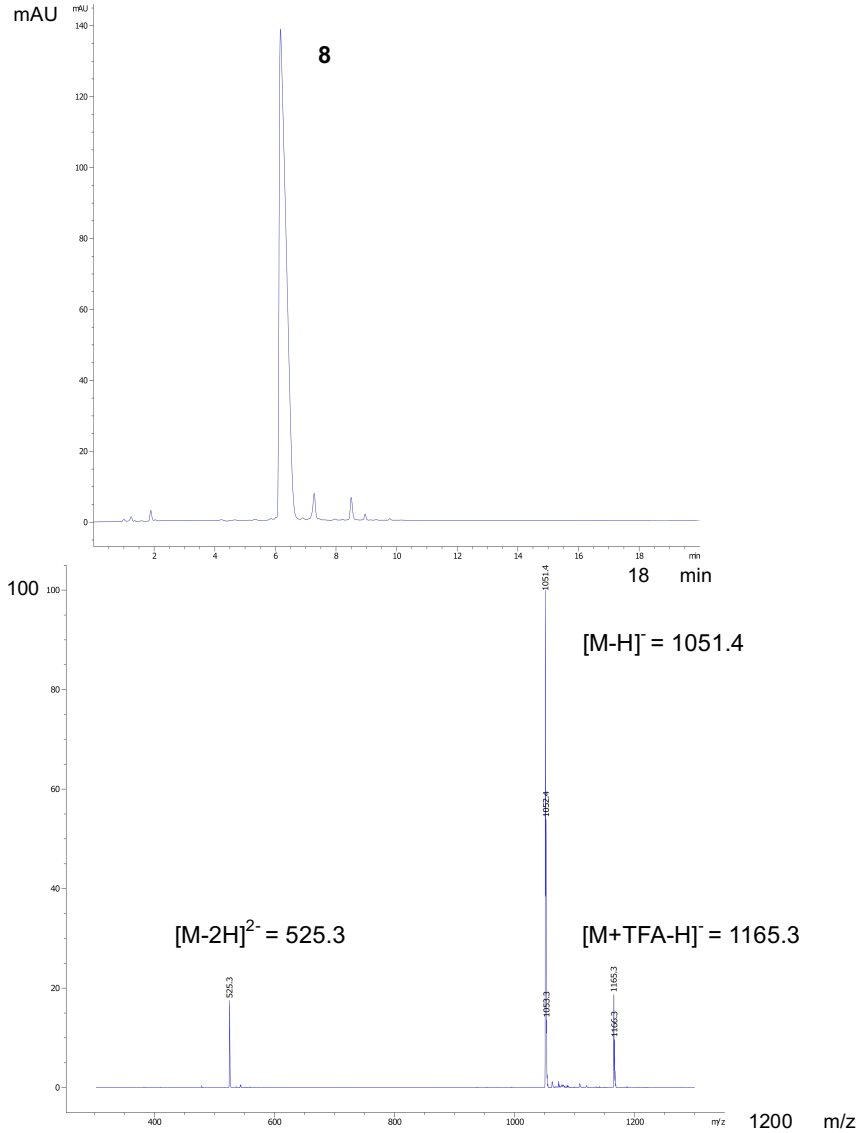

Figure S9. Analytical HPLC-MS spectra of pure phosphopeptide **8** in Method A. Calculated mass $[M-H]^-$: 1051.4, observed mass $[M-H]^-$: 1051.4; Calculated mass $[M-2H]^{2-}$: 525.2, observed mass $[M-2H]^{2-}$: 525.3; Calculated mass $[M+TFA-H]^-$: 1165.4, observed mass $[M+TFA-H]^-$: 1165.3.

Synthesis and analytical data for model phosphopeptide **9**

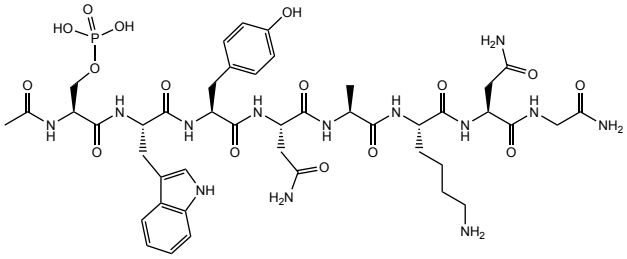

Phosphopeptide **9** was synthesized on the Fmoc-Rink amide resin (0.11 mmol). The crude peptide was purified by preparative reverse-phase HPLC and obtained as a lyophilized solid (54 mg, 0.050 mmol, 45%).

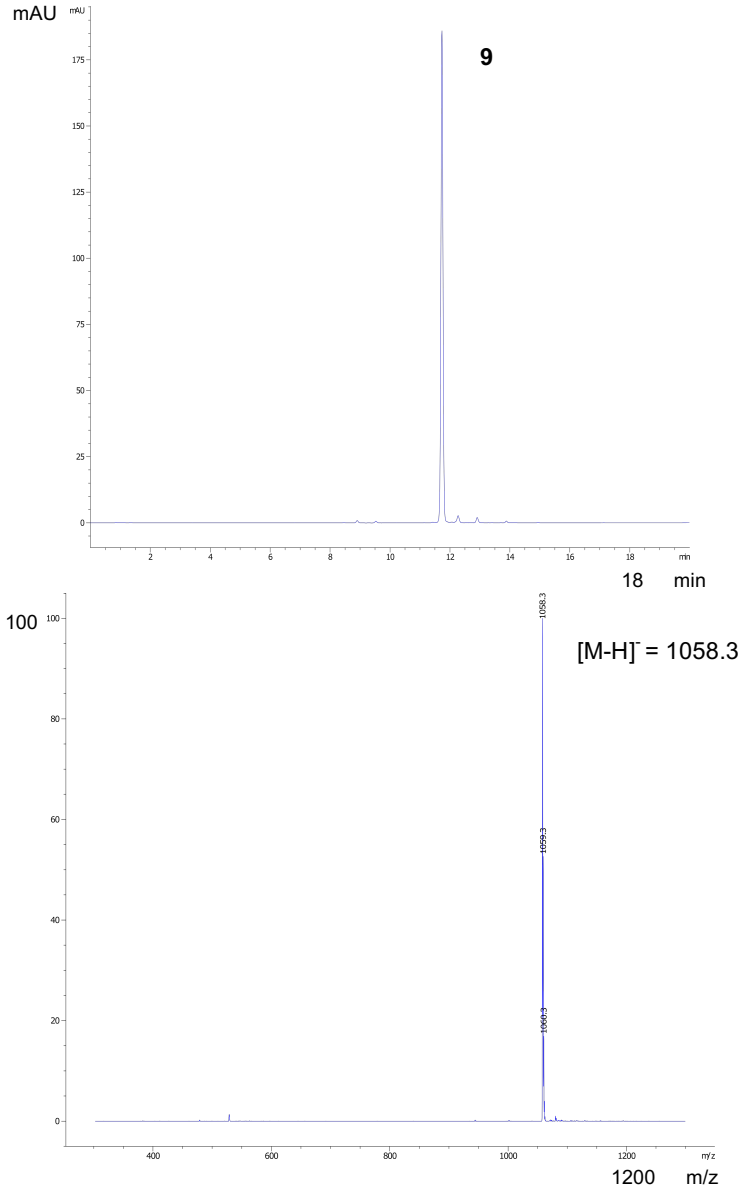

Figure S10. Analytical HPLC-MS spectra of pure phosphopeptide **9** in Method A. Calculated mass $[M-H]^-$: 1058.4, observed mass $[M-H]^-$: 1058.3.

Synthesis and analytical data for model phosphopeptide **10**

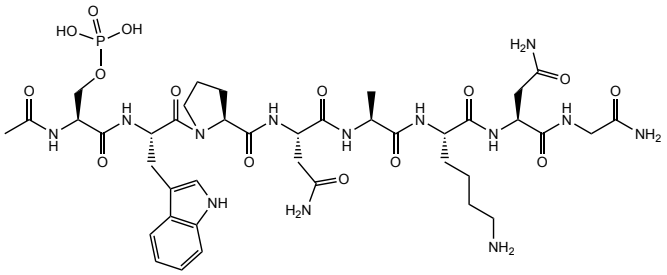

Phosphopeptide **10** was synthesized on the Fmoc-Rink amide resin (0.11 mmol). The crude peptide was purified by preparative reverse-phase HPLC and obtained as a lyophilized solid (53 mg, 0.053 mmol, 48%).

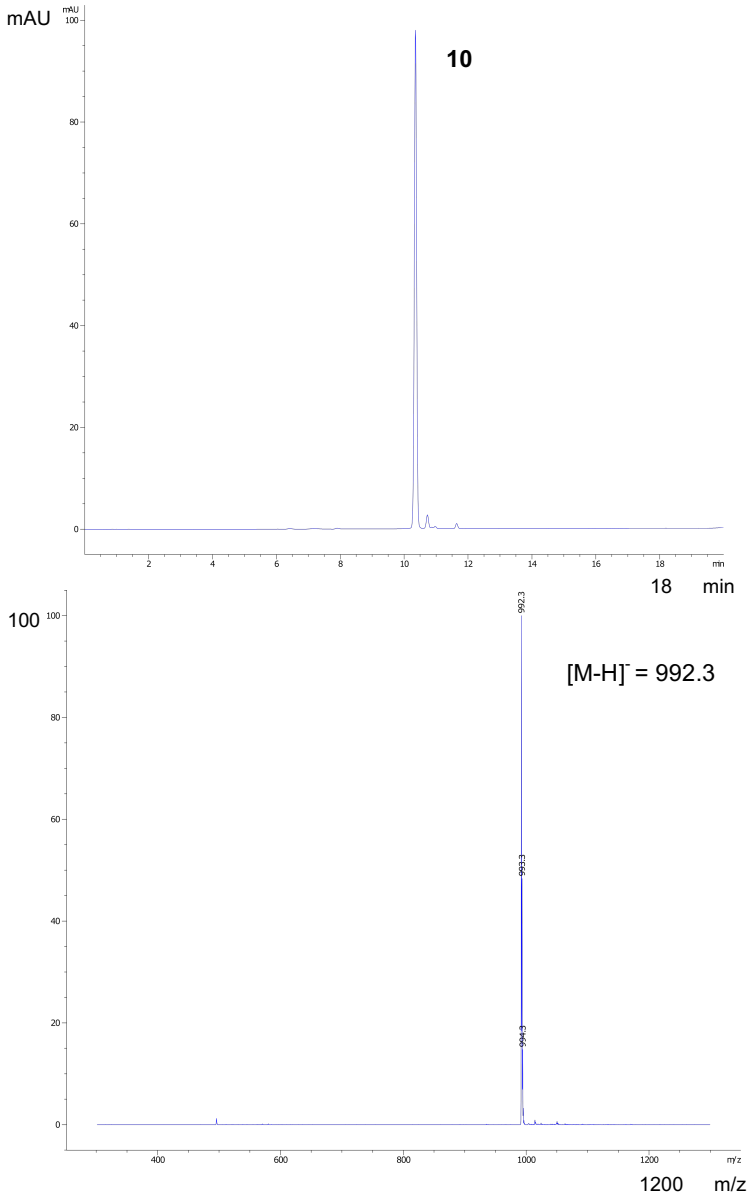

Figure S11. Analytical HPLC-MS spectra of pure phosphopeptide **10** in Method A. Calculated mass $[M-H]^-$: 992.4, observed mass $[M-H]^-$: 992.3.

Synthesis and analytical data for model phosphopeptide **11**

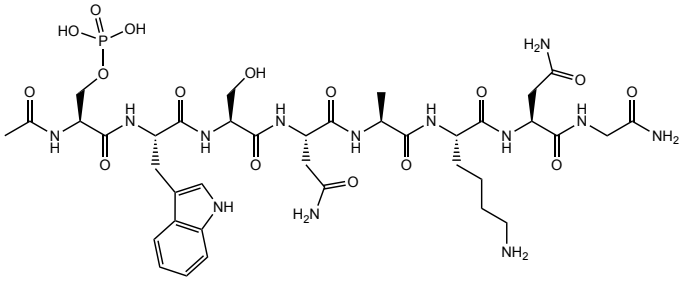

Phosphopeptide **11** was synthesized on the Fmoc-Rink amide resin (0.11 mmol). The crude peptide was purified by preparative reverse-phase HPLC and obtained as a lyophilized solid (38 mg, 0.039 mmol, 35%).

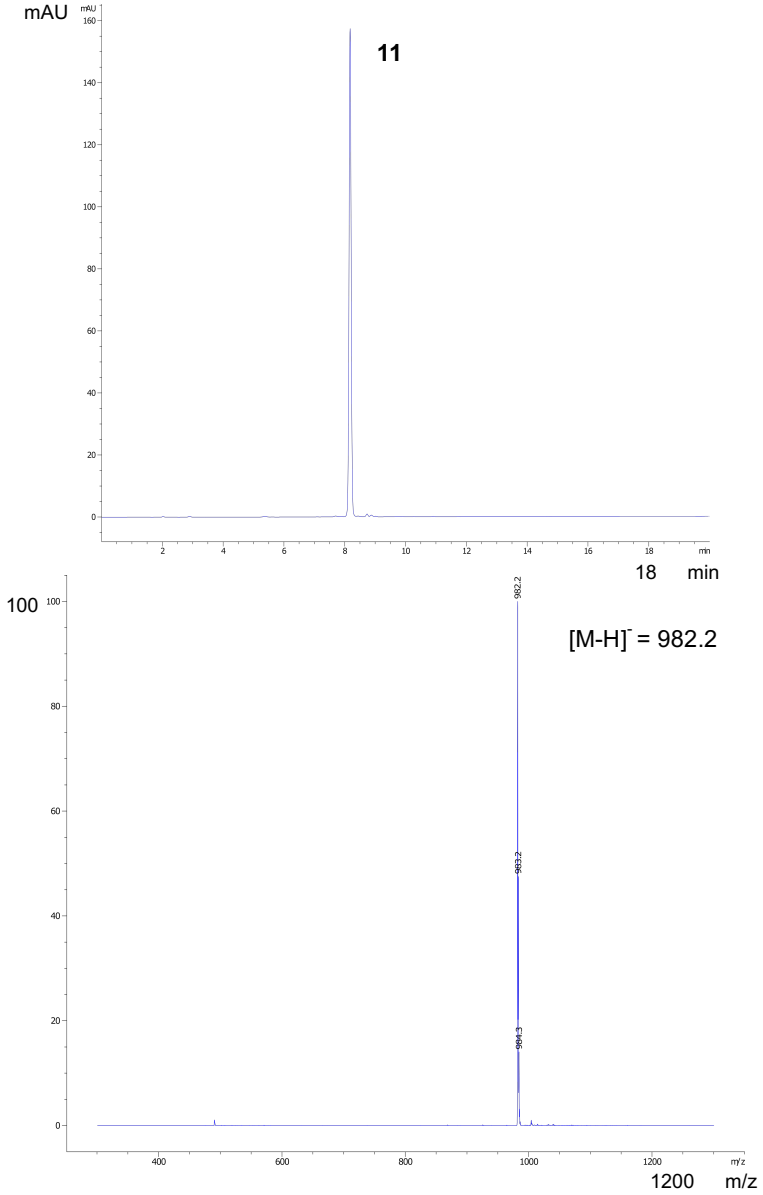

Figure S12. Analytical HPLC-MS spectra of pure phosphopeptide **11** in Method A. Calculated mass $[M-H]^-$: 982.4, observed mass $[M-H]^-$: 982.2.

Synthesis and analytical data for model phosphopeptide **12**

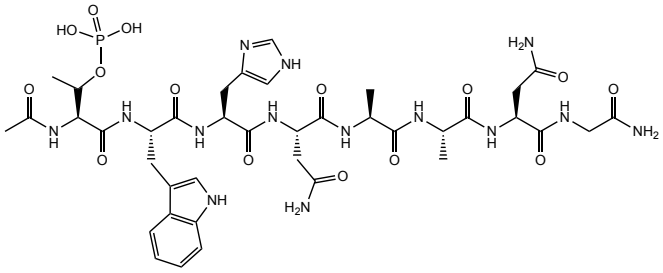

Phosphopeptide **12** was synthesized on the Fmoc-Rink amide resin (0.11 mmol). The crude peptide was purified by preparative reverse-phase HPLC and obtained as a lyophilized solid (62 mg, 0.063 mmol, 57%).

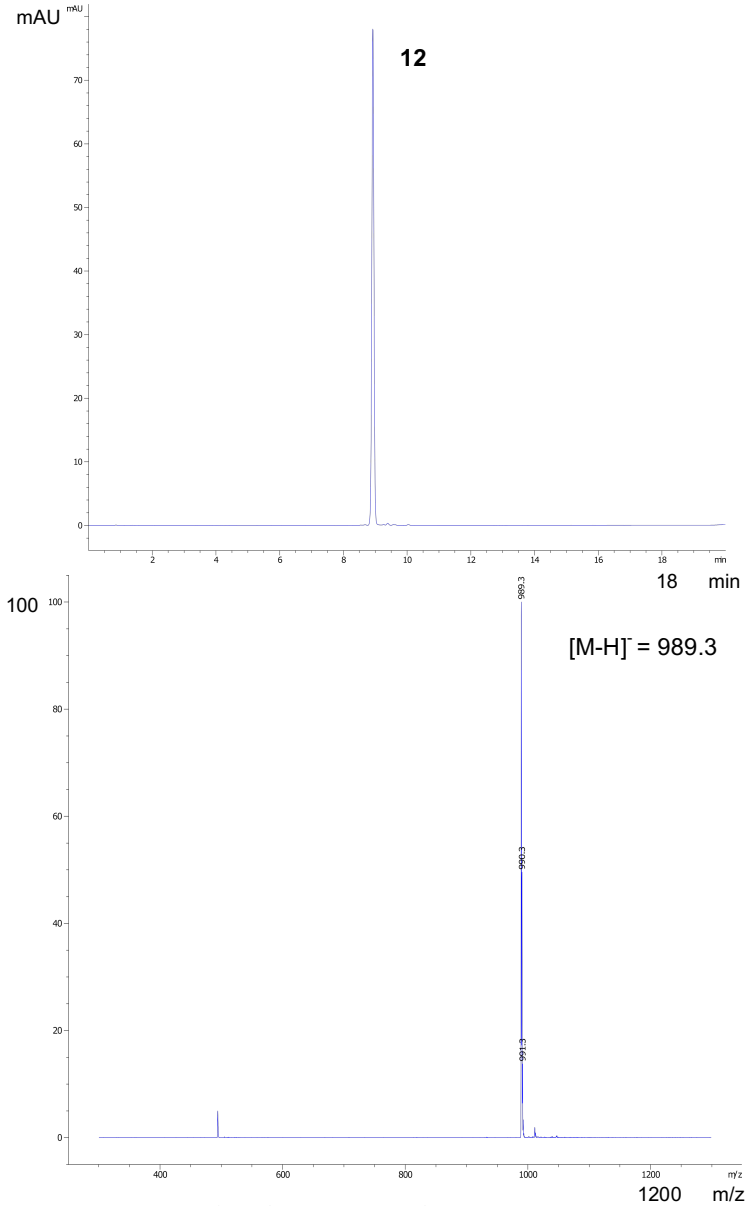

Figure S13. Analytical HPLC-MS spectra of pure phosphopeptide **12** in Method A. Calculated mass $[M-H]^-$: 989.4, observed mass $[M-H]^-$: 989.3.

Synthesis and analytical data for model phosphopeptide **13**

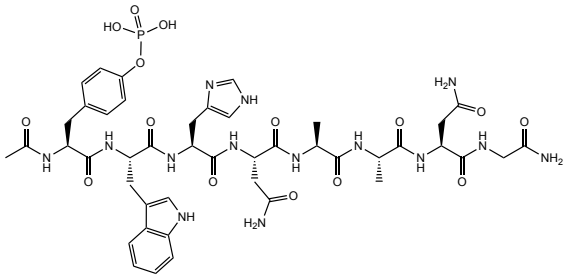

Phosphopeptide **13** was synthesized on the Fmoc-Rink amide resin (0.11 mmol). The crude peptide was purified by preparative reverse-phase HPLC and obtained as a lyophilized solid (35 mg, 0.033 mmol, 30%).

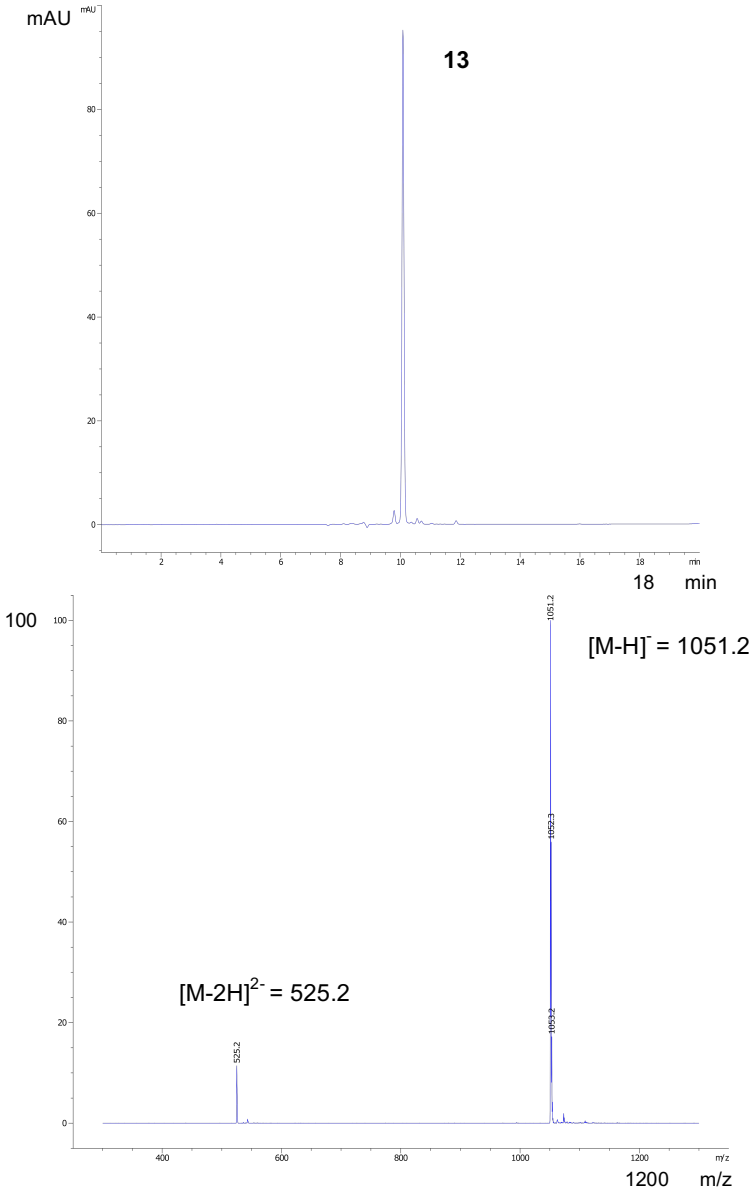

Figure S14. Analytical HPLC-MS spectra of pure phosphopeptide **13** in Method A. Calculated mass $[M-H]^-$: 1051.4, observed mass $[M-H]^-$: 1051.2; Calculated mass $[M-2H]^{2-}$: 525.2, observed mass $[M-2H]^{2-}$: 525.2.

Synthesis and analytical data for model phosphopeptide **14**

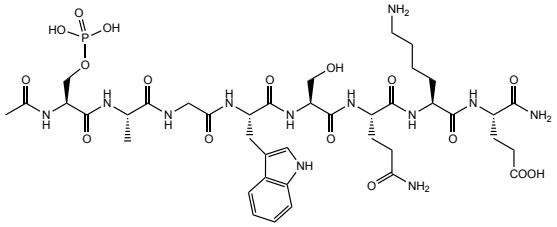

Phosphopeptide **14** was synthesized on the Fmoc-Rink amide resin (0.11 mmol). The crude peptide was purified by preparative reverse-phase HPLC and obtained as a lyophilized solid (39 mg, 0.038 mmol, 34%).

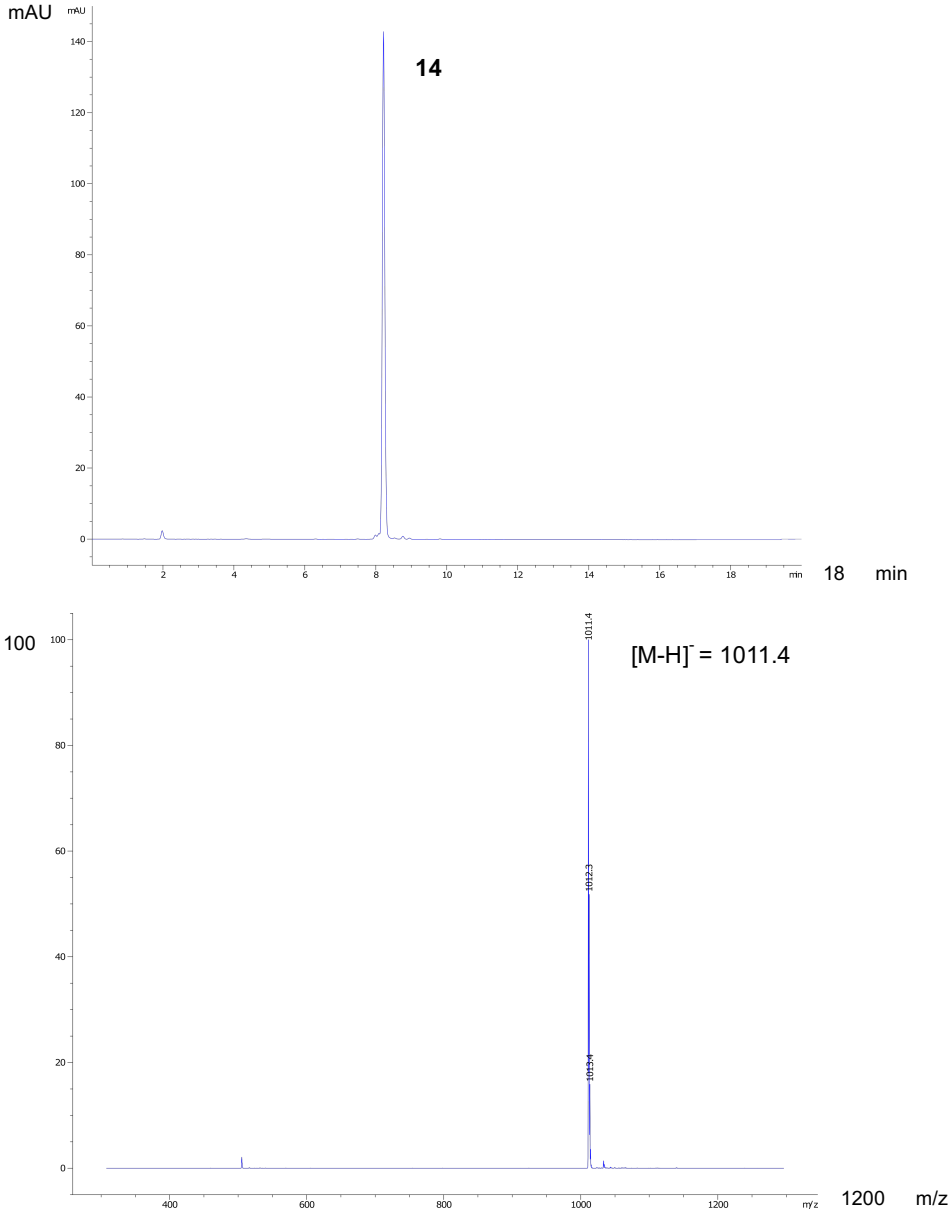

Figure S15. Analytical HPLC-MS spectra of pure phosphopeptide **14** in Method A. Calculated mass $[M-H]^-$: 1011.4, observed mass $[M-H]^-$: 1011.4.

Synthesis and analytical data for RPA190 fragment phosphopeptide **15**

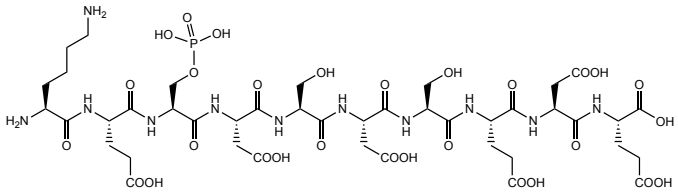

Phosphopeptide **15** was synthesized on the Fmoc-L-Glu(OtBu)-Wang resin (0.11 mmol). The crude peptide was purified by preparative reverse-phase HPLC and obtained as a lyophilized solid (58 mg, 0.047 mmol, 42%).

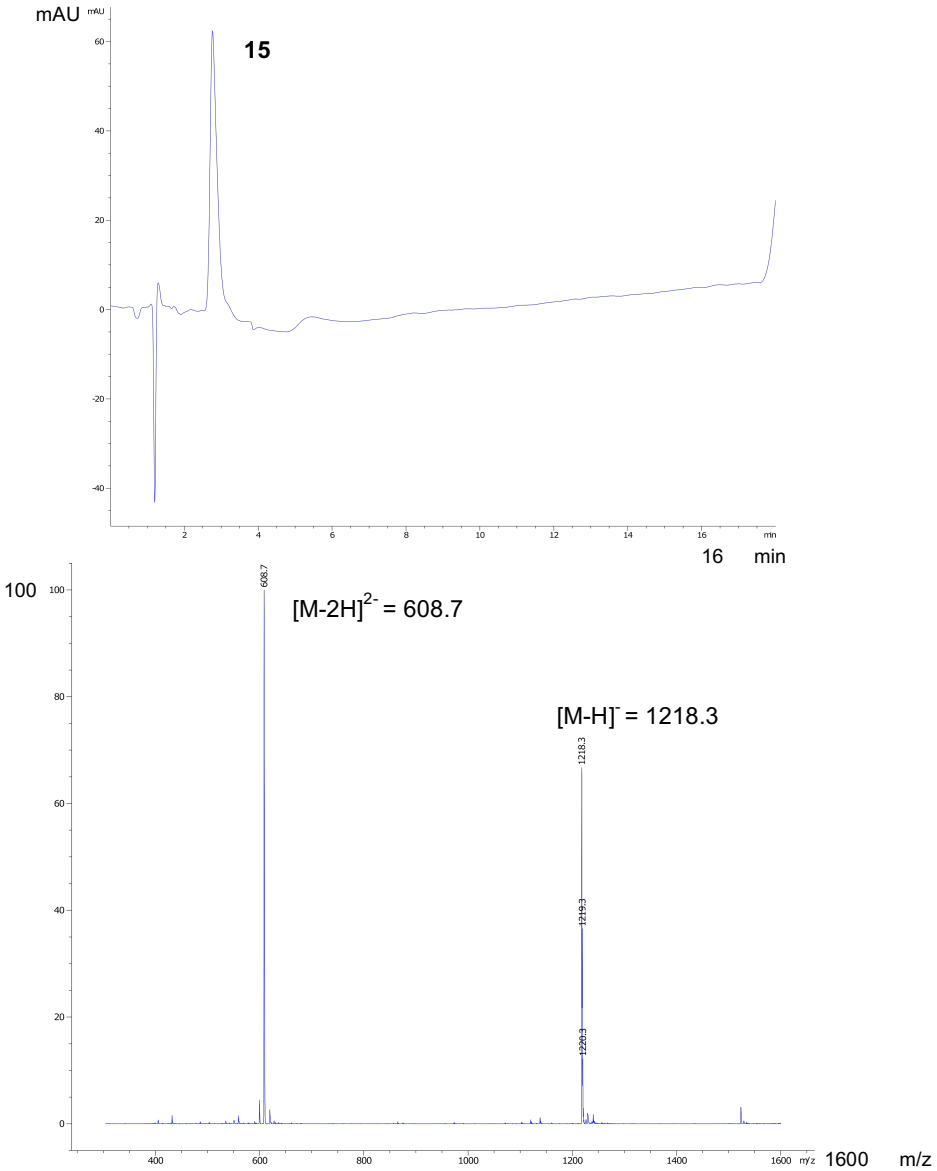

Figure S16. Analytical HPLC-MS spectra of pure phosphopeptide **15** in Method F. Calculated mass $[M-H]^-$: 1218.4, observed mass $[M-H]^-$: 1218.3; Calculated mass $[M-2H]^{2-}$: 608.7, observed mass $[M-2H]^{2-}$: 608.7.

Synthesis and analytical data for IC2C fragment phosphopeptide **16**

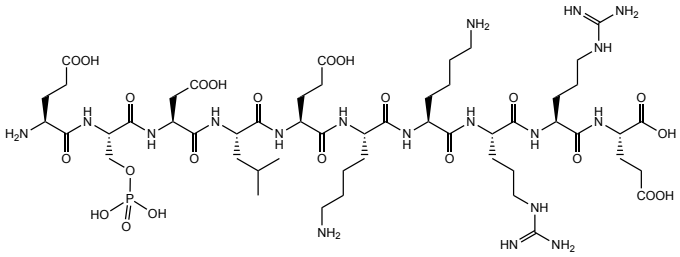

Phosphopeptide **16** was synthesized on the Fmoc-L-Glu(OtBu)-Wang resin (0.11 mmol). The crude peptide was purified by preparative reverse-phase HPLC and obtained as a lyophilized solid (49 mg, 0.036 mmol, 33%).

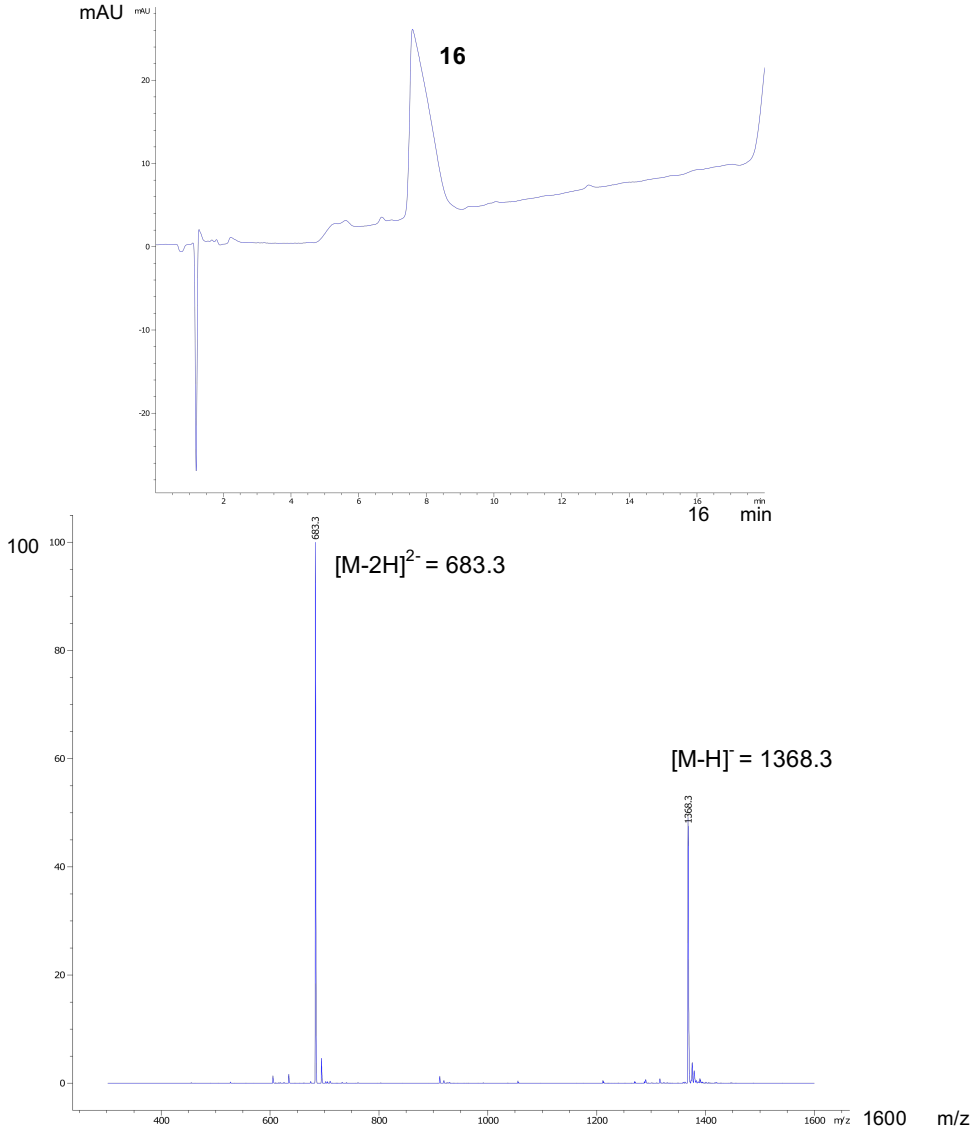

Figure S17. Analytical HPLC-MS spectra of pure phosphopeptide **16** in Method F. Calculated mass $[M-H]^-$: 1368.4, observed mass $[M-H]^-$: 1368.3; Calculated mass $[M-2H]^{2-}$: 683.3, observed mass $[M-2H]^{2-}$: 683.3.

Synthesis and analytical data for Gcr1 fragment phosphopeptide **17**

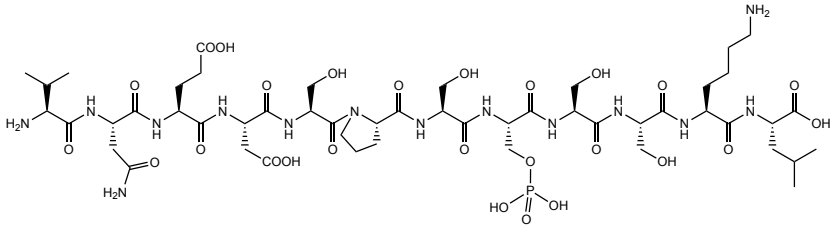

Phosphopeptide **17** was synthesized on the Fmoc-L-Leu-Wang resin (0.11 mmol). The crude peptide was purified by preparative reverse-phase HPLC and obtained as a lyophilized solid (18 mg, 0.014 mmol, 12%).

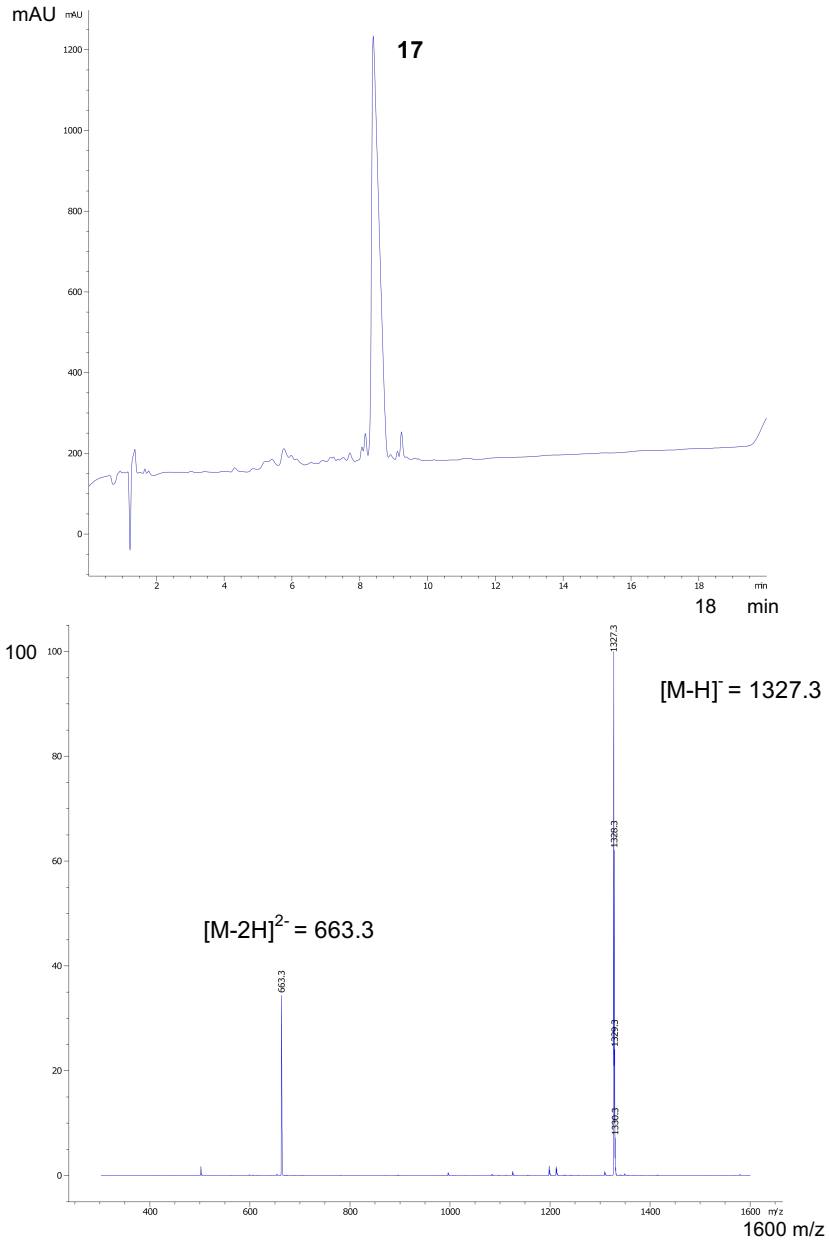

Figure S18. Analytical HPLC-MS spectra of pure phosphopeptide **17** in Method B. Calculated mass $[M-H]^-$: 1327.5, observed mass $[M-H]^-$: 1327.3; Calculated mass $[M-2H]^{2-}$: 663.2, observed mass $[M-2H]^{2-}$: 663.3.

Synthesis and analytical data for EIF2S2 fragment phosphopeptide **18**

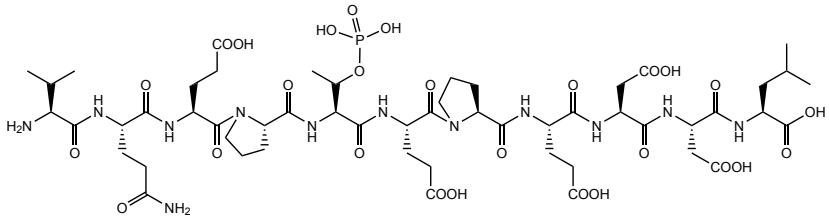

Phosphopeptide **18** was synthesized on the Fmoc-L-Leu-Wang resin (0.11 mmol). The crude peptide was purified by preparative reverse-phase HPLC and obtained as a lyophilized solid (24 mg, 0.018 mmol, 16%).

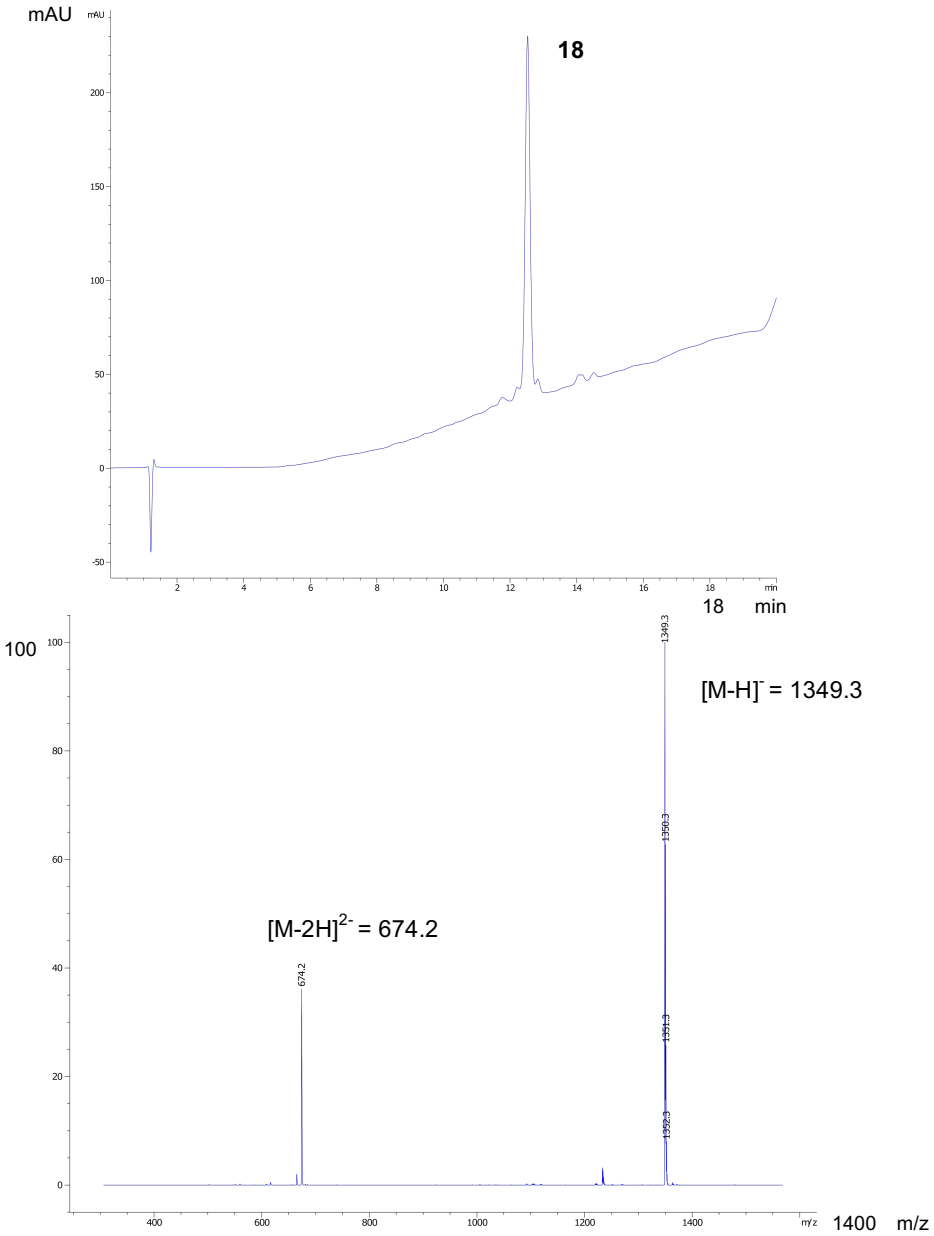

Figure S19. Analytical HPLC-MS spectra of pure phosphopeptide **18** in Method C. Calculated mass $[M-H]^-$: 1349.5, observed mass $[M-H]^-$: 1349.3; Calculated mass $[M-2H]^{2-}$: 674.2, observed mass $[M-2H]^{2-}$: 674.2.

Synthesis and analytical data for Nopp140 fragment precursor peptide **51**

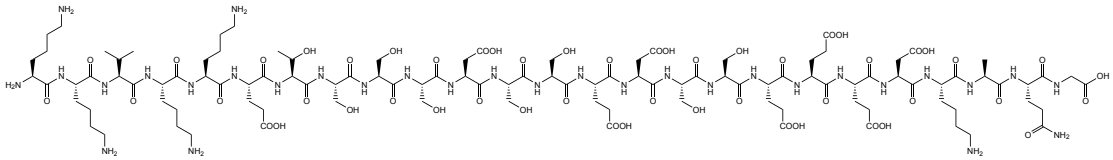

The precursor peptide **51** was synthesized on the Fmoc-Gly-Wang resin (0.11 mmol) and was used directly for the synthesis of phosphopeptide **52** on the resin without further purification.

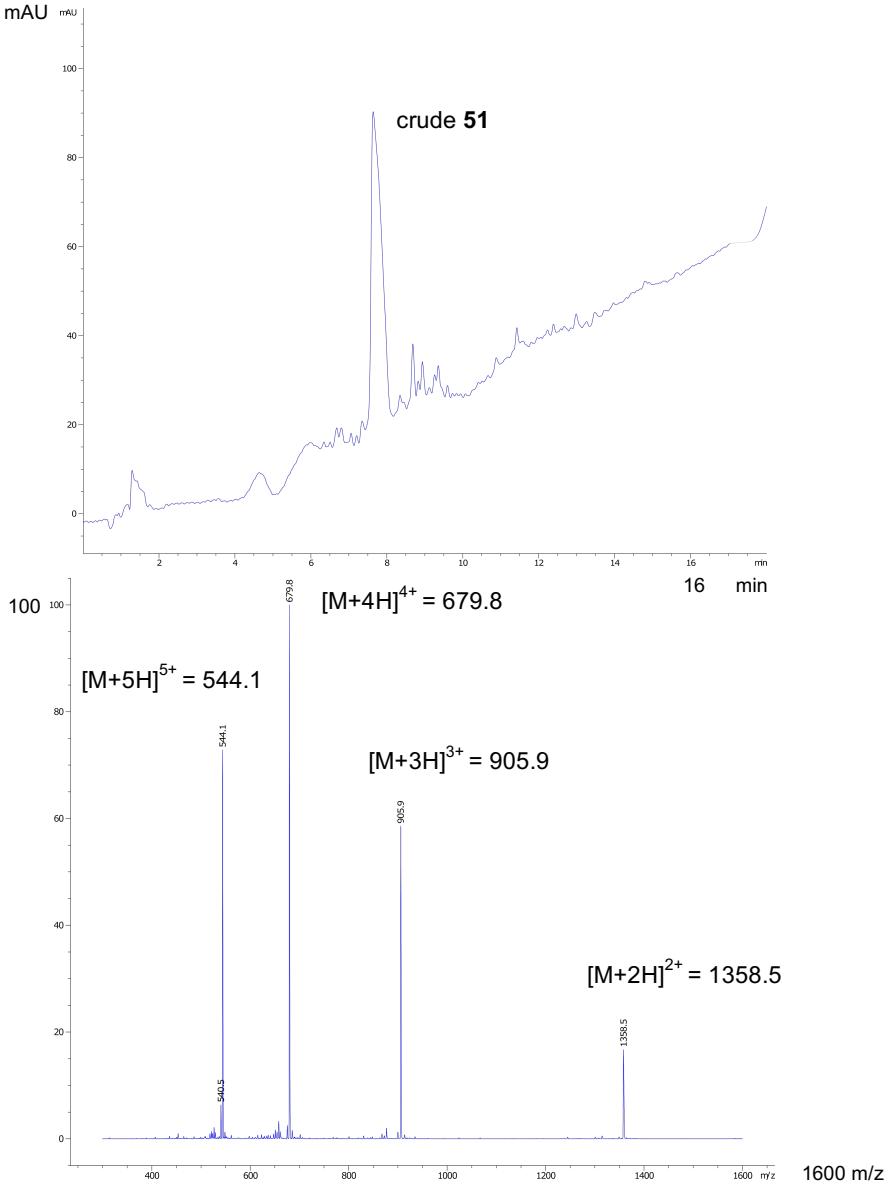

Figure S20. Analytical HPLC-MS spectra of crude precursor peptide **51** in Method D. Calculated mass $[M+2H]^{2+}$: 1358.6, observed mass $[M+2H]^{2+}$: 1358.5; Calculated mass $[M+3H]^{3+}$: 906.1, observed mass $[M+3H]^{3+}$: 905.9; Calculated mass $[M+4H]^{4+}$: 679.8, observed mass $[M+4H]^{4+}$: 679.8; Calculated mass $[M+5H]^{5+}$: 544.1, observed mass $[M+5H]^{5+}$: 544.1.

Synthesis and analytical data for Nopp140 fragment phosphopeptide **52**

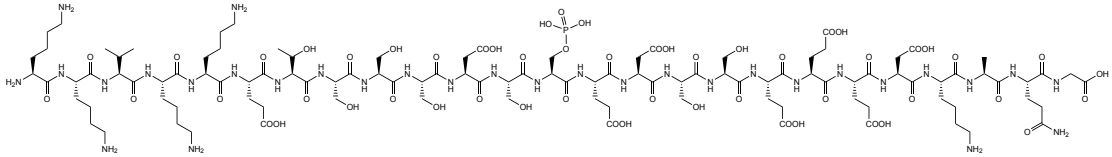

Phosphopeptide **52** was synthesized from the precursor peptide **51** via two-step phosphitylation and oxidation on resin (0.11 mmol). The crude peptide was purified by preparative reverse-phase HPLC and obtained as a lyophilized solid (88 mg, 0.031 mmol, 29%).

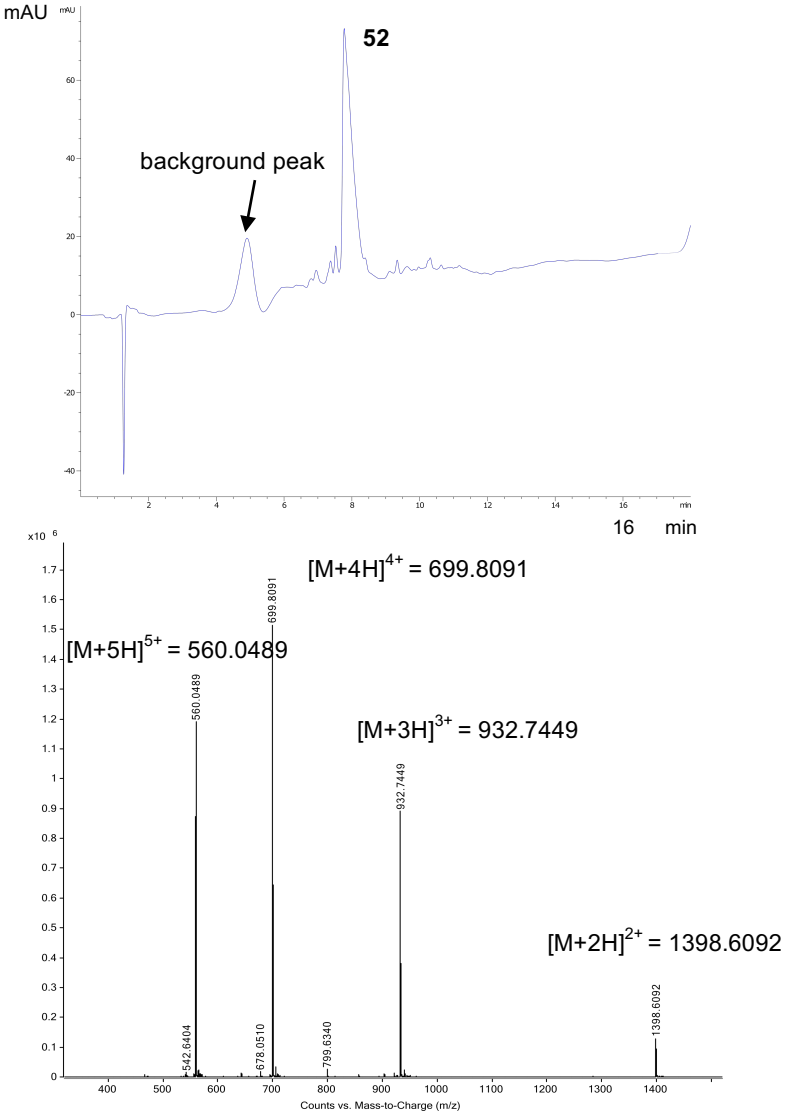

Figure S21. Analytical HPLC-MS spectra of pure phosphopeptide **52** in Method D. Calculated mass $[M+2H]^{2+}$: 1398.6104, observed mass $[M+2H]^{2+}$: 1398.6092; Calculated mass $[M+3H]^{3+}$: 932.7427, observed mass $[M+3H]^{3+}$: 932.7449; Calculated mass $[M+4H]^{4+}$: 699.8089, observed mass $[M+4H]^{4+}$: 699.8091; Calculated mass $[M+5H]^{5+}$: 560.0485, observed mass $[M+5H]^{5+}$: 560.0489.

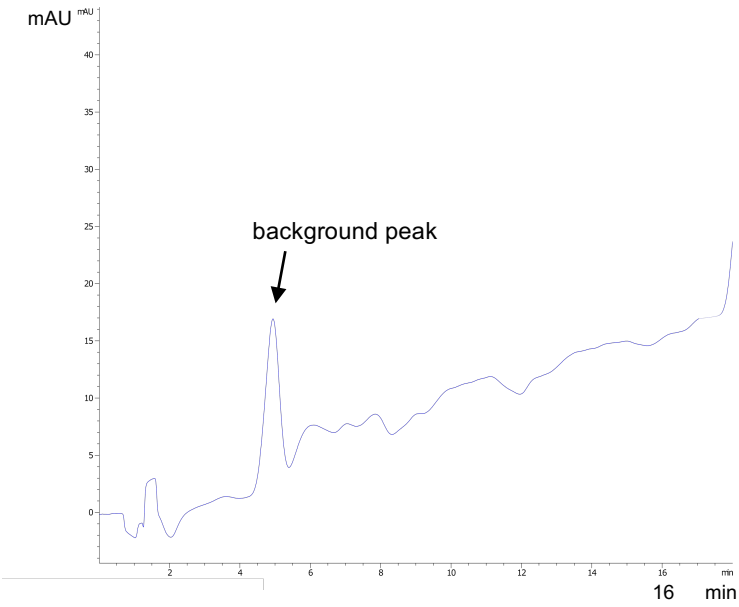

Figure S22. Analytical HPLC spectrum of injection with only H_2O in Method D indicating a background peak at around 5 min.

3. Synthesis of model pyrophosphopeptides

3.1 Investigation of temperature effect on peptide amidophosphorylation

In the initial investigation on the peptide amidophosphorylation, we set up the reactions at different temperature (room temperature, 45°C and -20°C in freezer) as the following. To a vial containing 1 mM of phosphopeptide **1** (1 equiv.) in 400 ul H_2O, was added DAP (30 equiv., 30 mM), magnesium chloride (10 equiv., 10 mM) and imidazole (10 equiv., 10 mM). The pH of the reaction mixture was adjusted to 5.5 with hydrochloric acid. The reactions were kept at different temperature for 2 days and the pH was adjusted to 5.5 once a day. Progress of reactions was monitored by LC-MS. Conversion of amidopyrophosphopeptide **19** was determined based on the area-under-the-curve (peak integration) at 280 nm by analytical HPLC.

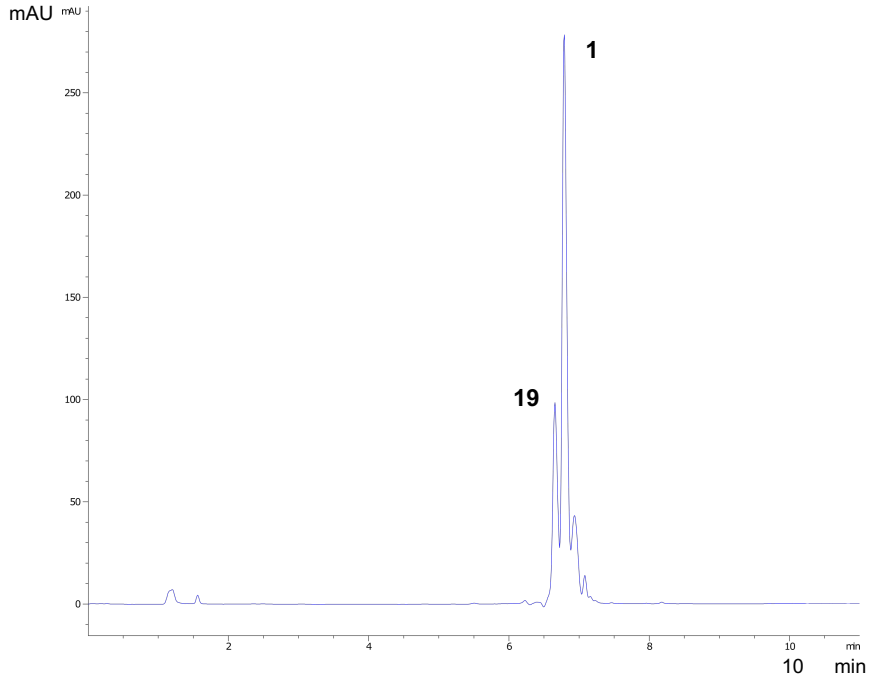

Figure S23. Analytical HPLC spectrum of the reaction crude showing the production of **19** from **1** in 22% conversion at room temperature.

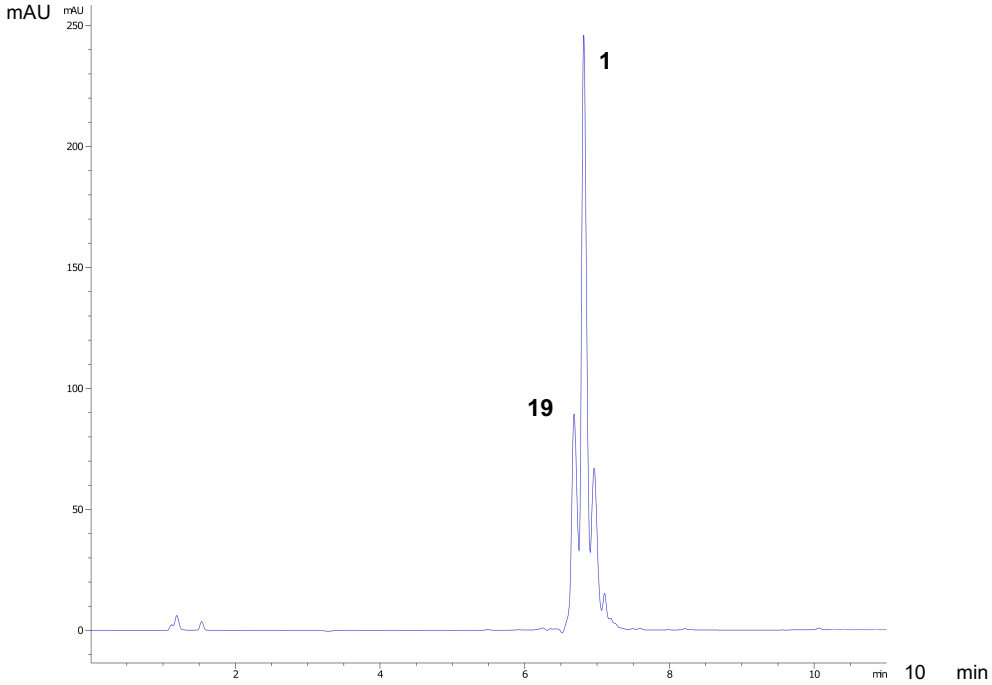

Figure S24. Analytical HPLC spectrum showing the production of **19** from **1** in 20% conversion at 45°C.

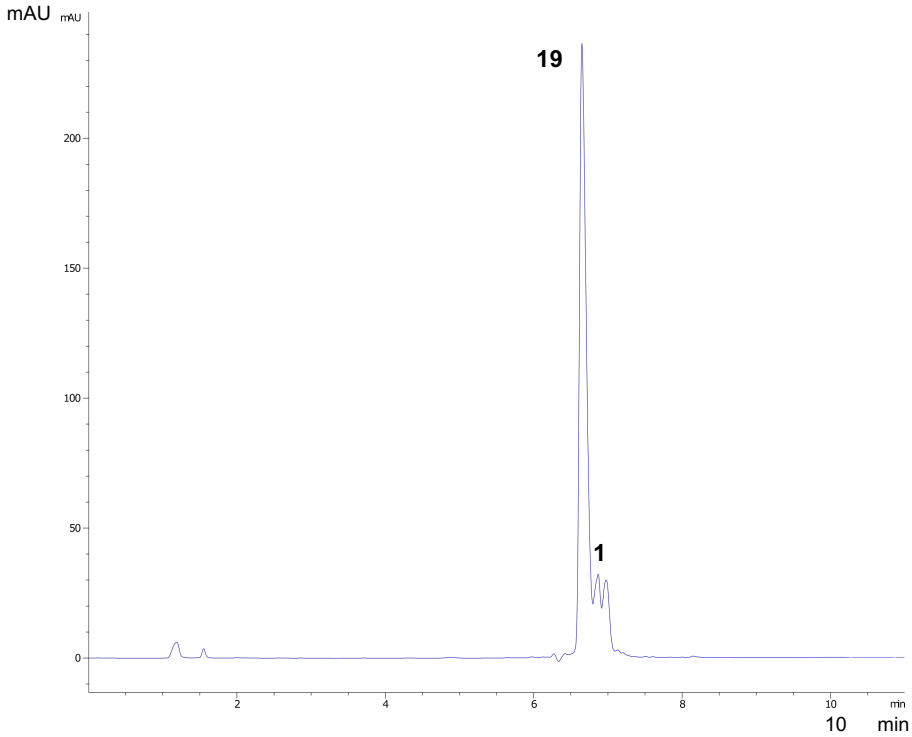

Figure S25. Analytical HPLC spectrum showing the production of **19** from **1** in 91% conversion at -20°C.

To further investigate the effect of temperature on the amidophosphorylation, phosphopeptide **3** was selected as substrate for reactions in a similar procedure as for phosphopeptide **1**. The concentration of DAP, magnesium chloride and imidazole were set at 30 mM, 10 mM and 10 mM, respectively in all cases. When the concentration of **3** was 1 mM, the amidophosphorylated product **21** was obtained in 25%, 93%, 23% conversion at room temperature, -20°C and 45°C, respectively. When the concentration of **3** was increased from 1 mM to 4 mM, **21** was obtained in improved conversions of 37% and 36% at room temperature and 45°C, respectively (Figure S26-S30). These results suggest that the high conversion observed at -20°C could be the result of eutectic freezing increasing the concentration beyond the normal increase of concentration at room temperature. The freeze concentration[3] of substrates at -20°C can be very high, thus giving greatly improved conversions.

The reactions of **3** starting in 1 mM at different temperature was monitored by ^{31}P NMR. DAP displayed a much slower hydrolysis rate at -20°C than at room temperature and 45°C. In fact, at 45°C no DAP was remaining following the reaction period and was hydrolyzed into orthophosphate and trimetaphosphate (Figure S31). These results indicated that the slower hydrolysis rate of DAP is also responsible for the higher conversions observed at -20°C.

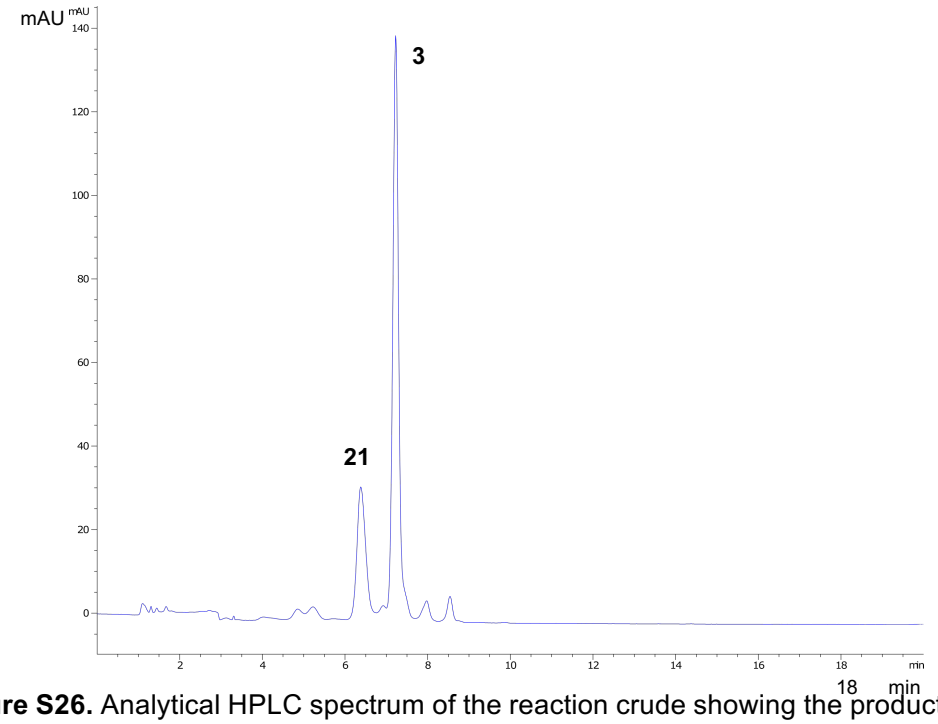

Figure S26. Analytical HPLC spectrum of the reaction crude showing the production of **21** from **3** (1 mM) in 25% conversion at room temperature in Method E.

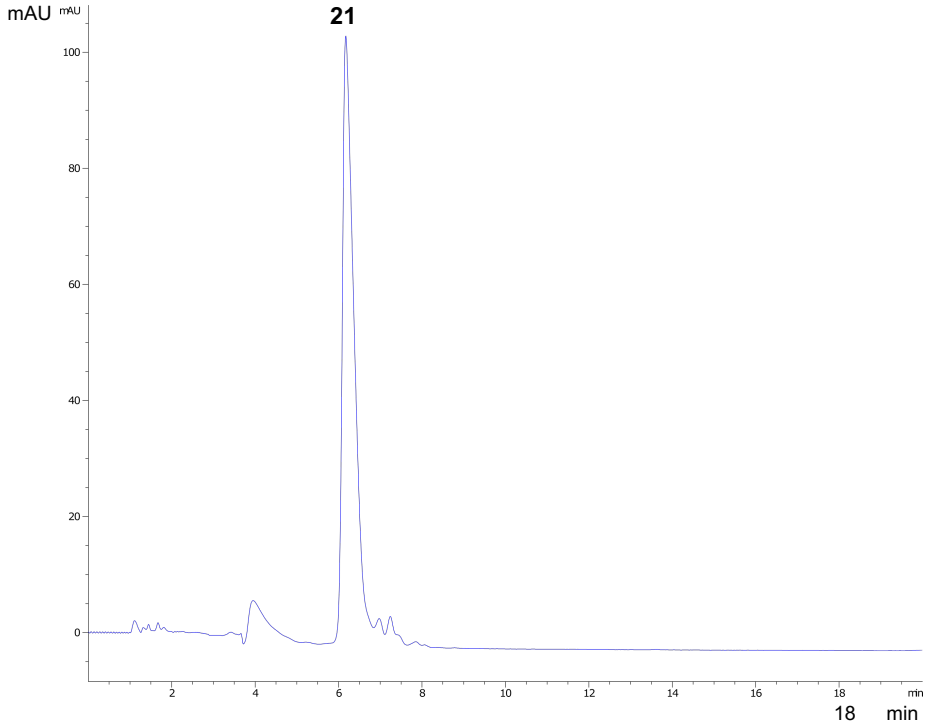

Figure S27. Analytical HPLC spectrum of the reaction crude showing the production of **21** from **3** (1 mM) in 93% conversion at -20°C in Method E.

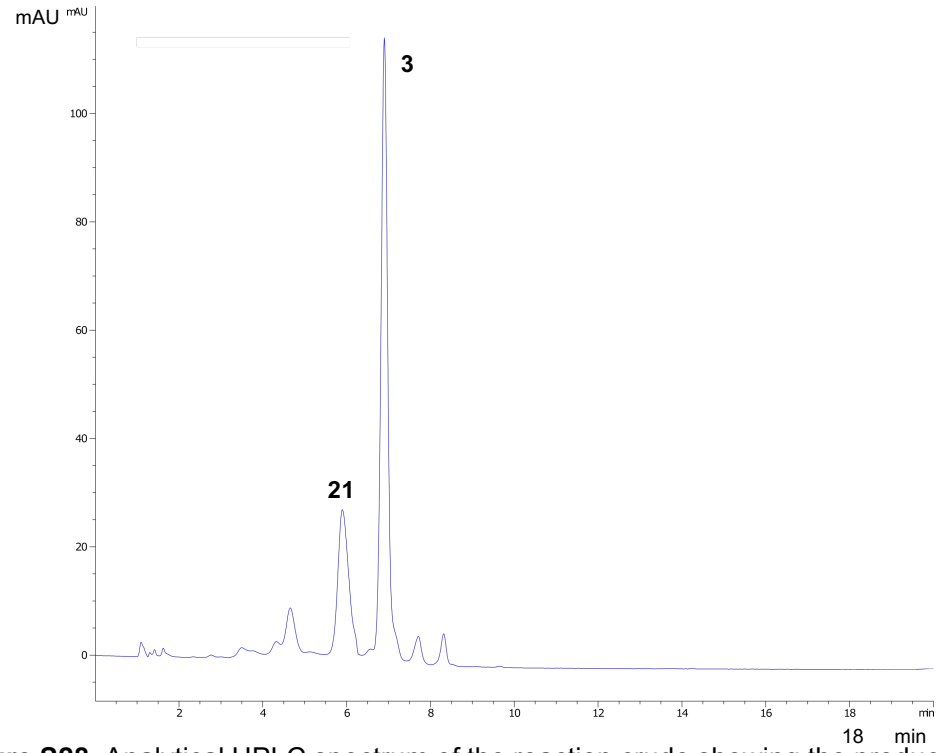

Figure S28. Analytical HPLC spectrum of the reaction crude showing the production of **21** from **3** (1 mM) in 23% conversion at 45°C in Method E.

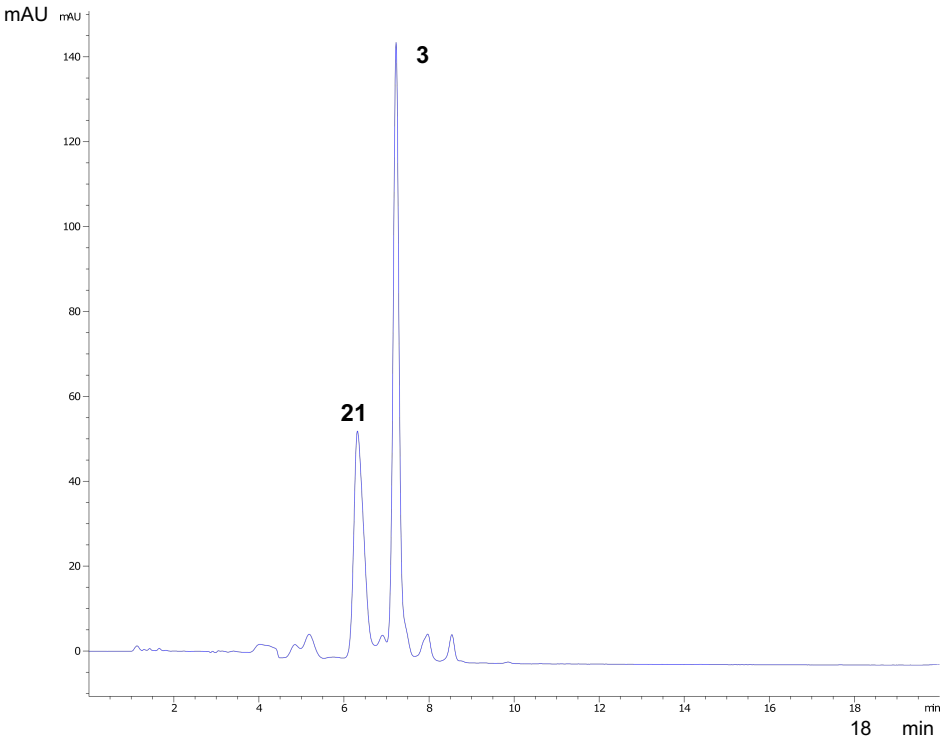

Figure S29. Analytical HPLC spectrum of the reaction crude showing the production of **21** from **3** (4 mM) in 37% conversion at room temperature in Method E.

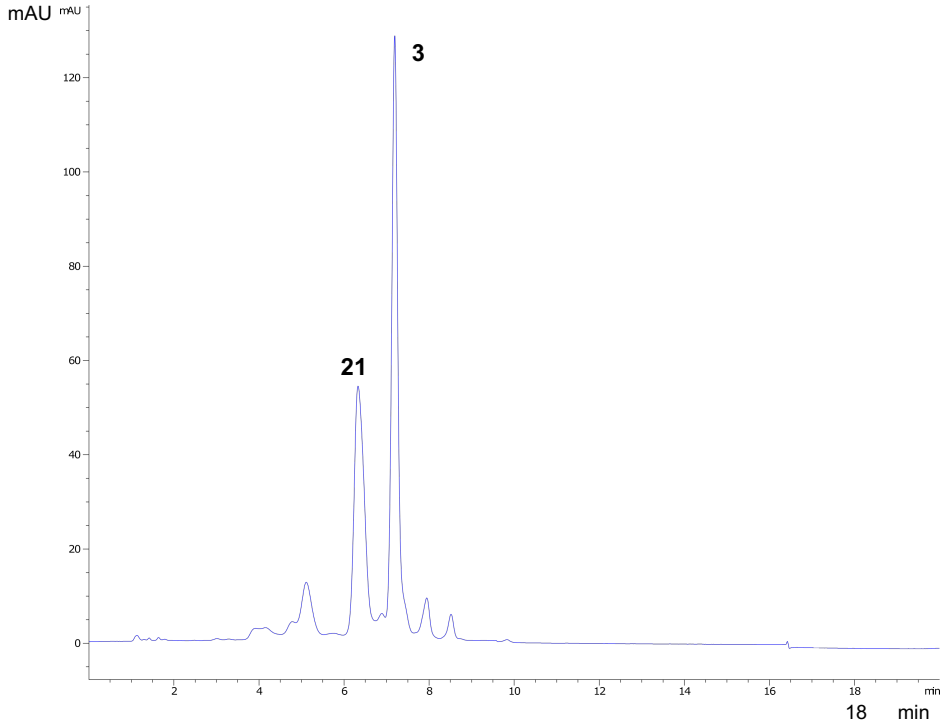

Figure S30. Analytical HPLC spectrum of the reaction crude showing the production of **21** from **3** (4 mM) in 36% conversion at 45°C in Method E.

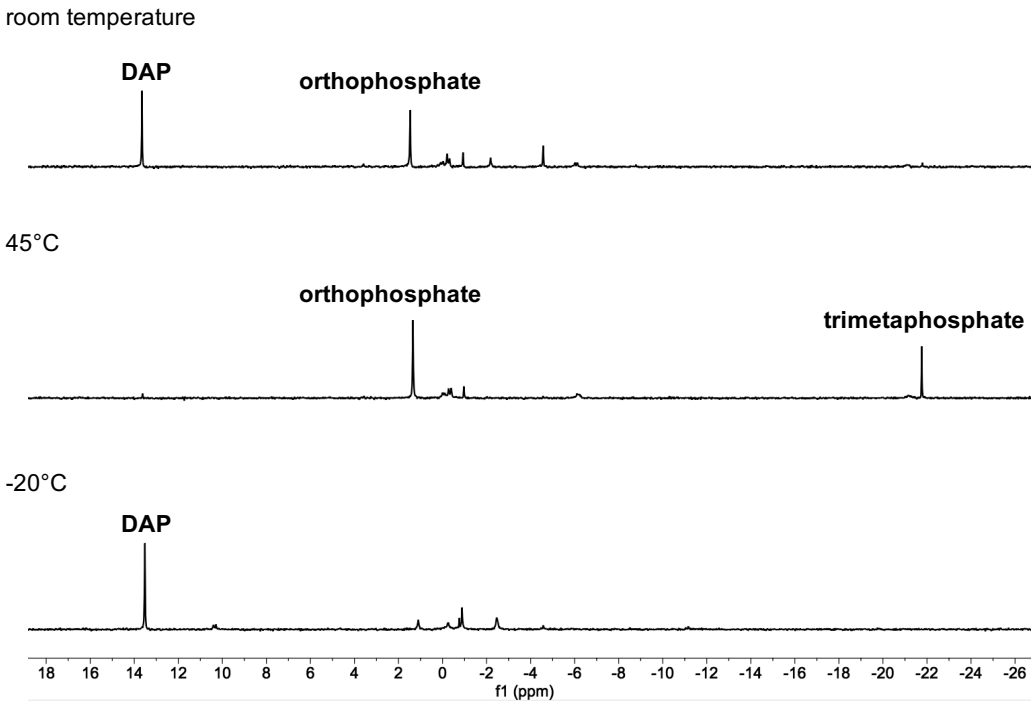

Figure S31. {H-decoupled} ^{31}P NMR spectra of the reaction crude of **3** starting in 1 mM at room temperature, 45°C and -20°C, respectively. It indicated that DAP displayed a much slower hydrolysis rate at -20°C than at room temperature and 45°C.

3.2 Procedure of pyrophosphorylation

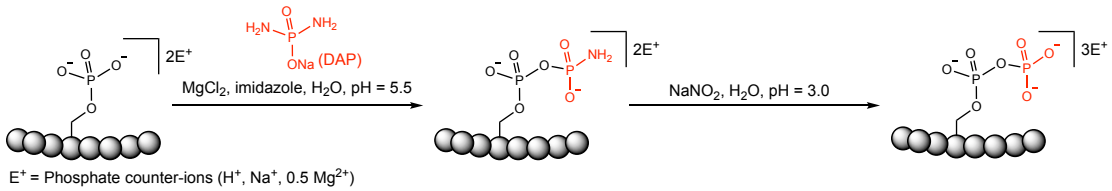

Figure S32. Synthesis of pyrophosphopeptides from respective phosphopeptides via one-pot sequential amidophosphorylation-hydrolysis scenario in water.

To a vial containing 1 mM of phosphopeptide (1 equiv.) in 400 ul H_2O, was added DAP (5 equiv.), magnesium chloride (2 equiv.) and imidazole (2 equiv.). The pH of the reaction mixture was adjusted to 5.5 with hydrochloric acid. The reactions were kept at -20°C in freezer. Progress of the amidophosphorylation reaction was monitored by LC-MS. After 2-3 days without further purification, sodium nitrite (5 equiv.) was added into the same-pot reaction mixture. The pH of the reaction mixture was adjusted to 3.0 with hydrochloric acid. The reactions were kept at -20°C for 20 hours. Progress of the hydrolysis was monitored by LC-MS. The conversion of amidopyrophosphopeptide and final pyrophosphopeptide were determined based on the area-under-the-curve at 280 nm by analytical HPLC.

For phosphopeptide **5** containing cysteine residue, sodium nitrite (8 equiv.) was added into the same-pot reaction mixture after the completion in the first step. After the hydrolysis, excess 4-mercaptophenylacetic acid (MPAA) was added to convert the nitrothioite peptide back to the desired pyrophosphopeptide **38** with the original thiol.

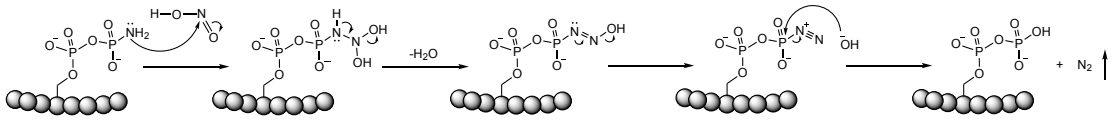

Figure S33. The mechanism of pyrophosphopeptide formation via nitrous acid induced hydrolysis from respective amidopyrophosphopeptide. The mechanism was given according to the reference.[4]

3.3 Liquid chromatography-mass spectrometry (LC-MS)

Synthesis and analytical data for model amidopyrophosphopeptide **19**

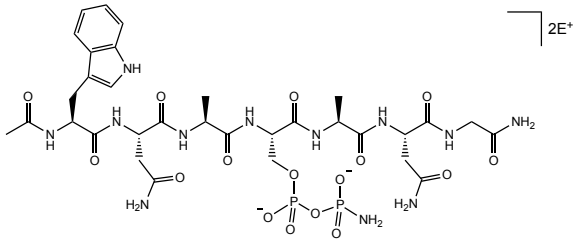

E^+ = Phosphate counter-ions (H^+, Na^+, 0.5 Mg^{2+})

Amidopyrophosphopeptide **19** was synthesized from **1** with the representative protocol using DAP, magnesium chloride and imidazole in 86% conversion indicated by HPLC and used for the next step without any further purification.

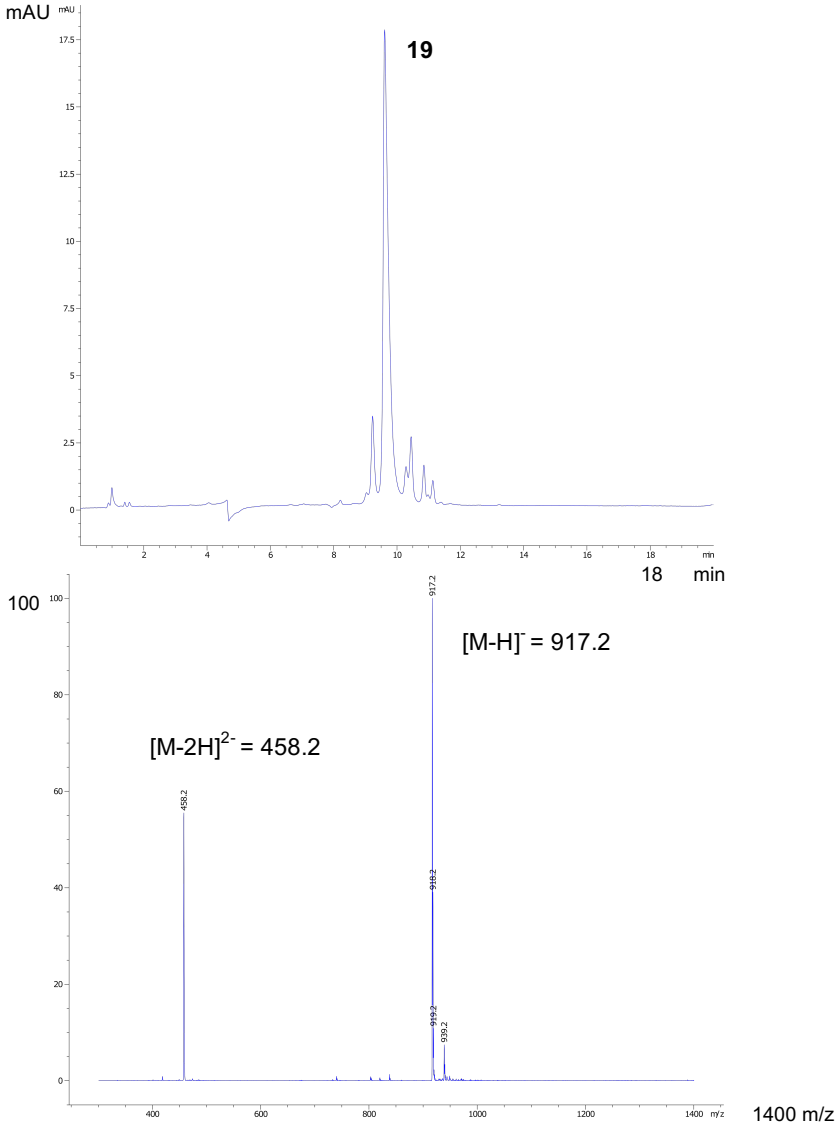

Figure S34. Analytical HPLC-MS spectra showing the production of **19** from **1** in Method A. Calculated mass $[M-H]^-$: 917.3, observed mass $[M-H]^-$: 917.2; Calculated mass $[M-2H]^{2-}$: 458.1, observed mass $[M-2H]^{2-}$: 458.2.

Synthesis and analytical data for model pyrophosphopeptide **35**

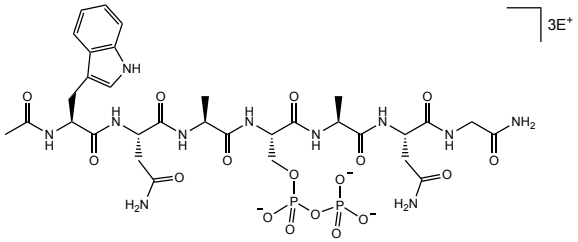

E^+ = Phosphate counter-ions (H^+, Na^+, 0.5 Mg^{2+})

Pyrophosphopeptide **35** was synthesized from **19** following the representative protocol using sodium nitrite in the same pot in 85% conversion over two steps indicated by HPLC.

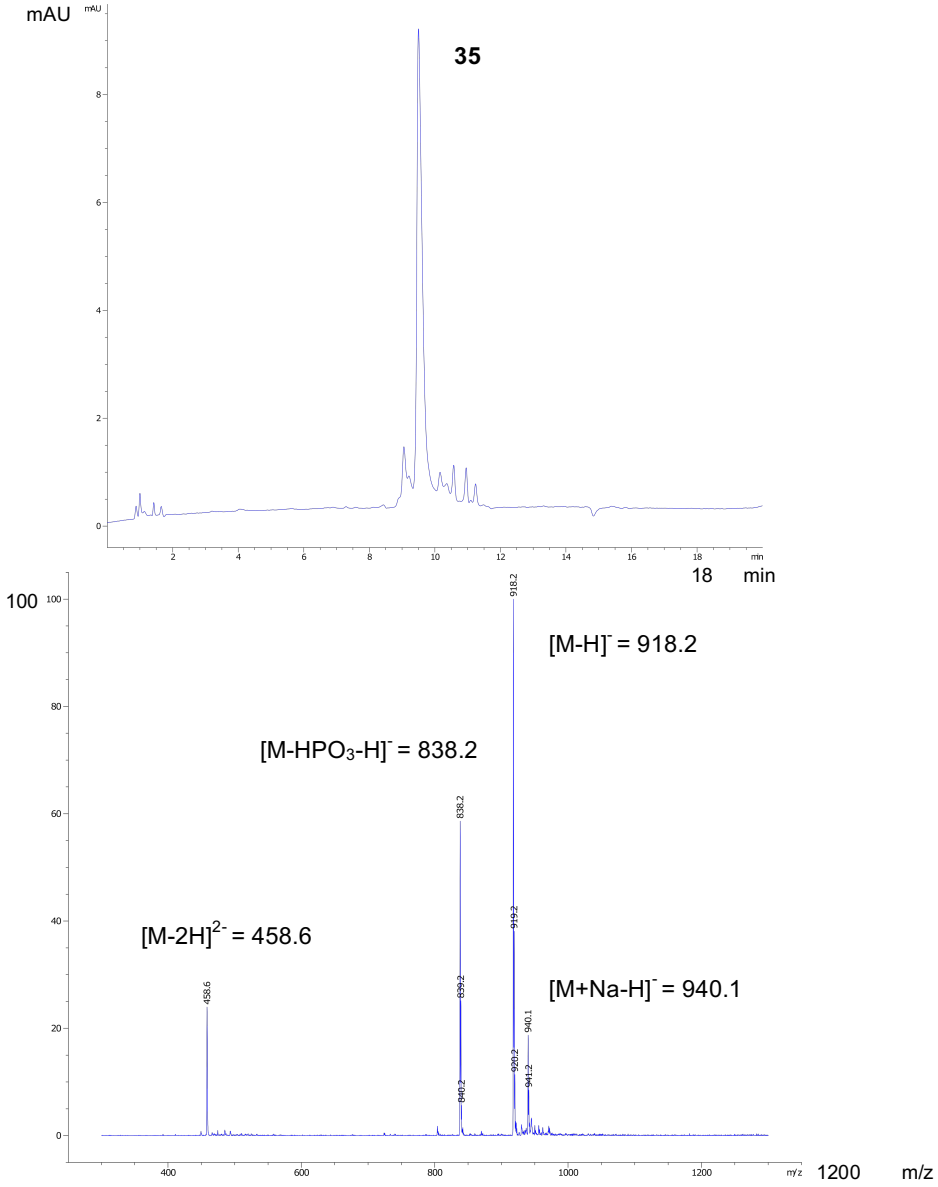

Figure S35. Analytical HPLC-MS spectra showing the production of **35** from **19** in Method A. Calculated mass $[M-H]^-$: 918.3, observed mass $[M-H]^-$: 918.2; Calculated mass $[M-2H]^{2-}$: 458.6, observed mass $[M-2H]^{2-}$: 458.6.

Synthesis and analytical data for model amidopyrophosphopeptide **20**

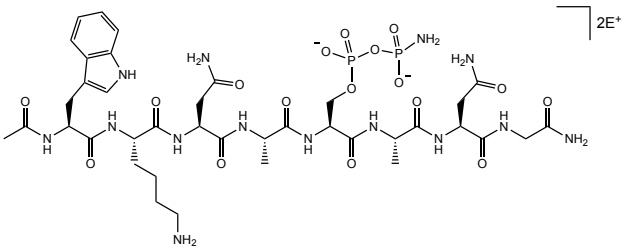

E^+ = Phosphate counter-ions (H^+, Na^+, 0.5 Mg^{2+})

Amidopyrophosphopeptide **20** was synthesized from **2** with the representative protocol using DAP, magnesium chloride and imidazole in 96% conversion indicated by HPLC and used for the next step without any further purification.

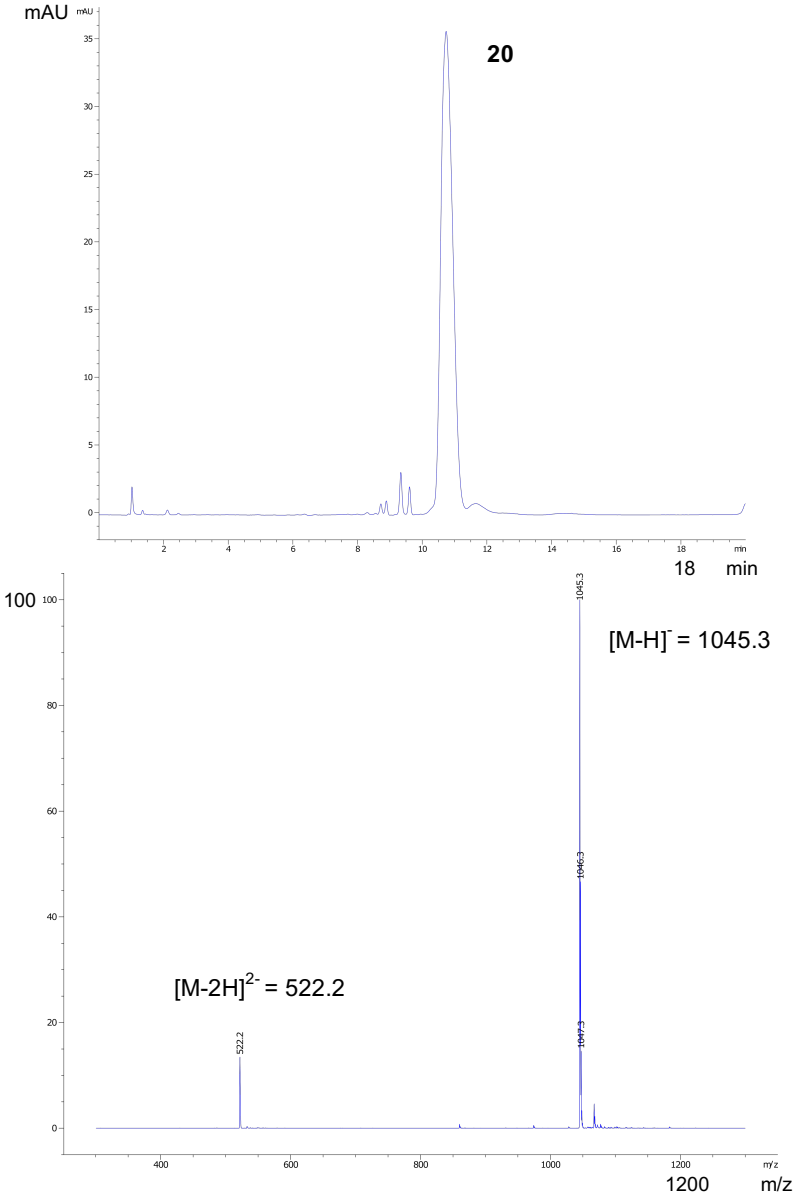

Figure S36. Analytical HPLC-MS spectra showing the production of **20** from **2** in Method A. Calculated mass $[M-H]^-$: 1045.4, observed mass $[M-H]^-$: 1045.3; Calculated mass $[M-2H]^{2-}$: 522.2, observed mass $[M-2H]^{2-}$: 522.2.

Synthesis and analytical data for model pyrophosphopeptide **36**

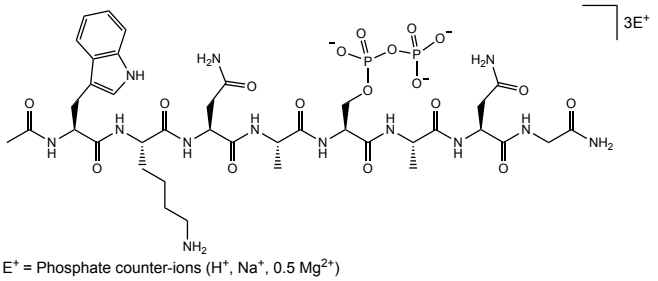

E^+ = Phosphate counter-ions (H^+, Na^+, 0.5 Mg^{2+})

Pyrophosphopeptide **36** was synthesized from **20** following the representative protocol using sodium nitrite in the same pot in 95% conversion over two steps indicated by HPLC.

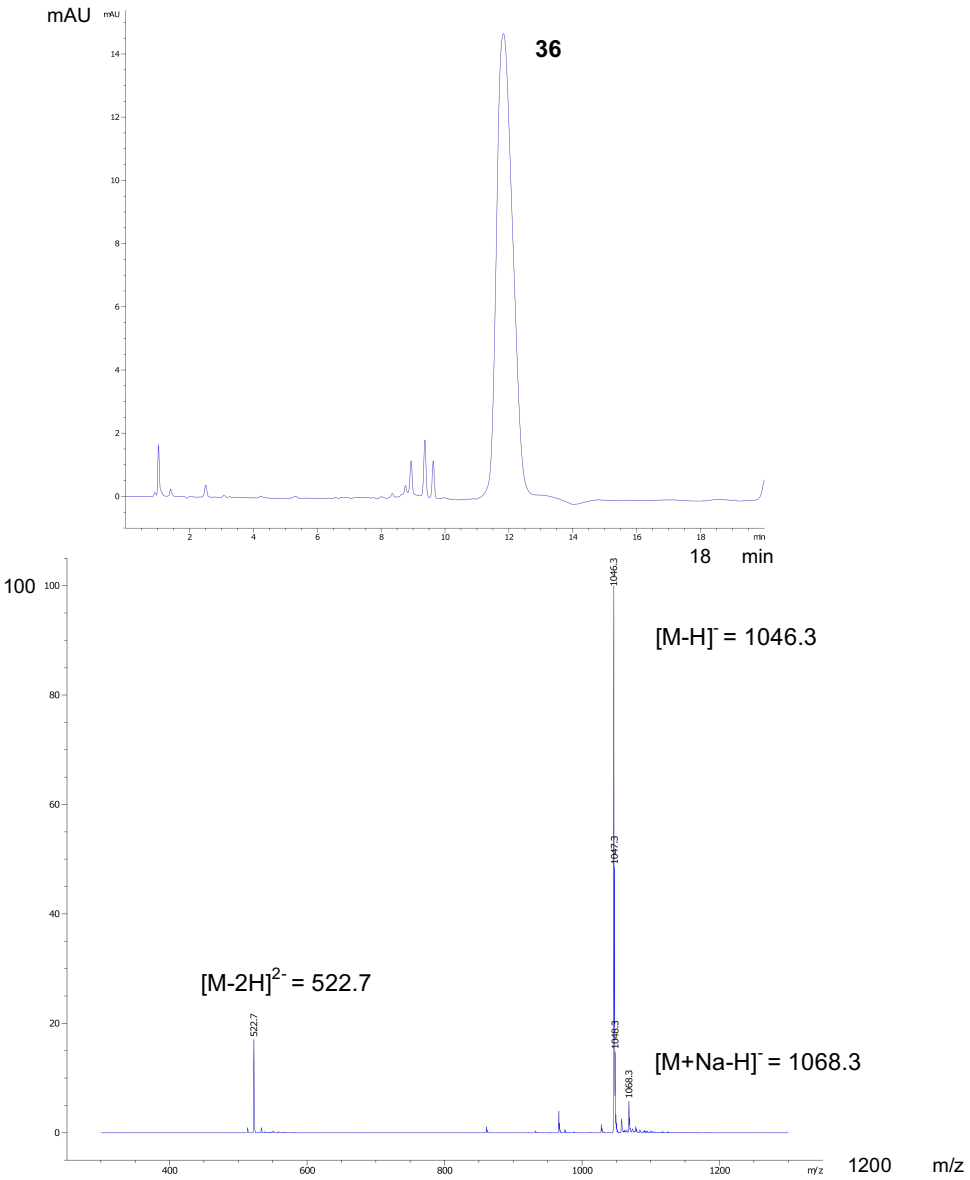

Figure S37. Analytical HPLC-MS spectra showing the production of **36** from **20** in Method A. Calculated mass $[M-H]^-$: 1046.4, observed mass $[M-H]^-$: 1046.3; Calculated mass $[M-2H]^{2-}$: 522.7, observed mass $[M-2H]^{2-}$: 522.7.

Synthesis and analytical data for model amidopyrophosphopeptide **21**

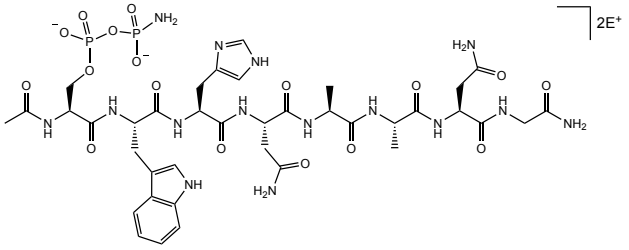

Amidopyrophosphopeptide **21** was synthesized from **3** with the representative protocol using DAP, magnesium chloride and imidazole in 97% conversion indicated by HPLC and used for the next step without any further purification.

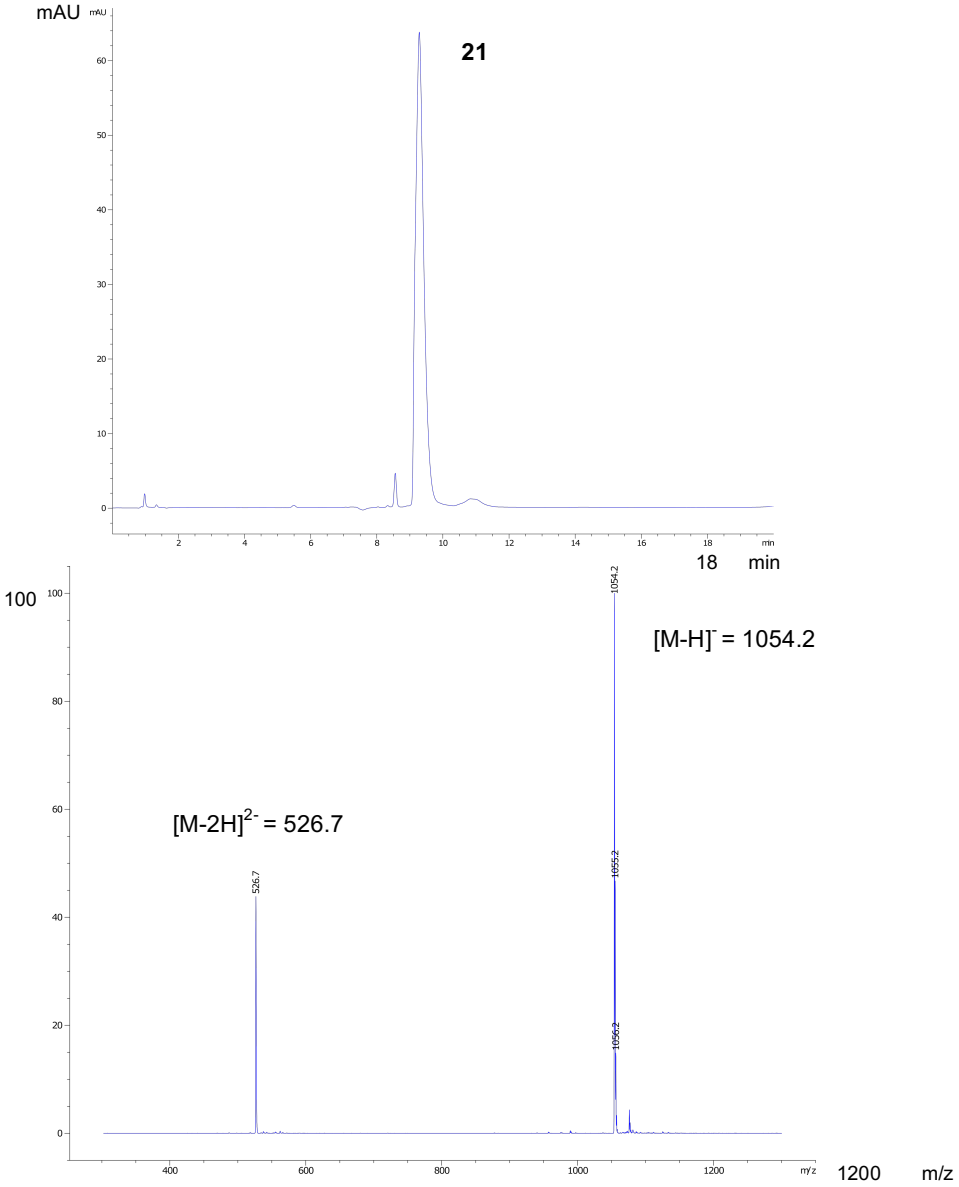

Figure S38. Analytical HPLC-MS spectra showing the production of **21** from **3** in Method A. Calculated mass $[M-H]^-$: 1054.3, observed mass $[M-H]^-$: 1054.2; Calculated mass $[M-2H]^{2-}$: 526.7, observed mass $[M-2H]^{2-}$: 526.7.

Synthesis and analytical data for model pyrophosphopeptide **37**

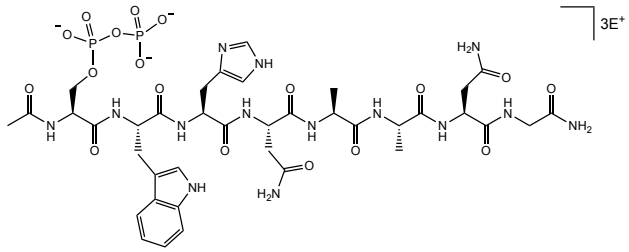

Pyrophosphopeptide **37** was synthesized from **21** following the representative protocol using sodium nitrite in the same pot in 96% conversion over two steps indicated by HPLC.

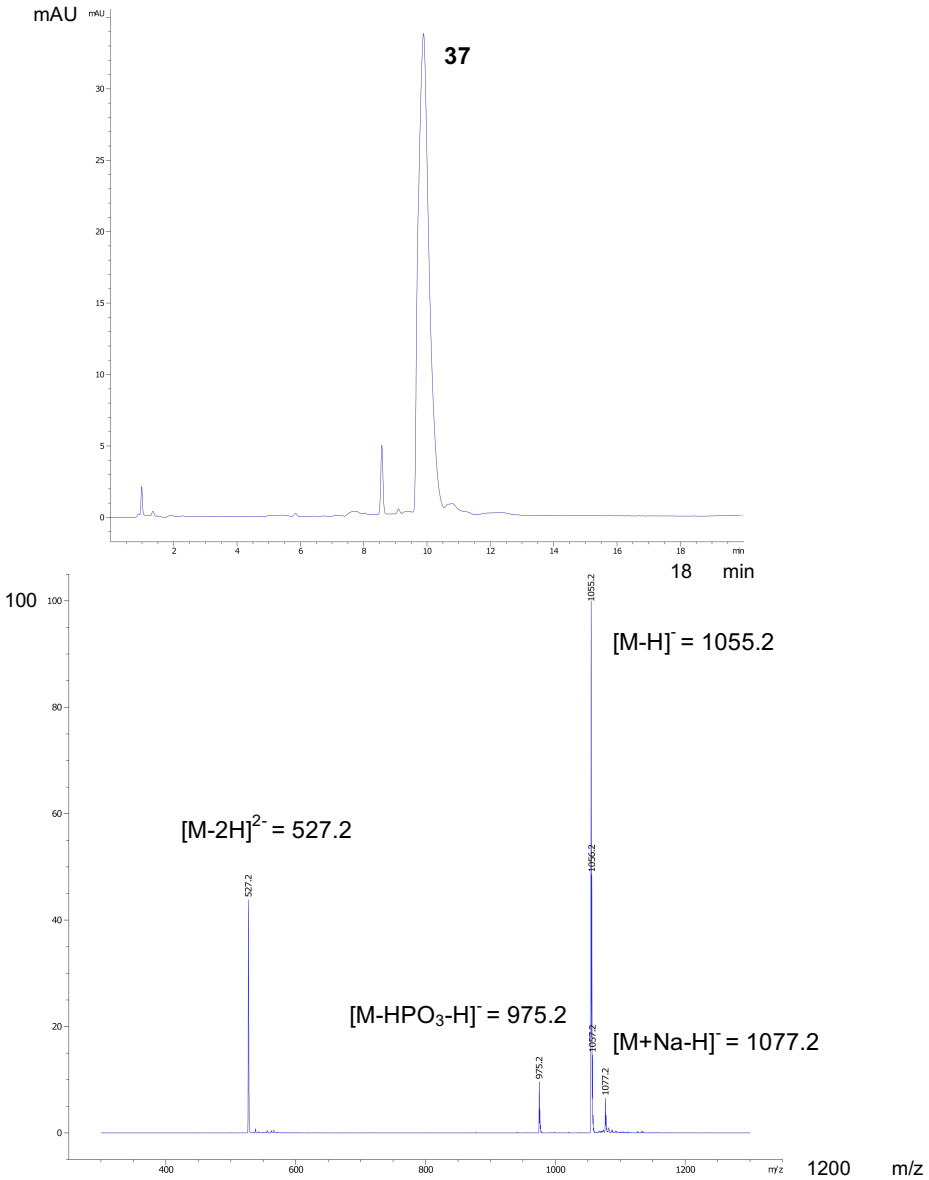

Figure S39. Analytical HPLC-MS spectra showing the production of **37** from **21** in Method A. Calculated mass $[M-H]^-$: 1055.3, observed mass $[M-H]^-$: 1055.2; Calculated mass $[M-2H]^{2-}$: 527.2, observed mass $[M-2H]^{2-}$: 527.2.

Analytical data for the control reaction with model peptide **4**

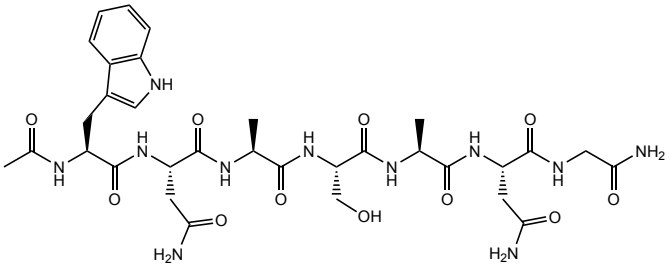

The control reaction of peptide **4** (lacking phosphoserine residue) was set up following the representative protocol using DAP, magnesium chloride and imidazole. No amidophosphorylation was observed indicated by HPLC.

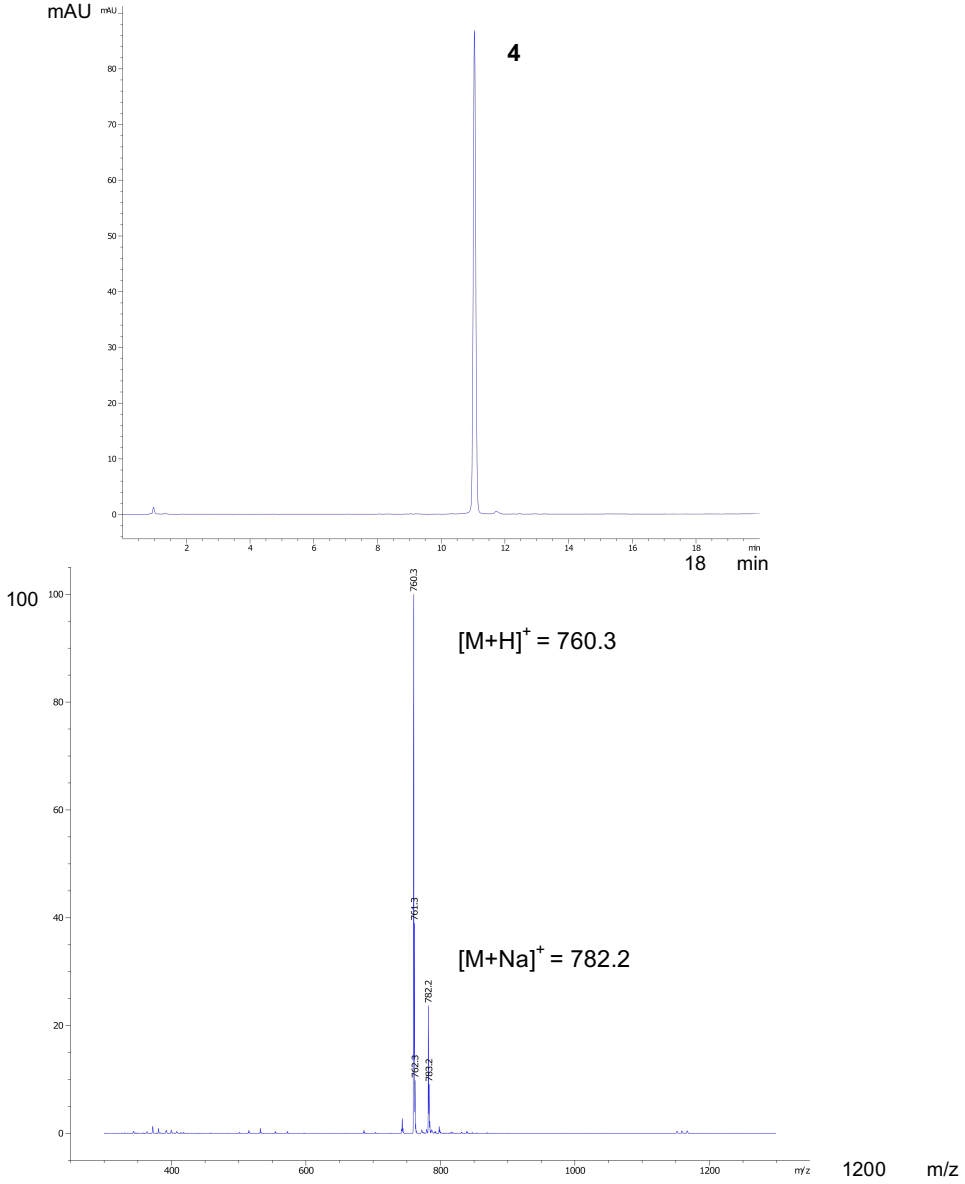

Figure S40. Analytical HPLC-MS spectra showing no amidophosphorylation of **4** in Method A. Calculated mass $[M+H]^+$: 760.3, observed mass $[M+H]^+$: 760.3; Calculated mass $[M+Na]^+$: 782.3, observed mass $[M+Na]^+$: 782.2.

Synthesis and analytical data for model amidopyrophosphopeptide **22**

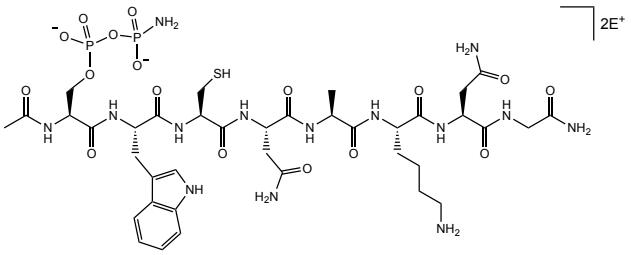

Amidopyrophosphopeptide **22** was synthesized from **5** with the representative protocol using DAP, magnesium chloride and imidazole in 95% conversion indicated by HPLC and used for the next step without any further purification.

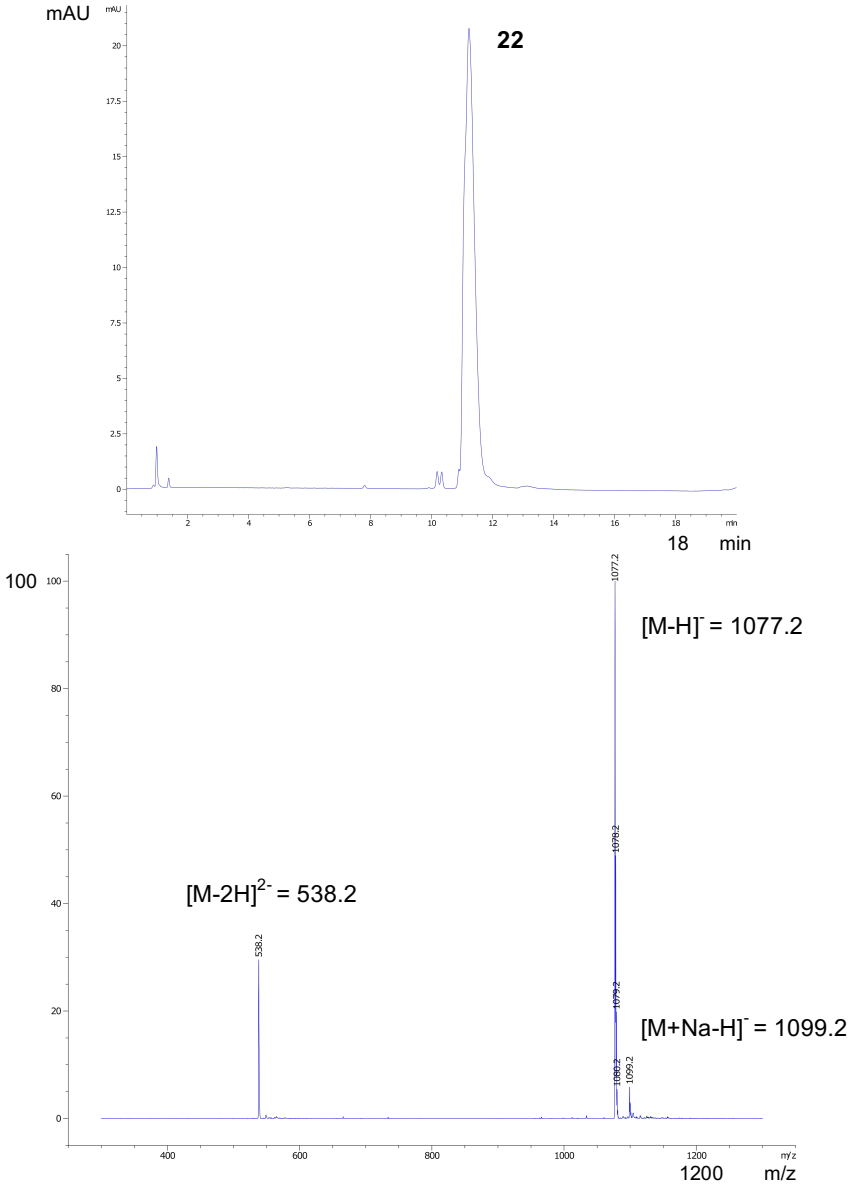

Figure S41. Analytical HPLC-MS spectra showing the production of **22** from **5** in Method A. Calculated mass $[M-H]^-$: 1077.3, observed mass $[M-H]^-$: 1077.2; Calculated mass $[M-2H]^{2-}$: 538.2, observed mass $[M-2H]^{2-}$: 538.2.

Synthesis and analytical data for model pyrophosphopeptide **38**

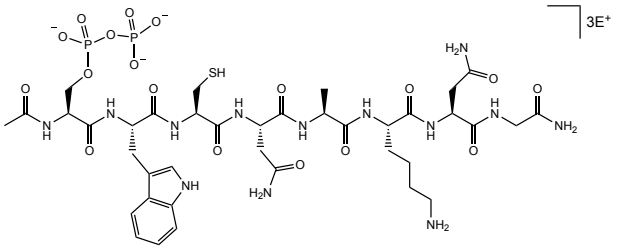

E^+ = Phosphate counter-ions (H^+, Na^+, 0.5 Mg^{2+})

Pyrophosphopeptide **38** was synthesized from **22** following the general protocol using sodium nitrite and MPAA in the same pot in 66% conversion over three steps indicated by HPLC. After the hydrolysis, the nitrothioite peptide with the pyrophosphate group was observed as the major product from oxidation of the thiol group by HNO_2. The desired **38** with the original thiol was formed from reduction of nitrothioite at pH 7.0 by the addition of excess MPAA.

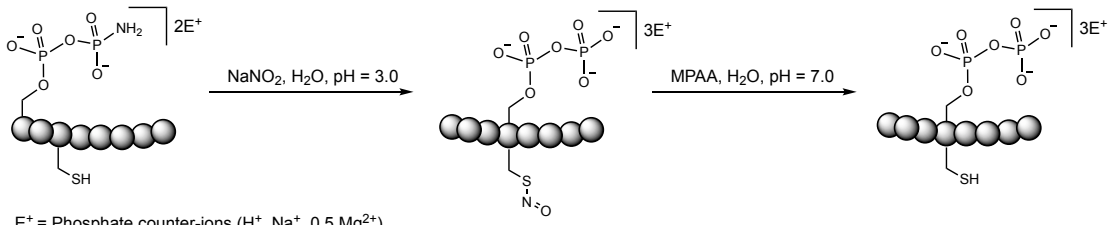

Figure S42. Synthesis of pyrophosphopeptide **38** containing the original thiol group from amidopyrophosphopeptide **22** via hydrolysis and reduction.

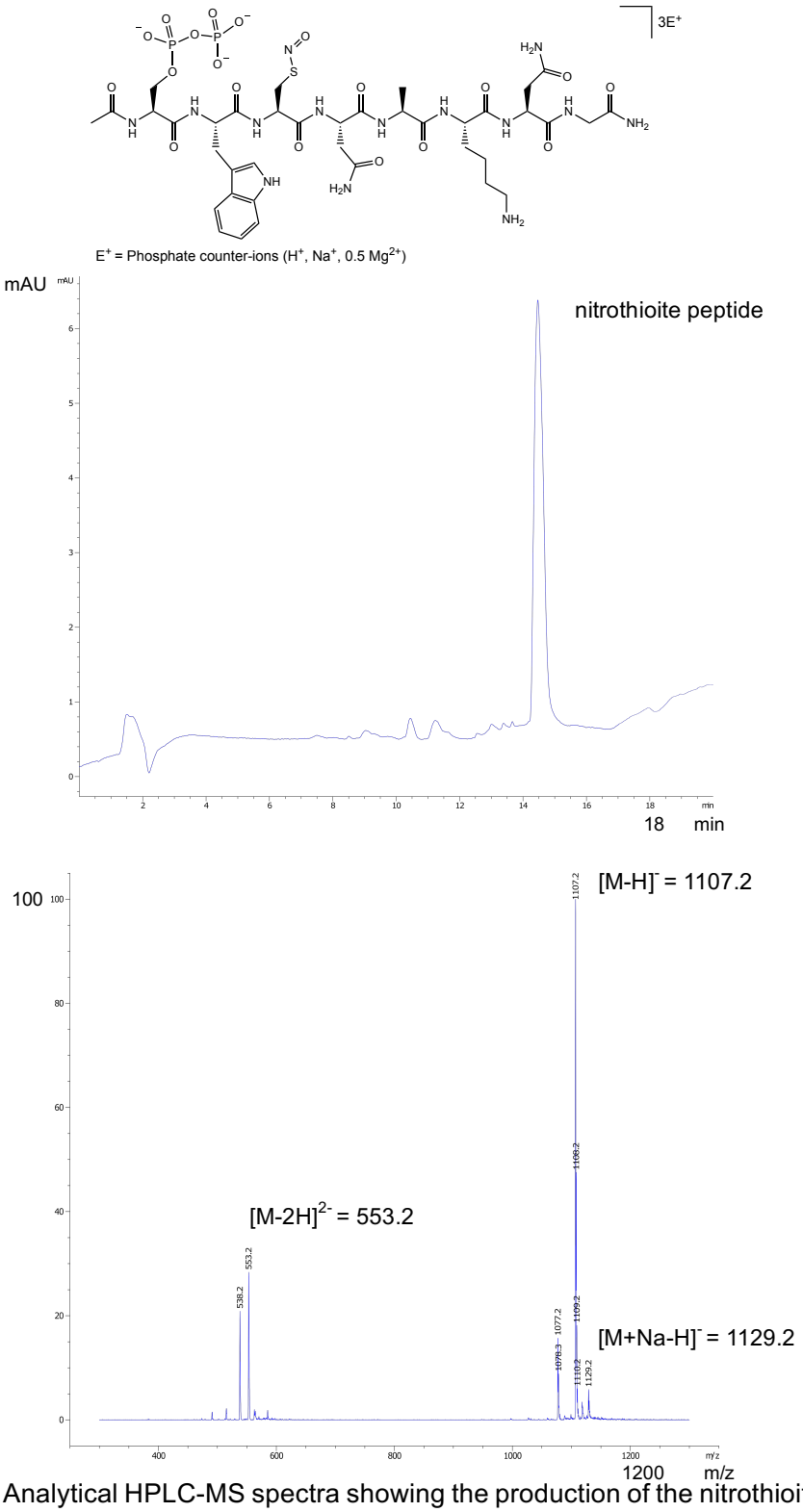

Figure S43. Analytical HPLC-MS spectra showing the production of the nitrothioite peptide from **22** in Method A. Calculated mass $[M-H]^-$: 1107.3, observed mass $[M-H]^-$: 1107.2; Calculated mass $[M-2H]^{2-}$: 553.2, observed mass $[M-2H]^{2-}$: 553.2.

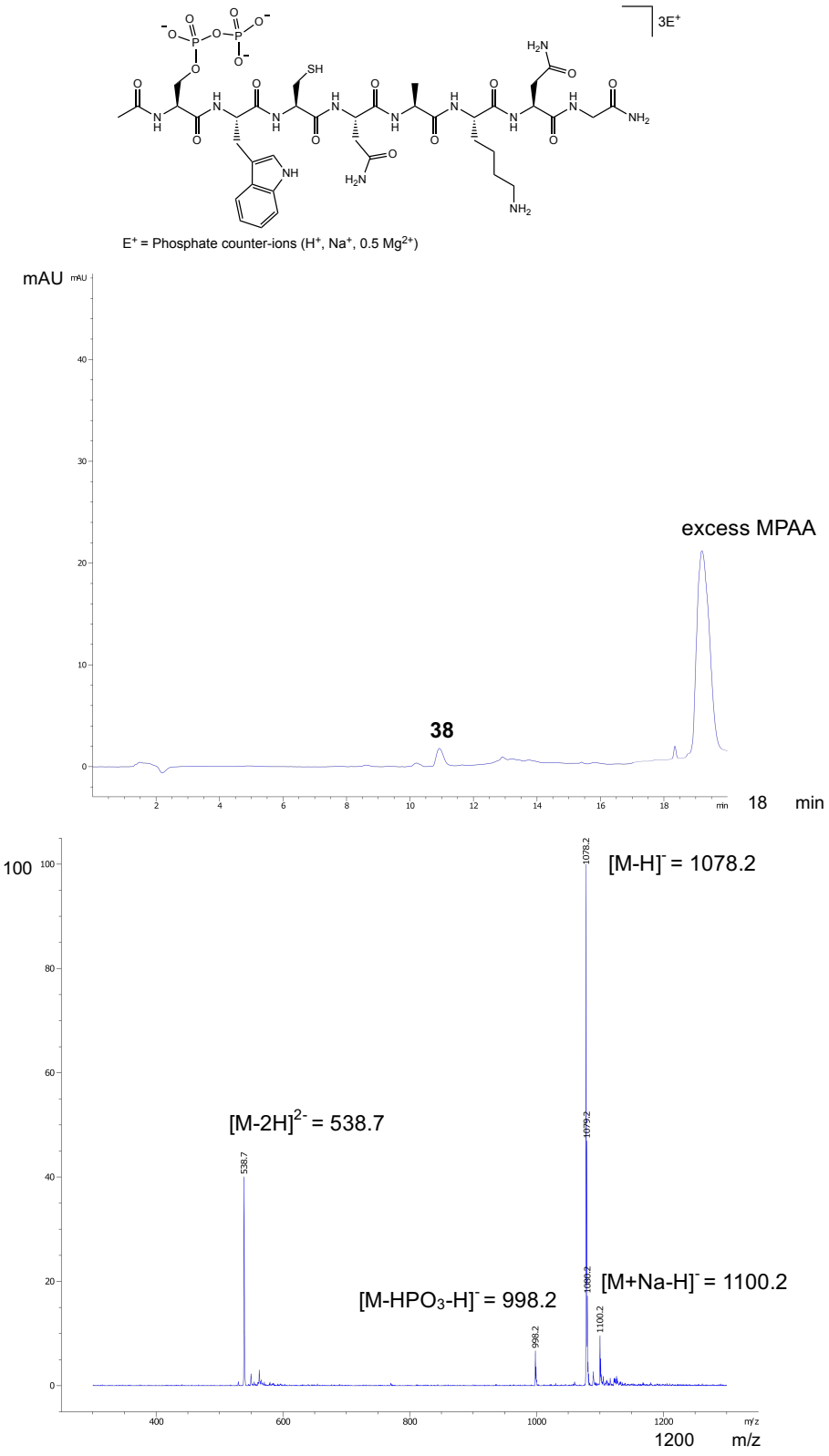

Figure S44. Analytical HPLC-MS spectra showing the production of **38** from the nitrothioite peptide in Method A. Calculated mass $[M-H]^-$: 1078.3, observed mass $[M-H]^-$: 1078.2; Calculated mass $[M-2H]^{2-}$: 538.7, observed mass $[M-2H]^{2-}$: 538.7.

Analytical data for the control reaction with model peptide **6**

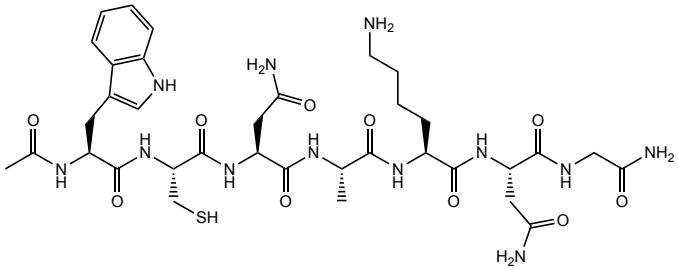

The control reaction of peptide **6** (lacking phosphoserine residue) was set up following the representative protocol using DAP, magnesium chloride and imidazole. No amidophosphorylation was observed indicated by HPLC.

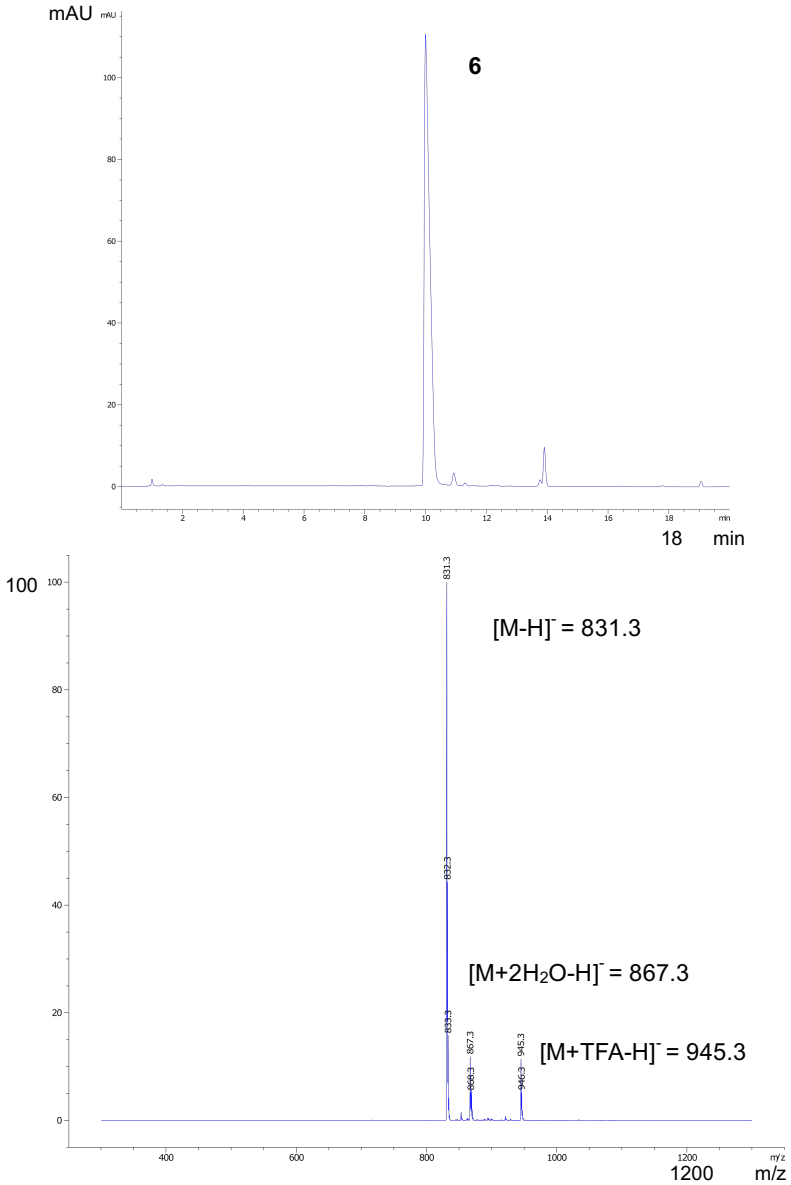

Figure S45. Analytical HPLC-MS spectra showing no amidophosphorylation of **6** in Method A. Calculated mass $[M-H]^-$: 831.4, observed mass $[M-H]^-$: 831.3; Calculated mass $[M+2H_2O-H]^-$: 867.4, observed mass $[M+2H_2O-H]^-$: 867.3.

Synthesis and analytical data for model amidopyrophosphopeptide **23**

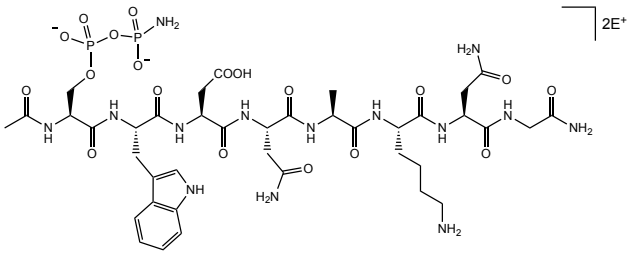

E^+ = Phosphate counter-ions (H^+, Na^+, 0.5 Mg^{2+})

Amidopyrophosphopeptide **23** was synthesized from **7** with the representative protocol using DAP, magnesium chloride and imidazole in 94% conversion indicated by HPLC and used for the next step without any further purification.

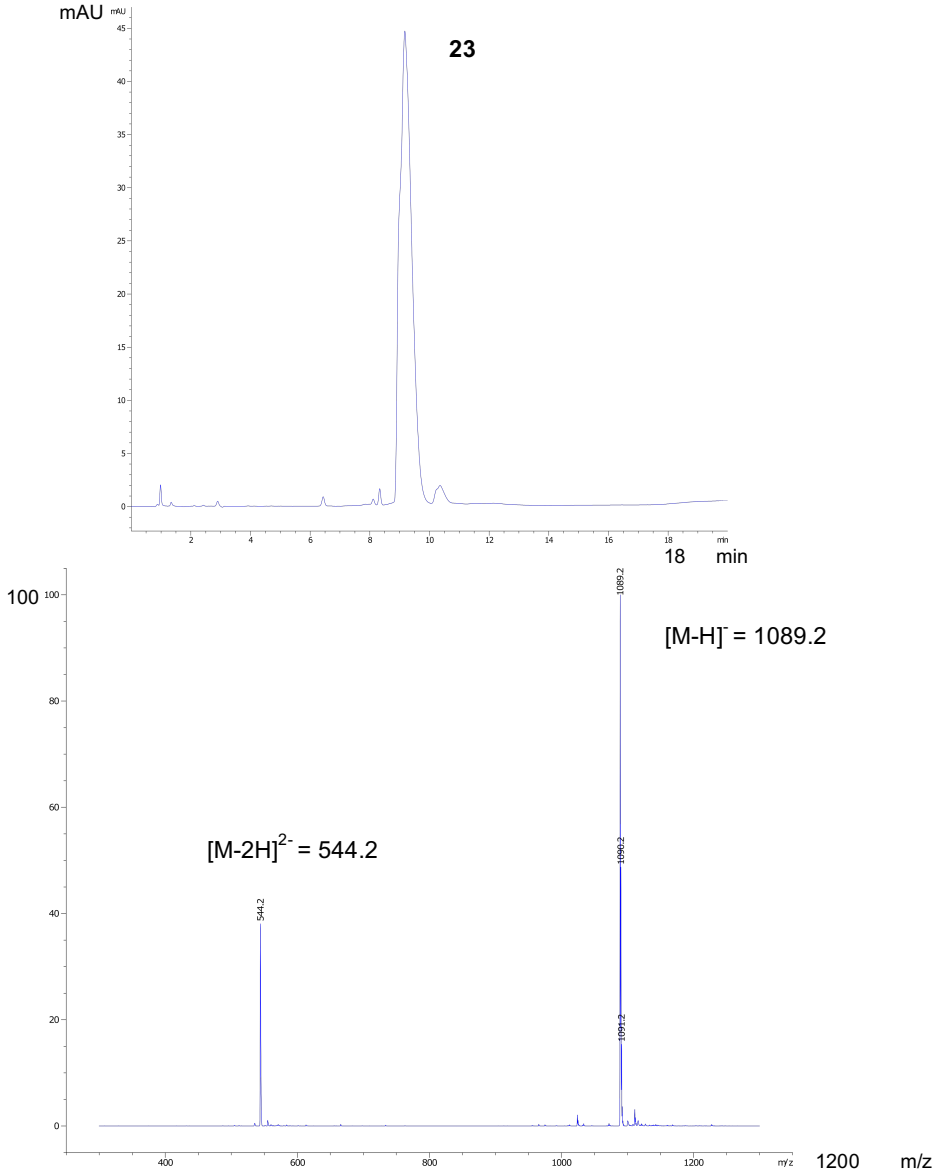

Figure S46. Analytical HPLC-MS spectra showing the production of **23** from **7** in Method A. Calculated mass $[M-H]^-$: 1089.4, observed mass $[M-H]^-$: 1089.2; Calculated mass $[M-2H]^{2-}$: 544.2, observed mass $[M-2H]^{2-}$: 544.2.

Synthesis and analytical data for model pyrophosphopeptide **39**

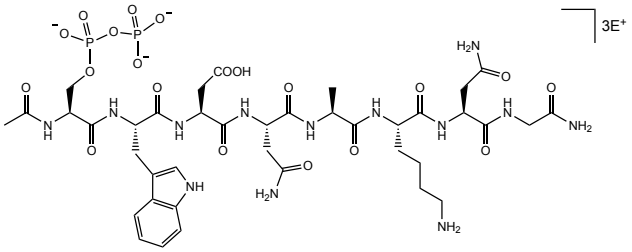

E^+ = Phosphate counter-ions (H^+, Na^+, 0.5 Mg^{2+})

Pyrophosphopeptide **39** was synthesized from **23** following the representative protocol using sodium nitrite in the same pot in 92% conversion over two steps indicated by HPLC.

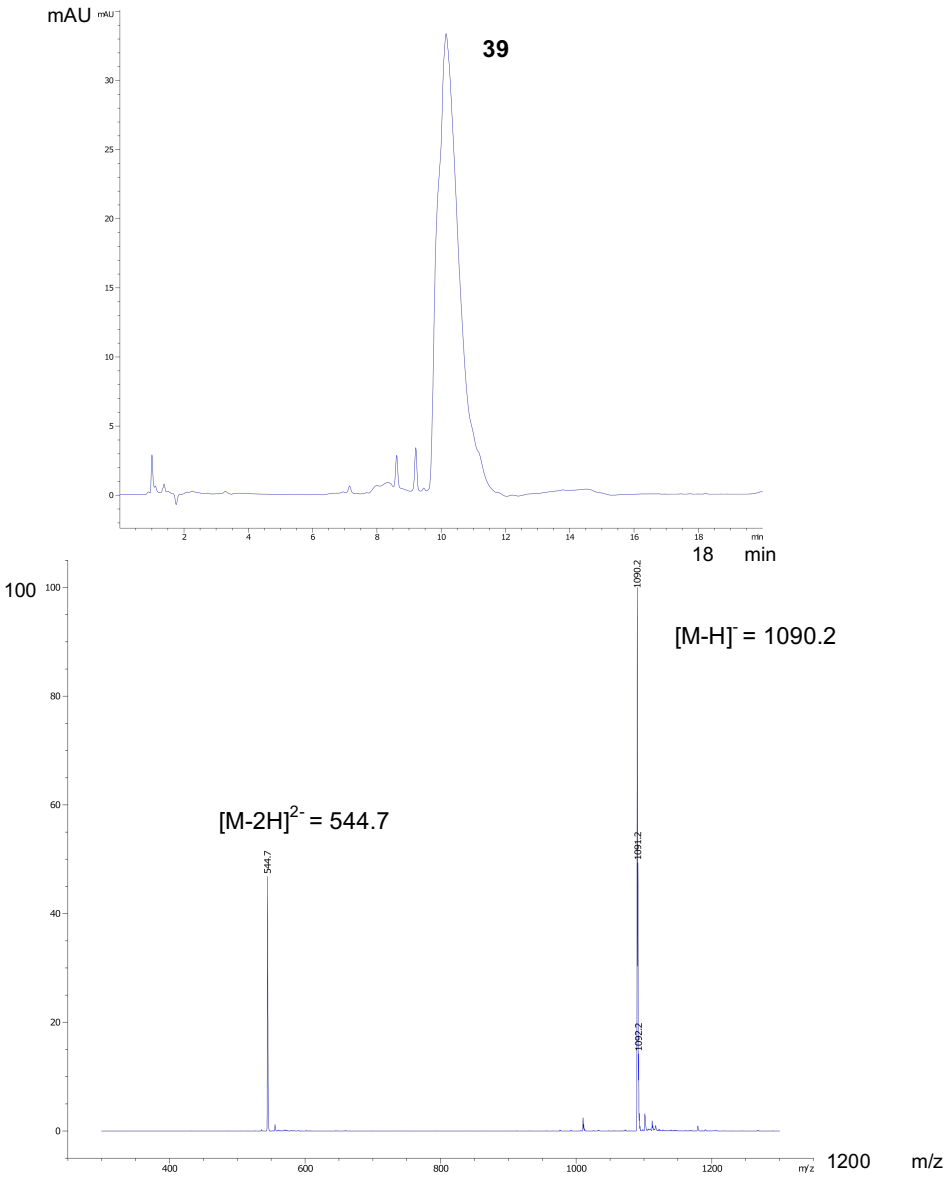

Figure S47. Analytical HPLC-MS spectra showing the production of **39** from **23** in Method A. Calculated mass $[M-H]^-$: 1090.3, observed mass $[M-H]^-$: 1090.2; Calculated mass $[M-2H]^{2-}$: 544.7, observed mass $[M-2H]^{2-}$: 544.7.

Synthesis and analytical data for model amidopyrophosphopeptide **24**

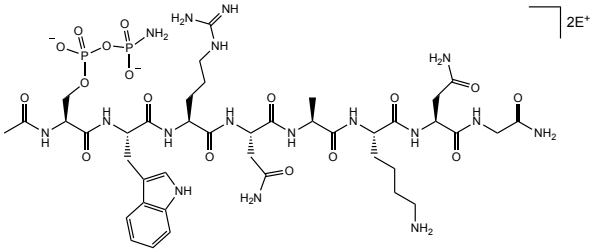

E^+ = Phosphate counter-ions (H^+, Na^+, 0.5 Mg^{2+})

Amidopyrophosphopeptide **24** was synthesized from **8** with the representative protocol using DAP, magnesium chloride and imidazole in 93% conversion indicated by HPLC and used for the next step without any further purification.

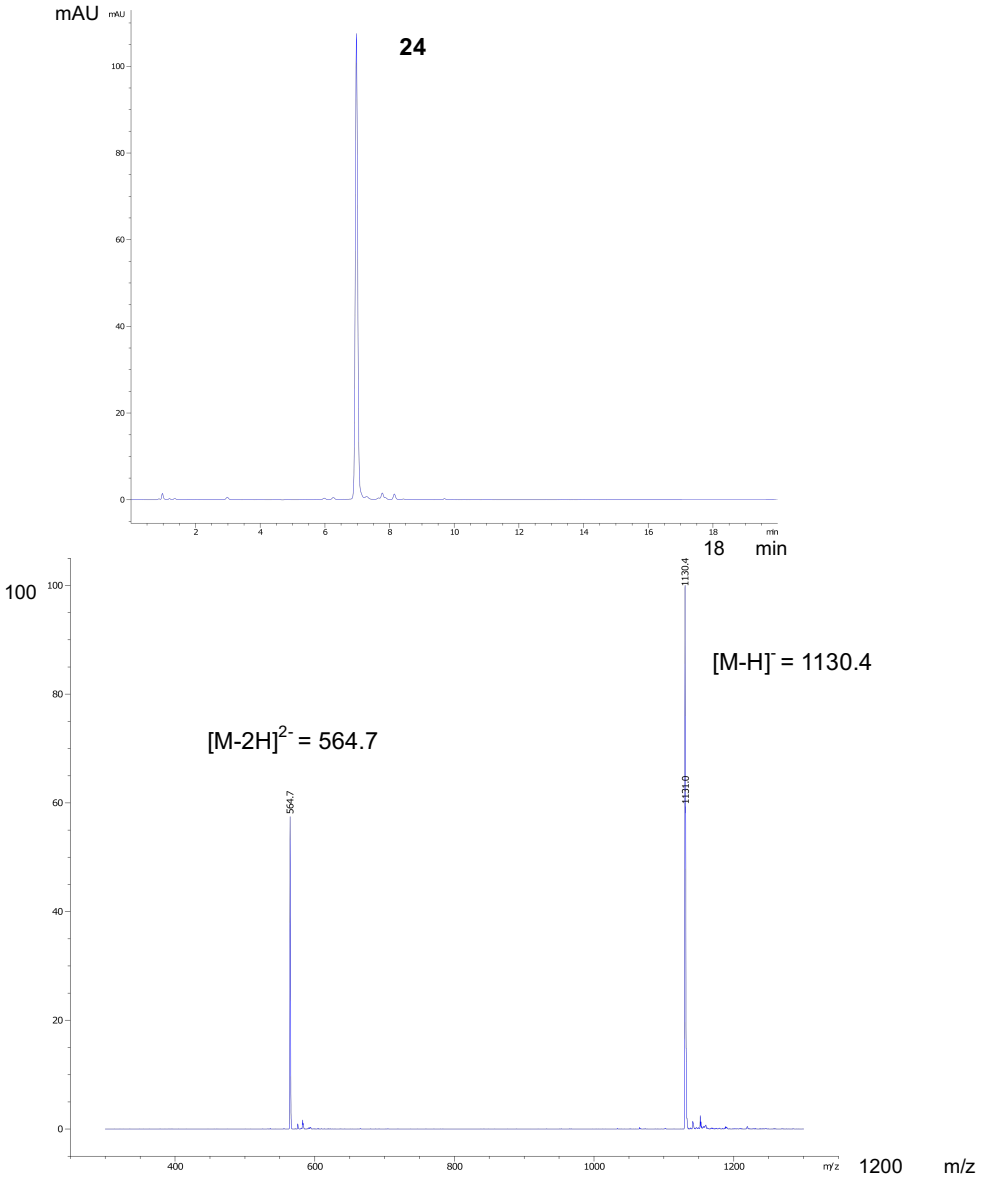

Figure S48. Analytical HPLC-MS spectra showing the production of **24** from **8** in Method A. Calculated mass $[M-H]^-$: 1130.4, observed mass $[M-H]^-$: 1130.4; Calculated mass $[M-2H]^{2-}$: 564.7, observed mass $[M-2H]^{2-}$: 564.7.

Synthesis and analytical data for model pyrophosphopeptide **40**

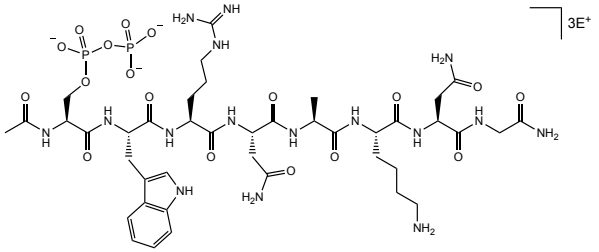

Pyrophosphopeptide **40** was synthesized from **24** following the representative protocol using sodium nitrite in the same pot in 86% conversion over two steps indicated by HPLC.

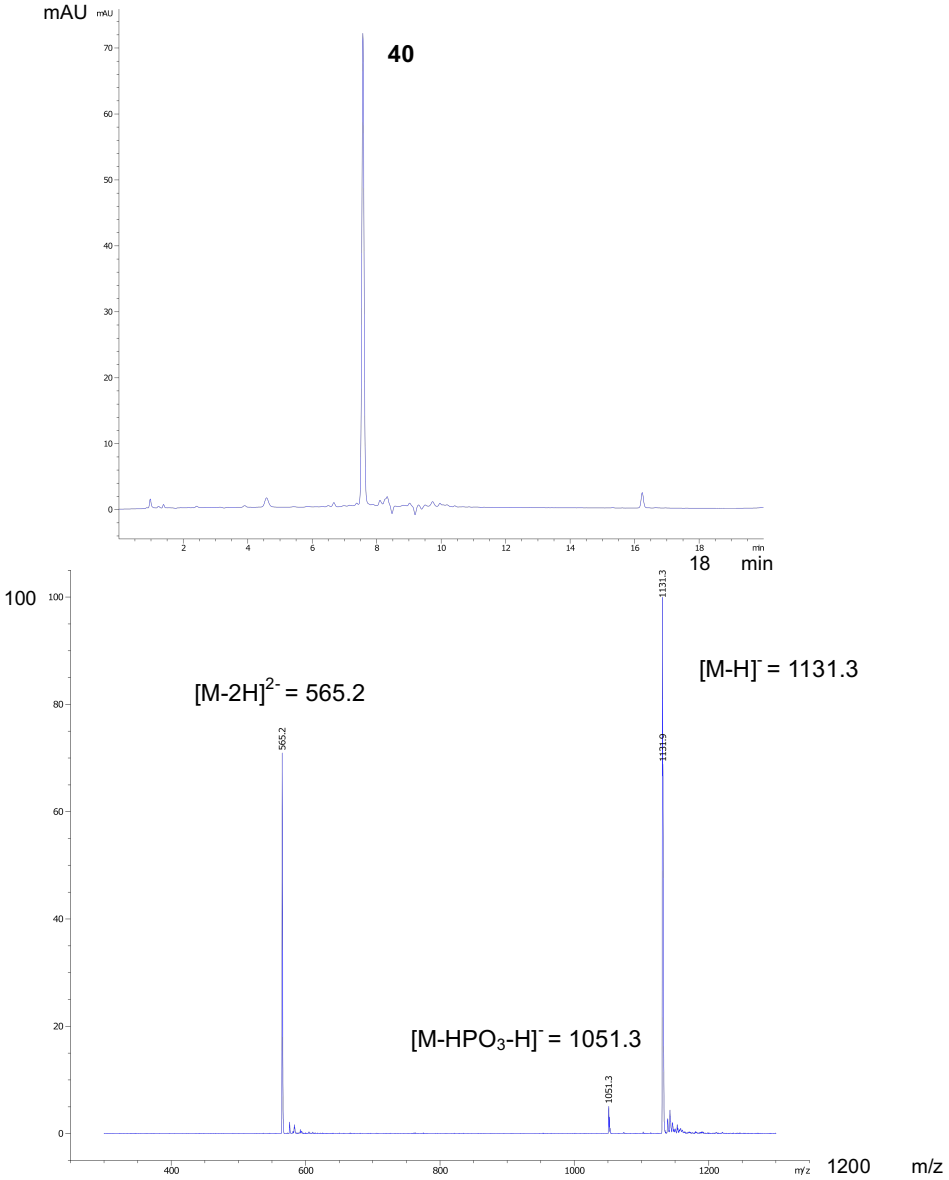

Figure S49. Analytical HPLC-MS spectra showing the production of **40** from **24** in Method A. Calculated mass $[M-H]^-$: 1131.4, observed mass $[M-H]^-$: 1131.3; Calculated mass $[M-2H]^{2-}$: 565.2, observed mass $[M-2H]^{2-}$: 565.2.

Synthesis and analytical data for model amidopyrophosphopeptide **25**

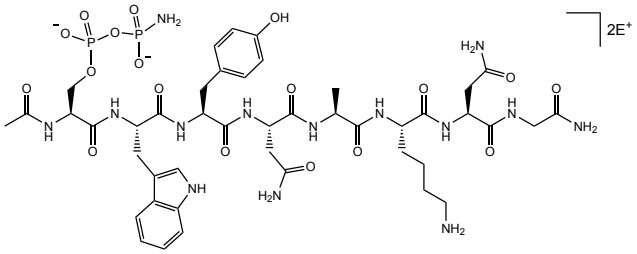

E^+ = Phosphate counter-ions (H^+, Na^+, 0.5 Mg^{2+})

Amidopyrophosphopeptide **25** was synthesized from **9** with the representative protocol using DAP, magnesium chloride and imidazole in 96% conversion indicated by HPLC and used for the next step without any further purification.

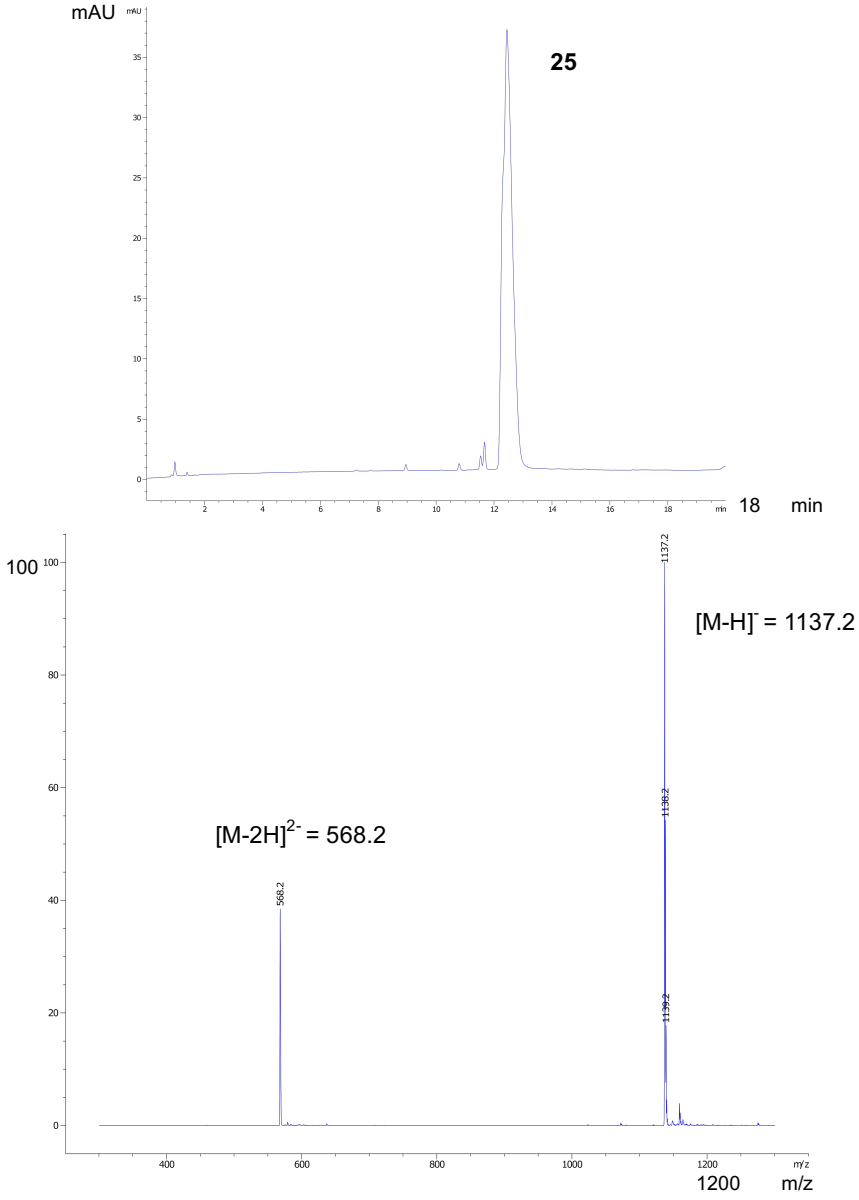

Figure S50. Analytical HPLC-MS spectra showing the production of **25** from **9** in Method A. Calculated mass $[M-H]^-$: 1137.4, observed mass $[M-H]^-$: 1137.2; Calculated mass $[M-2H]^{2-}$: 568.2, observed mass $[M-2H]^{2-}$: 568.2.

Synthesis and analytical data for model pyrophosphopeptide **41**

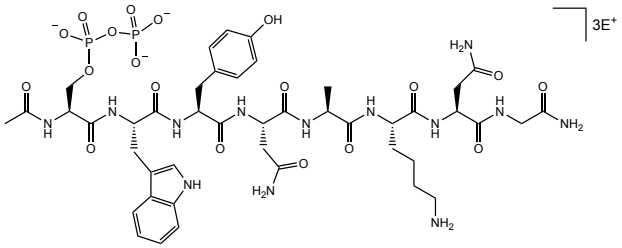

E^+ = Phosphate counter-ions (H^+, Na^+, 0.5 Mg^{2+})

Pyrophosphopeptide **41** was synthesized from **25** following the representative protocol using sodium nitrite in the same pot in 90% conversion over two steps indicated by HPLC.

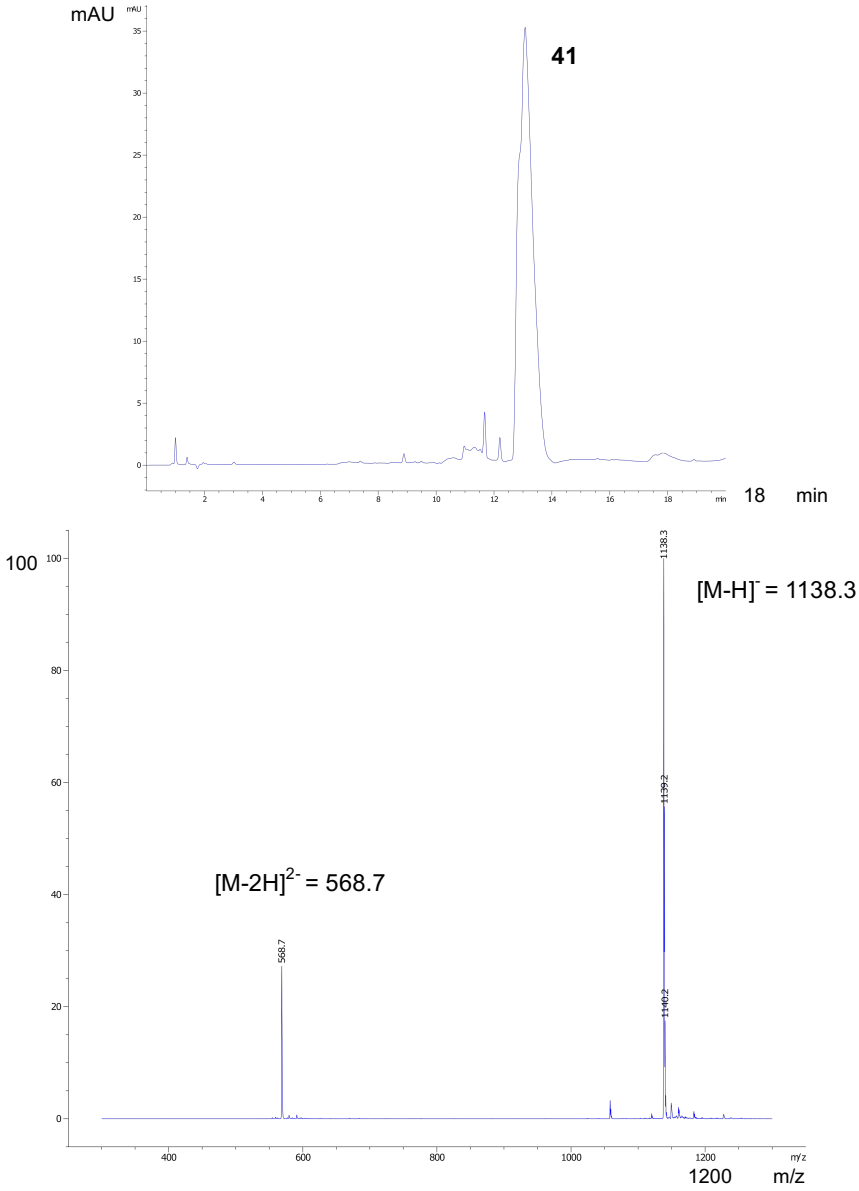

Figure S51. Analytical HPLC-MS spectra showing the production of **41** from **25** in Method A. Calculated mass $[M-H]^-$: 1138.4, observed mass $[M-H]^-$: 1138.3; Calculated mass $[M-2H]^{2-}$: 568.7, observed mass $[M-2H]^{2-}$: 568.7.

Synthesis and analytical data for model amidopyrophosphopeptide **26**

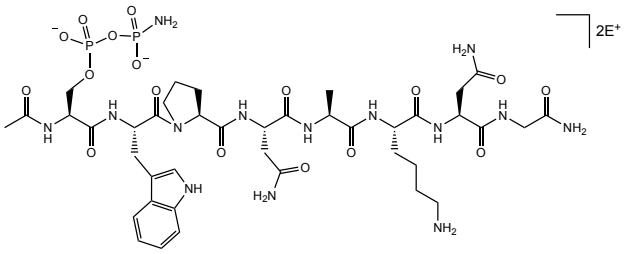

Amidopyrophosphopeptide **26** was synthesized from **10** with the representative protocol using DAP, magnesium chloride and imidazole in 94% conversion indicated by HPLC and used for the next step without any further purification.

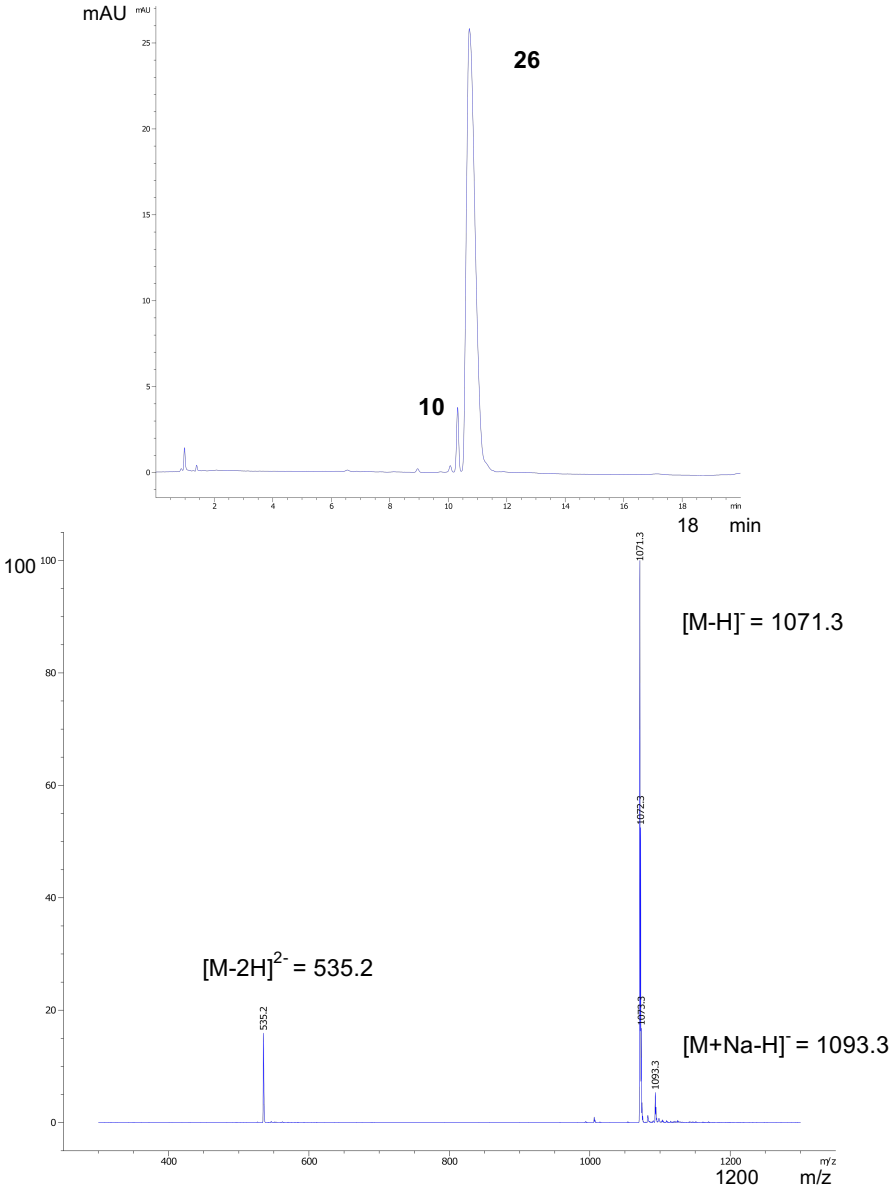

Figure S52. Analytical HPLC-MS spectra showing the production of **26** from **10** in Method A. Calculated mass $[M-H]^-$: 1071.4, observed mass $[M-H]^-$: 1071.3; Calculated mass $[M-2H]^{2-}$: 535.2, observed mass $[M-2H]^{2-}$: 535.2.

Synthesis and analytical data for model pyrophosphopeptide **42**

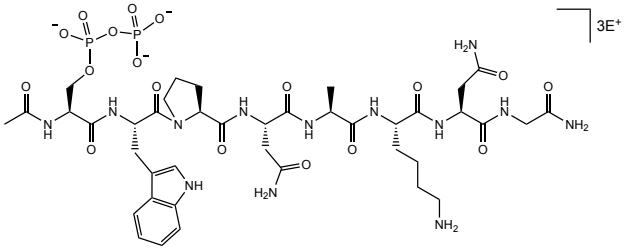

Pyrophosphopeptide **42** was synthesized from **26** following the representative protocol using sodium nitrite in the same pot in 86% conversion over two steps indicated by HPLC.

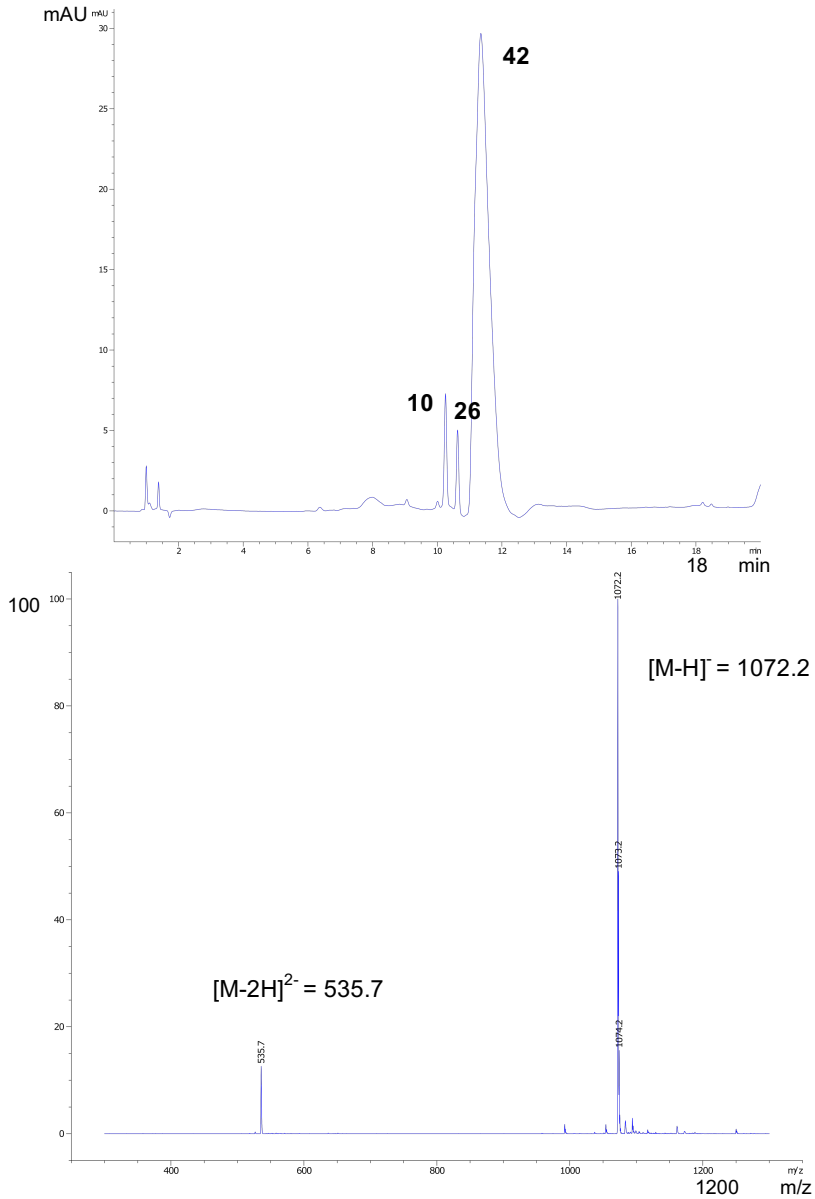

Figure S53. Analytical HPLC-MS spectra showing the production of **42** from **26** in Method A. Calculated mass $[M-H]^-$: 1072.4, observed mass $[M-H]^-$: 1072.2; Calculated mass $[M-2H]^{2-}$: 535.7, observed mass $[M-2H]^{2-}$: 535.7.

Synthesis and analytical data for model amidopyrophosphopeptide **27**

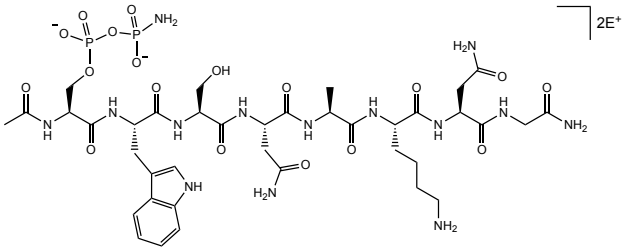

Amidopyrophosphopeptide **27** was synthesized from **11** with the representative protocol using DAP, magnesium chloride and imidazole in 96% conversion indicated by HPLC and used for the next step without any further purification.

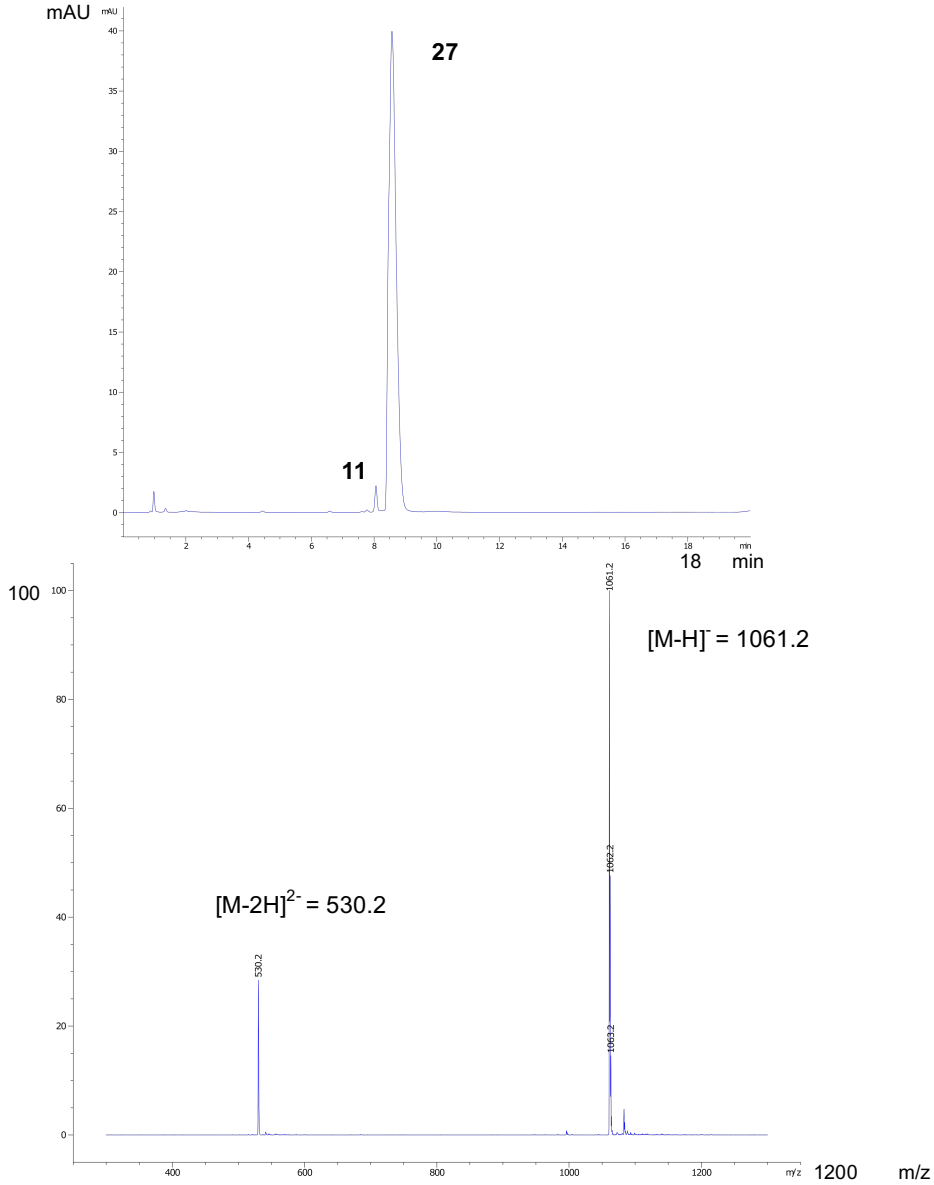

Figure S54. Analytical HPLC-MS spectra showing the production of **27** from **11** in Method A. Calculated mass $[M-H]^-$: 1061.4, observed mass $[M-H]^-$: 1061.2; Calculated mass $[M-2H]^{2-}$: 530.2, observed mass $[M-2H]^{2-}$: 530.2.

Synthesis and analytical data for model pyrophosphopeptide **43**

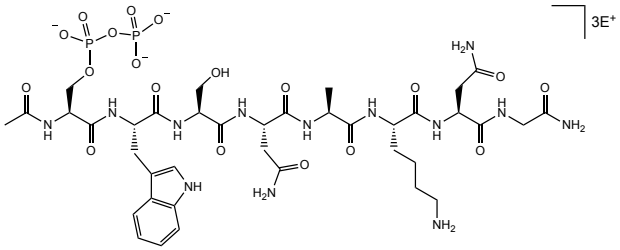

Pyrophosphopeptide **43** was synthesized from **27** following the representative protocol using sodium nitrite in the same pot in 90% conversion over two steps indicated by HPLC.

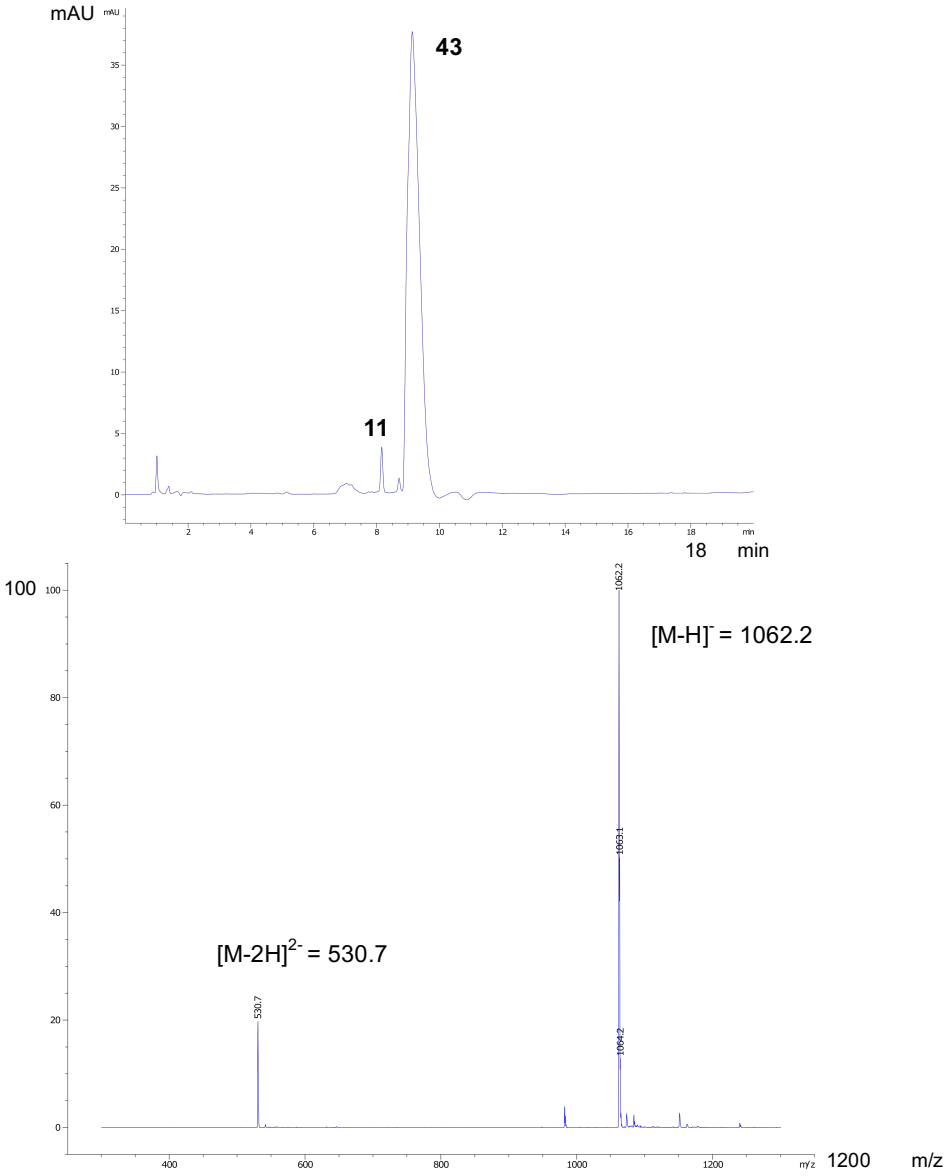

Figure S55. Analytical HPLC-MS spectra showing the production of **43** from **27** in Method A. Calculated mass $[M-H]^-$: 1062.3, observed mass $[M-H]^-$: 1062.2; Calculated mass $[M-2H]^{2-}$: 530.7, observed mass $[M-2H]^{2-}$: 530.7.

Synthesis and analytical data for model amidopyrophosphopeptide **28**

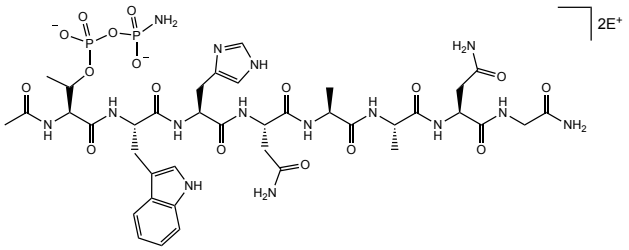

E^+ = Phosphate counter-ions (H^+, Na^+, 0.5 Mg^{2+})

Amidopyrophosphopeptide **28** was synthesized from **12** with the representative protocol using DAP, magnesium chloride and imidazole in 94% conversion indicated by HPLC and used for the next step without any further purification.

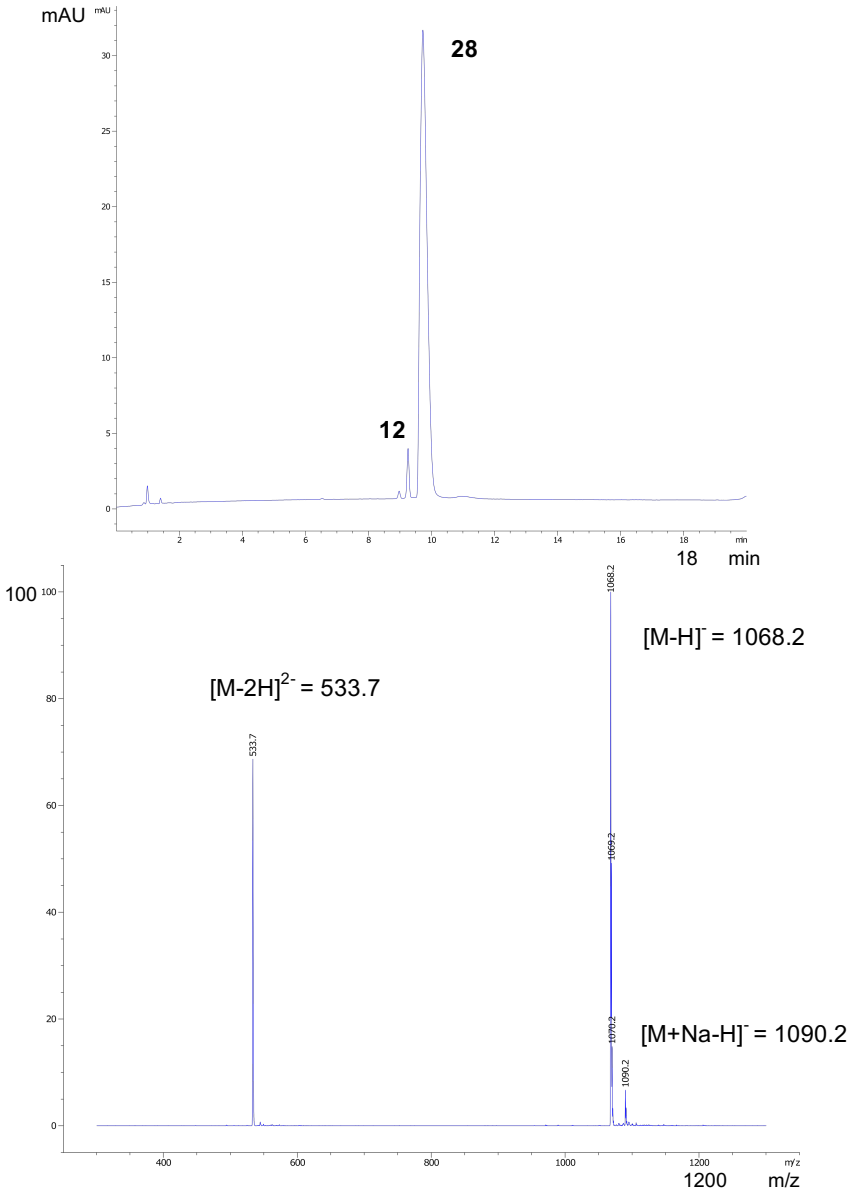

Figure S56. Analytical HPLC-MS spectra showing the production of **28** from **12** in Method A. Calculated mass $[M-H]^-$: 1068.3, observed mass $[M-H]^-$: 1068.2; Calculated mass $[M-2H]^{2-}$: 533.7, observed mass $[M-2H]^{2-}$: 533.7.

Synthesis and analytical data for model pyrophosphopeptide **44**

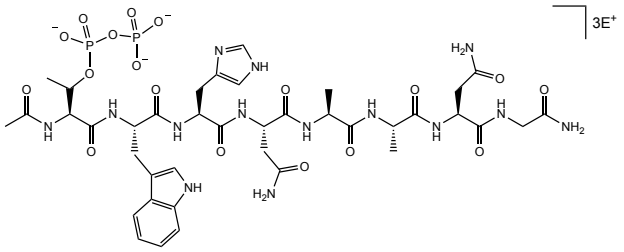

Pyrophosphopeptide **44** was synthesized from **28** following the representative protocol using sodium nitrite in the same pot in 93% conversion over two steps indicated by HPLC.

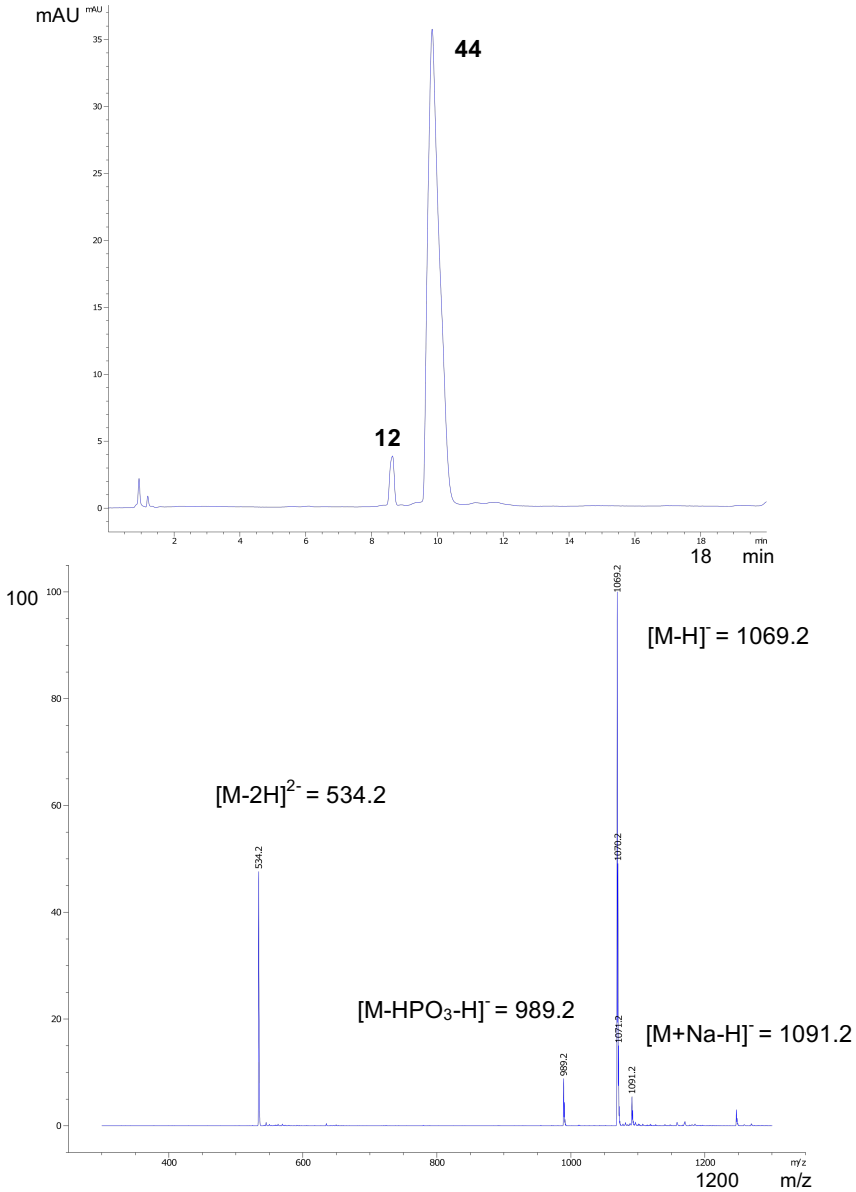

Figure S57. Analytical HPLC-MS spectra showing the production of **44** from **28** in Method A. Calculated mass $[M-H]^-$: 1069.3, observed mass $[M-H]^-$: 1069.2; Calculated mass $[M-2H]^{2-}$: 534.2, observed mass $[M-2H]^{2-}$: 534.2.

Synthesis and analytical data for model amidopyrophosphopeptide **29**

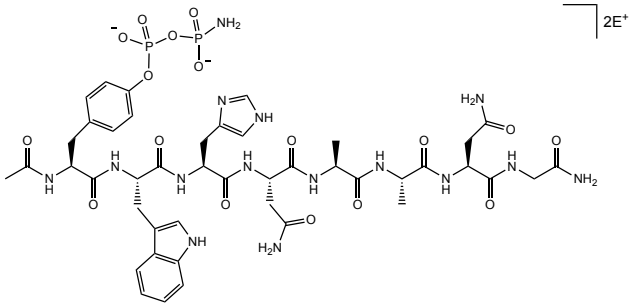

E^+ = Phosphate counter-ions (H^+, Na^+, 0.5 Mg^{2+})

Amidopyrophosphopeptide **29** was synthesized from **13** with the representative protocol using DAP, magnesium chloride and imidazole in 90% conversion indicated by HPLC and used for the next step without any further purification.

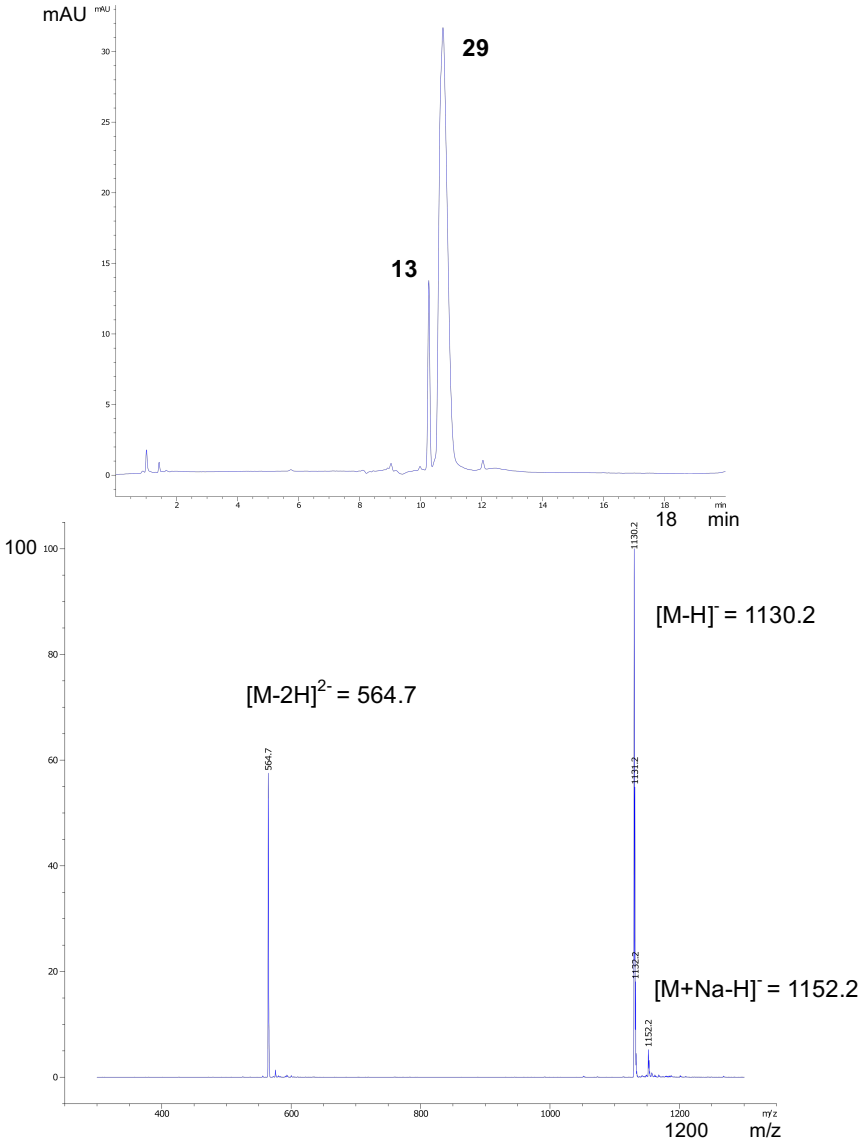

Figure S58. Analytical HPLC-MS spectra showing the production of **29** from **13** in Method A. Calculated mass $[M-H]^-$: 1130.4, observed mass $[M-H]^-$: 1130.2; Calculated mass $[M-2H]^{2-}$: 564.7, observed mass $[M-2H]^{2-}$: 564.7.

Synthesis and analytical data for model pyrophosphopeptide **45**

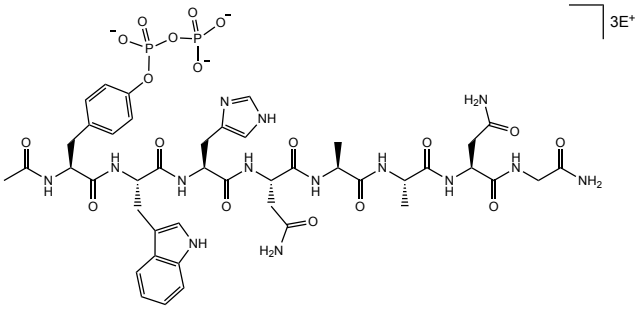

E^+ = Phosphate counter-ions (H^+, Na^+, 0.5 Mg^{2+})

Pyrophosphopeptide **45** was synthesized from **29** following the representative protocol using sodium nitrite in the same pot in 83% conversion over two steps indicated by HPLC.

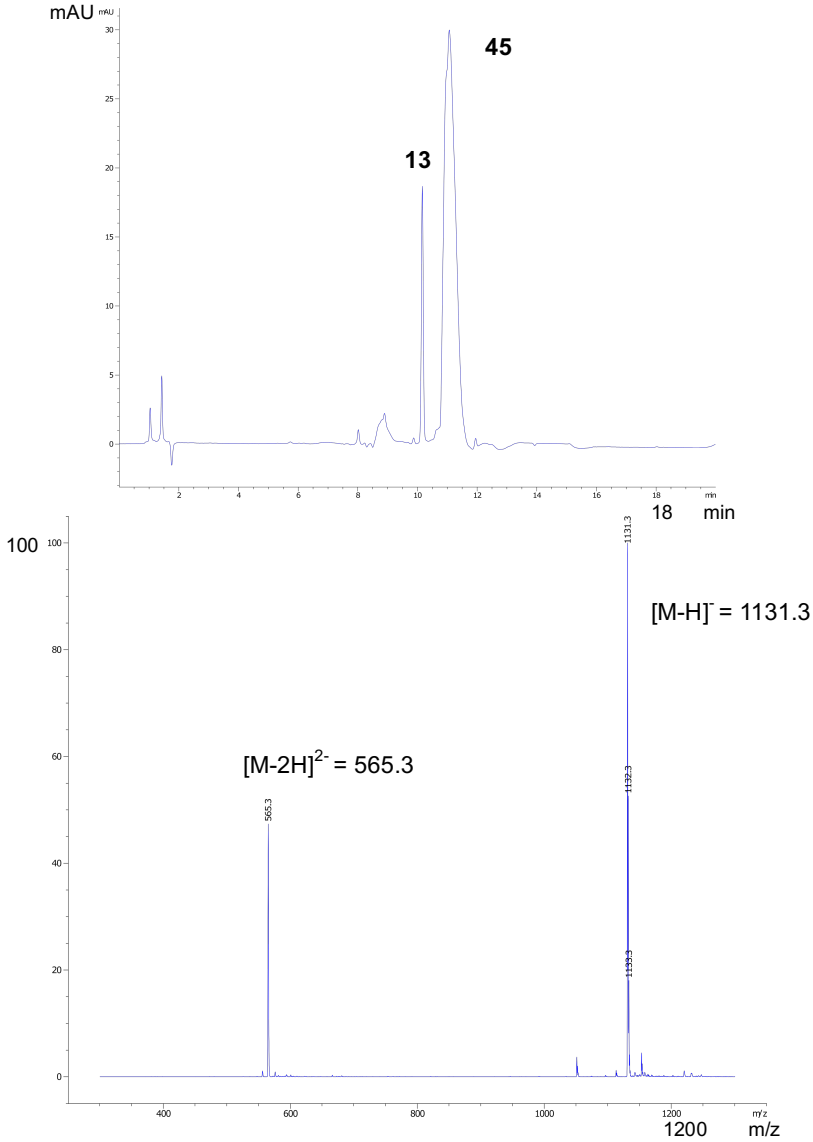

Figure S59. Analytical HPLC-MS spectra showing the production of **45** from **29** in Method A. Calculated mass $[M-H]^-$: 1131.3, observed mass $[M-H]^-$: 1131.3; Calculated mass $[M-2H]^{2-}$: 565.2, observed mass $[M-2H]^{2-}$: 565.3.

Synthesis and analytical data for model amidopyrophosphopeptide **30**

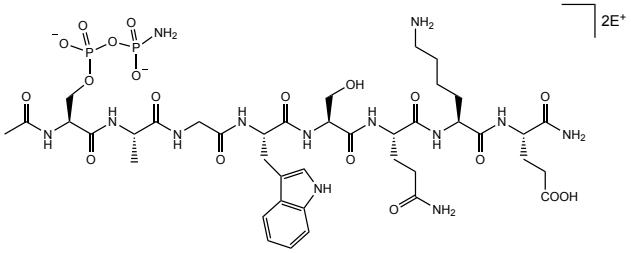

Amidopyrophosphopeptide **30** was synthesized from **14** with the representative protocol using DAP, magnesium chloride and imidazole in 95% conversion indicated by HPLC and used for the next step without any further purification.

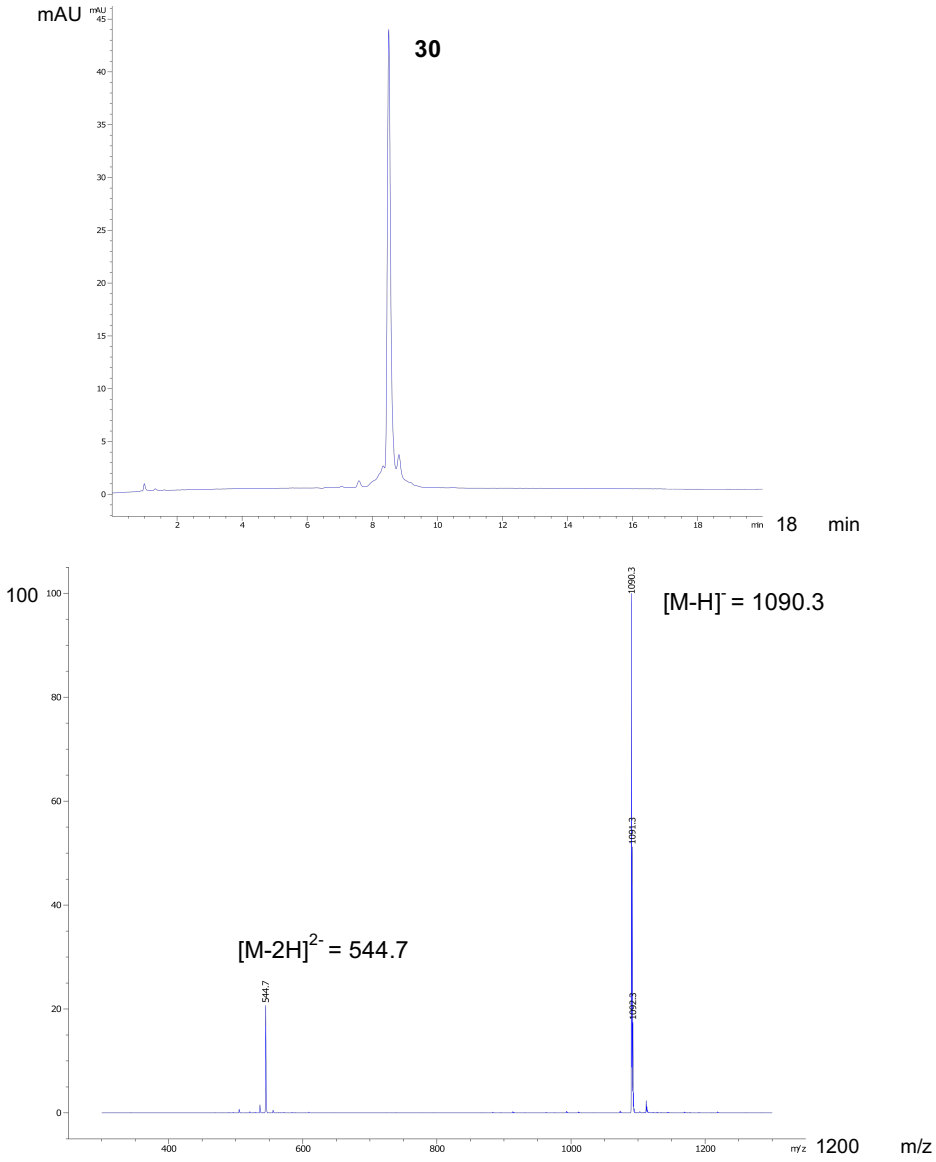

Figure S60. Analytical HPLC-MS spectra showing the production of **30** from **14** in Method A. Calculated mass $[M-H]^-$: 1090.4, observed mass $[M-H]^-$: 1090.3; Calculated mass $[M-2H]^{2-}$: 544.7, observed mass $[M-2H]^{2-}$: 544.7.

Synthesis and analytical data for model pyrophosphopeptide **46**

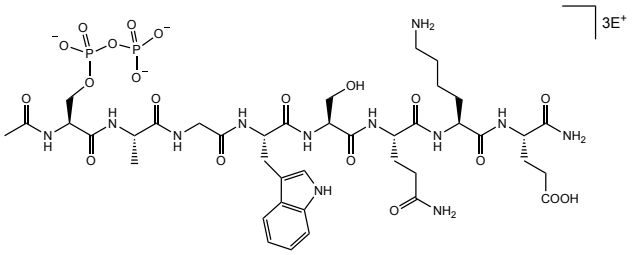

E^+ = Phosphate counter-ions (H^+, Na^+, 0.5 Mg^{2+})

Pyrophosphopeptide **46** was synthesized from **30** following the representative protocol using sodium nitrite in the same pot in 94% conversion over two steps indicated by HPLC.

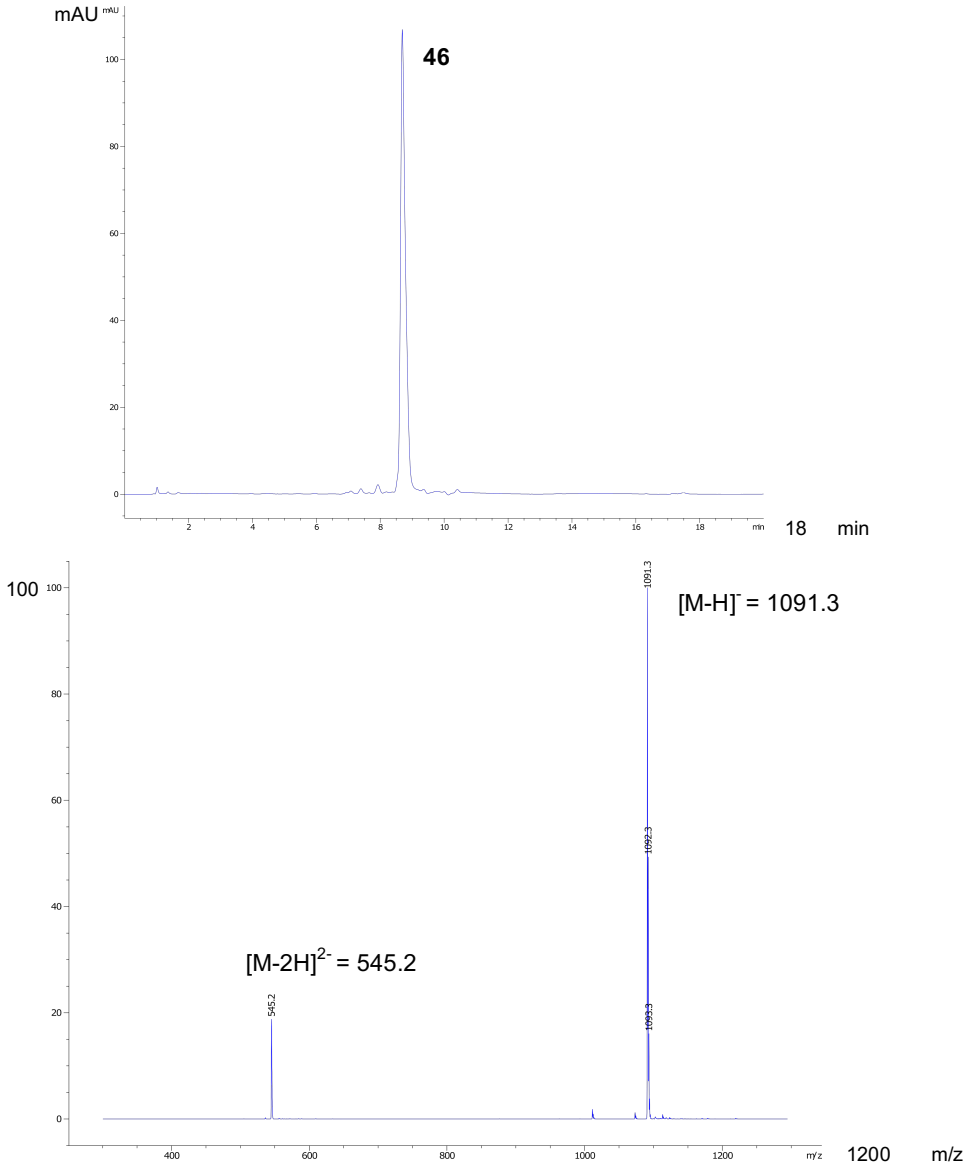

Figure S61. Analytical HPLC-MS spectra showing the production of **46** from **30** in Method A. Calculated mass $[M-H]^-$: 1091.4, observed mass $[M-H]^-$: 1091.3; Calculated mass $[M-2H]^{2-}$: 545.2, observed mass $[M-2H]^{2-}$: 545.2.

3.4 Scale-up synthesis of model pyrophosphopeptides

3.4.1 Procedure of pyrophosphorylation

To a vial containing 10 mM of phosphopeptide (1 equiv.) in 1 ml H_2O, was added DAP (5 equiv.), magnesium chloride (2 equiv.) and imidazole (2 equiv.). The pH of the reaction mixture was adjusted to 5.5 with hydrochloric acid. The reactions were kept at -20°C in freezer. Progress of the amidophosphorylation was monitored by LC-MS. After 2 days without any further purification, sodium nitrite (5 equiv.) was added into the same-pot reaction mixture. The pH of the reaction mixture was adjusted to 3.0 with hydrochloric acid. The reactions were kept at -20°C for 20 hours. Progress of the hydrolysis was monitored by LC-MS. The crude pyrophosphopeptides were purified by preparative reverse-phase HPLC.

3.4.2 Liquid chromatography-mass spectrometry (LC-MS)

Synthesis and analytical data for model amidopyrophosphopeptide **21**

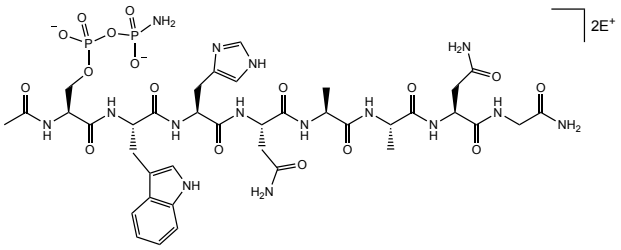

E^+ = Phosphate counter-ions (H^+, Na^+, 0.5 Mg^{2+})

Amidopyrophosphopeptide **21** was synthesized from **3** (9.8 mg) following the representative protocol using DAP, magnesium chloride and imidazole and used for the next step without any further purification.

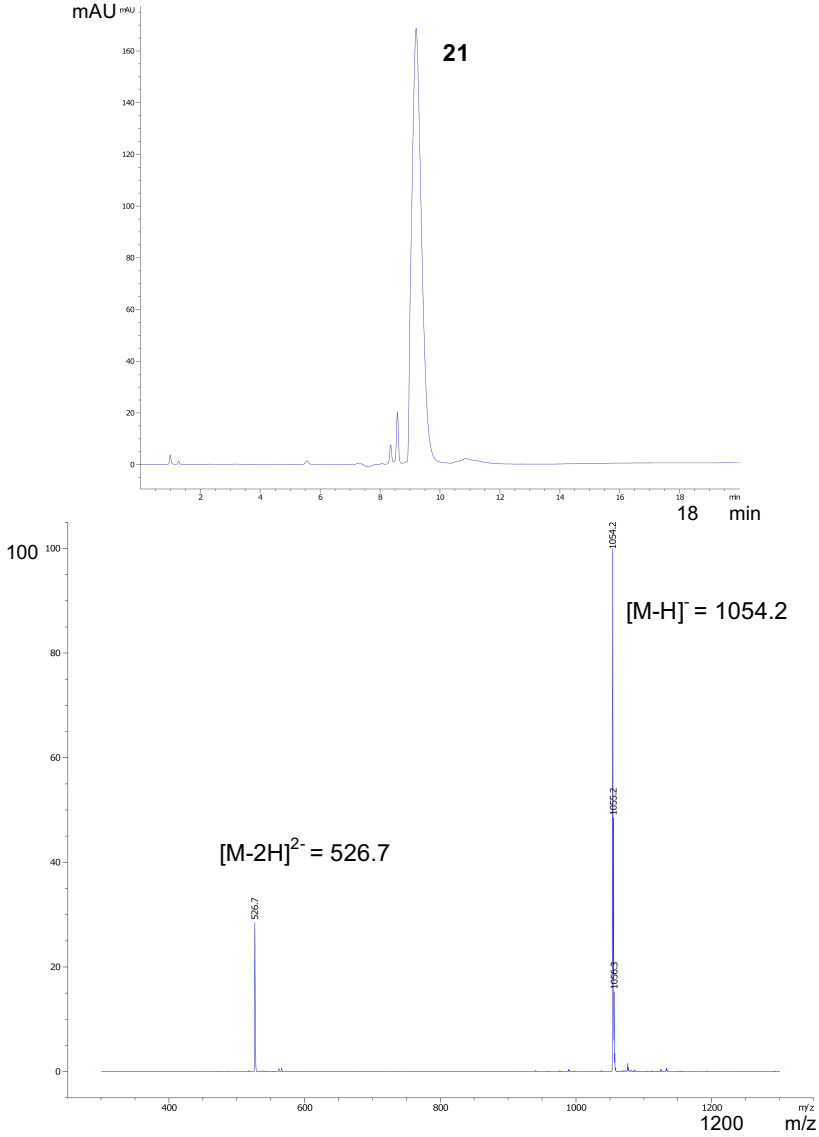

Figure S62. Analytical HPLC-MS spectra showing the production of **21** from **3** in Method A. Calculated mass $[M-H]^-$: 1054.3, observed mass $[M-H]^-$: 1054.2; Calculated mass $[M-2H]^{2-}$: 526.7, observed mass $[M-2H]^{2-}$: 526.7.

Synthesis and analytical data for model pyrophosphopeptide **37**

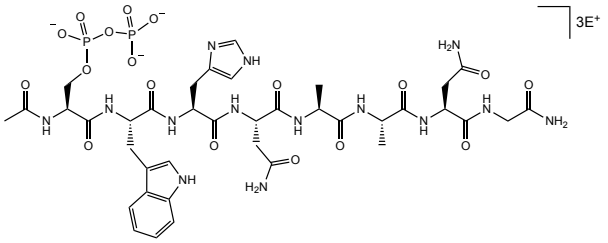

E^+ = Phosphate counter-ions (H^+, Na^+, 0.5 Mg^{2+})

Pyrophosphopeptide **37** was synthesized from **21** following the representative protocol using sodium nitrite in the same pot and then purified by preparative reverse-phase HPLC and obtained as a lyophilized solid (6.9 mg, 65%).

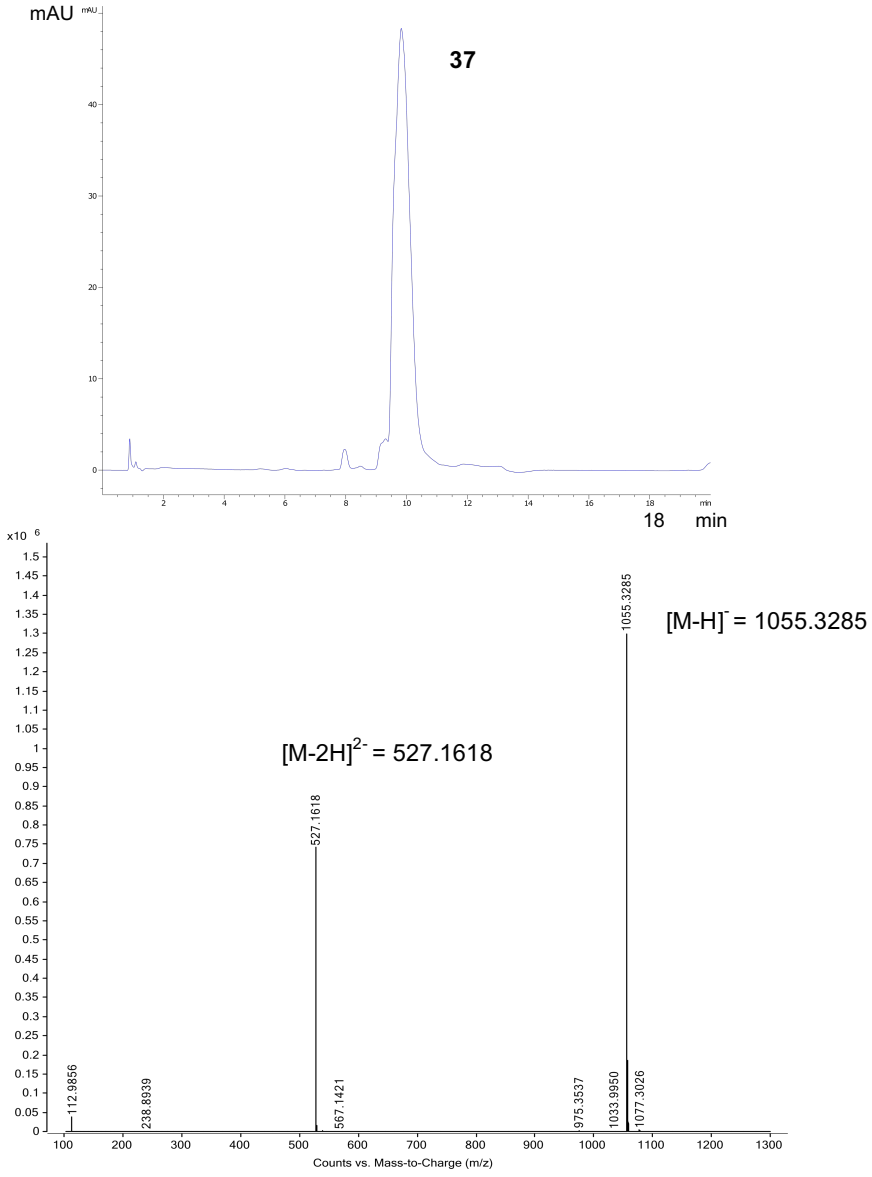

Figure S63. Analytical HPLC-MS spectra showing the production of **37** from **21** in Method A. Calculated mass $[M-H]^-$: 1055.3143, observed mass $[M-H]^-$: 1055.3285; Calculated mass $[M-2H]^{2-}$: 527.1535, observed mass $[M-2H]^{2-}$: 527.1618.

Synthesis and analytical data for model amidopyrophosphopeptide **25**

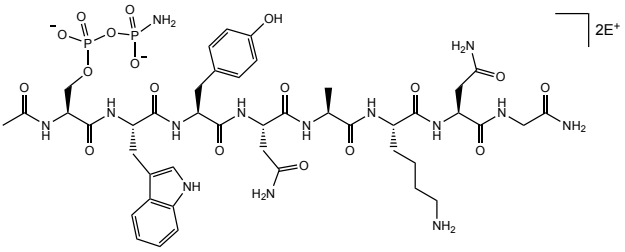

E+ = Phosphate counter-ions (H^+, Na^+, 0.5 Mg^{2+})

Amidopyrophosphopeptide **25** was synthesized from **9** (10.6 mg) following the representative protocol using DAP, magnesium chloride and imidazole and used for the next step without any further purification.

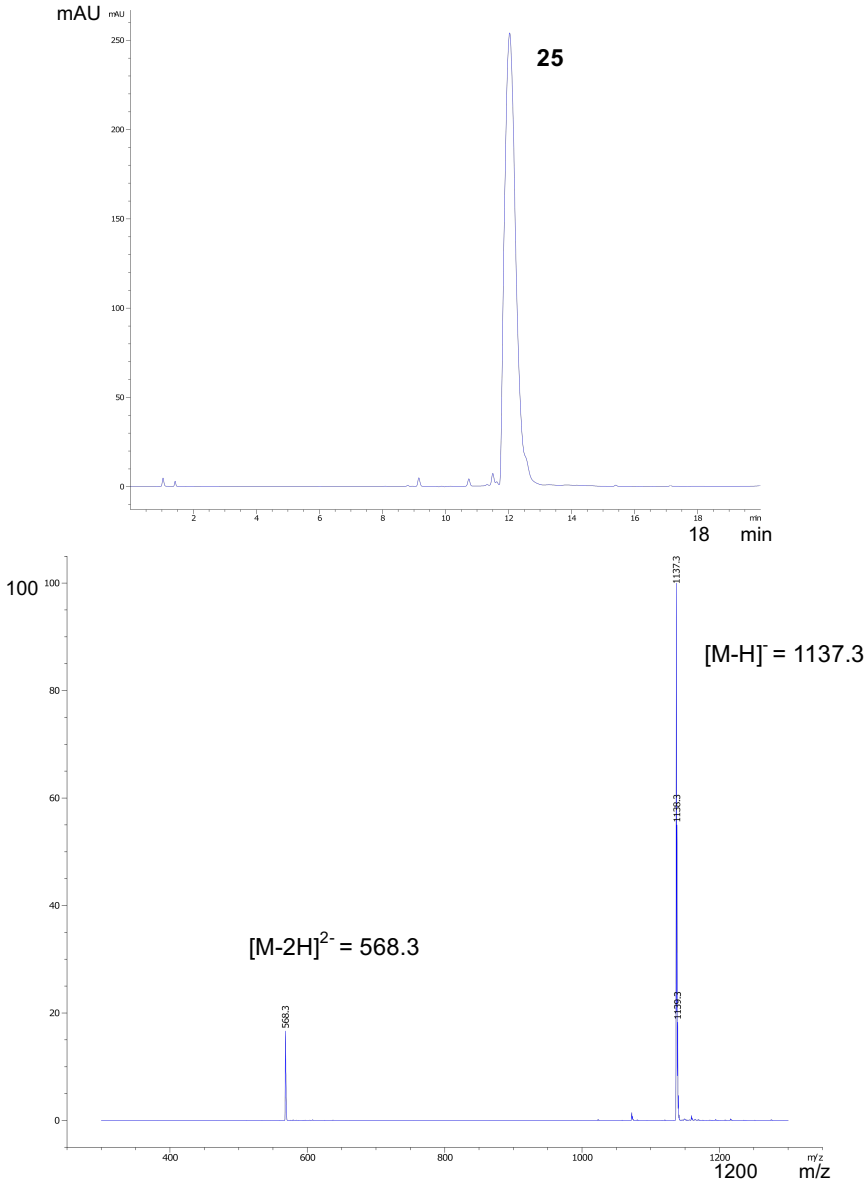

Figure S64. Analytical HPLC-MS spectra showing the production of **25** from **9** in Method A. Calculated mass $[M-H]^-$: 1137.4, observed mass $[M-H]^-$: 1137.3; Calculated mass $[M-2H]^{2-}$: 568.2, observed mass $[M-2H]^{2-}$: 568.3.

Synthesis and analytical data for model pyrophosphopeptide **41**

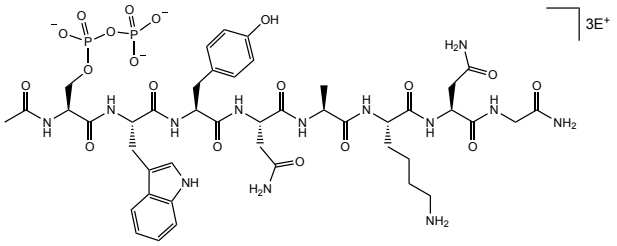

E^+ = Phosphate counter-ions (H^+, Na^+, 0.5 Mg^{2+})

Pyrophosphopeptide **41** was synthesized from **25** following the representative protocol using sodium nitrite in the same pot and then purified by preparative reverse-phase HPLC and obtained as a lyophilized solid (7.2 mg, 63%).

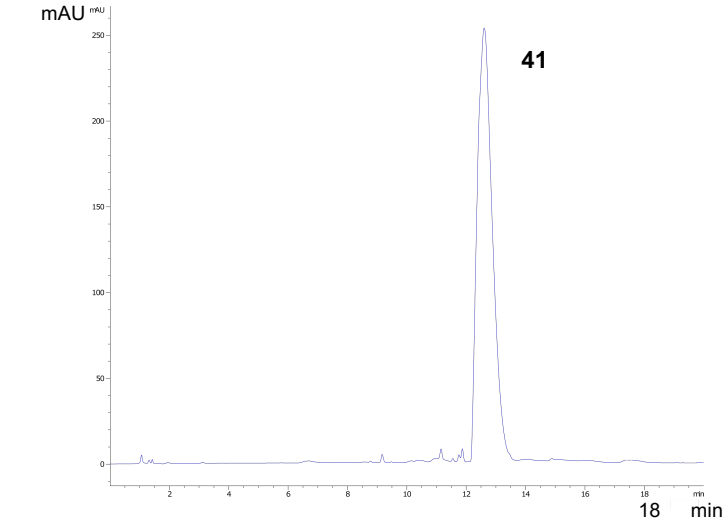

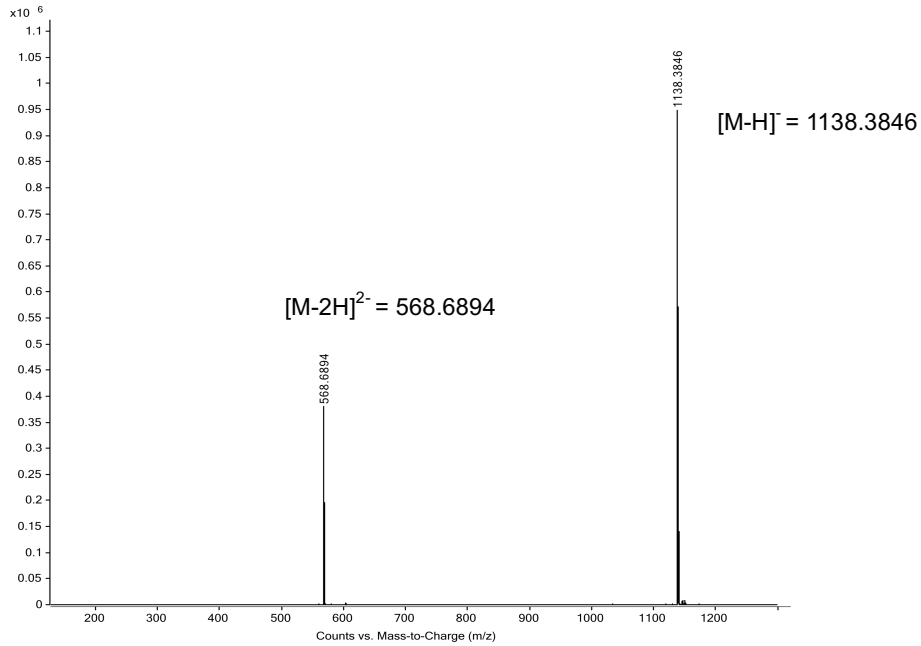

Figure S65. Analytical HPLC-MS spectra showing the production of **41** from **25** in Method A. Calculated mass $[M-H]^-$: 1138.3766, observed mass $[M-H]^-$: 1138.3846; Calculated mass $[M-2H]^{2-}$: 568.6846, observed mass $[M-2H]^{2-}$: 568.6894.

Synthesis and analytical data for model amidopyrophosphopeptide **27**

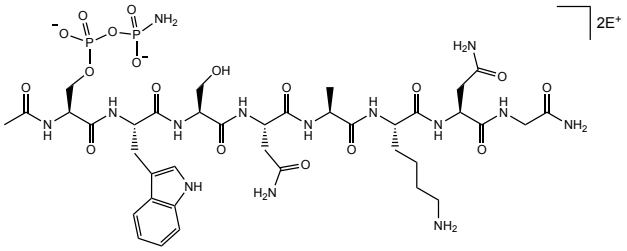

Amidopyrophosphopeptide **27** was synthesized from **11** (9.8 mg) following the representative protocol using DAP, magnesium chloride and imidazole and used for the next step without any further purification.

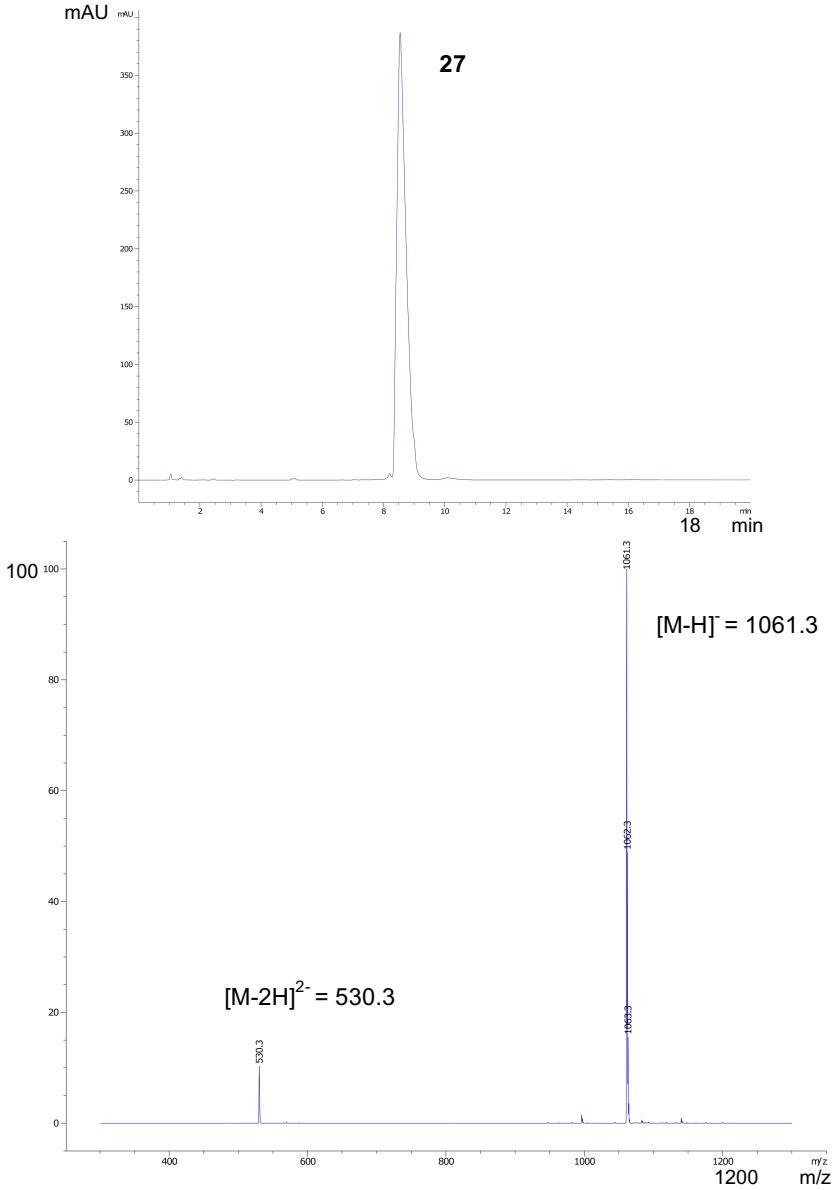

Figure S66. Analytical HPLC-MS spectra showing the production of **27** from **11** in Method A. Calculated mass $[M-H]^-$: 1061.4, observed mass $[M-H]^-$: 1061.3; Calculated mass $[M-2H]^{2-}$: 530.2, observed mass $[M-2H]^{2-}$: 530.3.

Synthesis and analytical data for model pyrophosphopeptide **43**

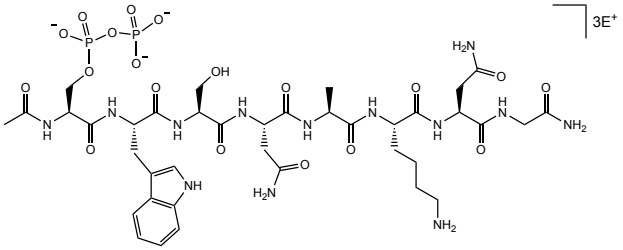

E^+ = Phosphate counter-ions (H^+, Na^+, 0.5 Mg^{2+})

Pyrophosphopeptide **43** was synthesized from **27** following the representative protocol using sodium nitrite in the same pot and then purified by preparative reverse-phase HPLC and obtained as a lyophilized solid (7.6 mg, 71%).

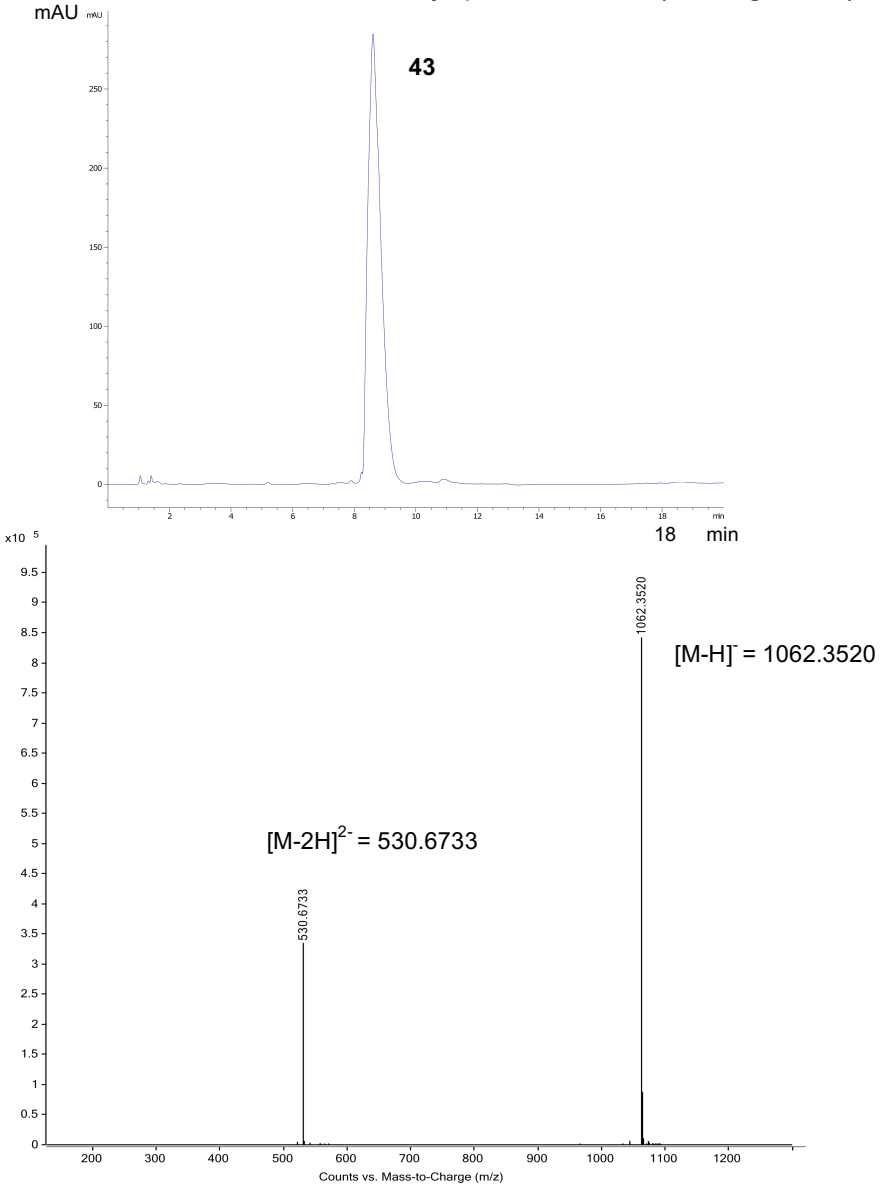

Figure S67. Analytical HPLC-MS spectra showing the production of **43** from **27** in Method A. Calculated mass $[M-H]^-$: 1062.3453, observed mass $[M-H]^-$: 1062.3520; Calculated mass $[M-2H]^{2-}$: 530.6690, observed mass $[M-2H]^{2-}$: 530.6733.

Synthesis and analytical data for model amidopyrophosphopeptide **28**

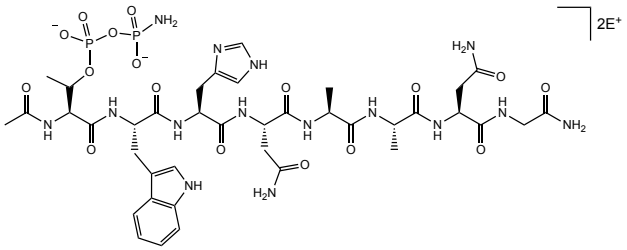

E^+ = Phosphate counter-ions (H^+, Na^+, 0.5 Mg^{2+})

Amidopyrophosphopeptide **28** was synthesized from **12** (9.9 mg) following the representative protocol using DAP, magnesium chloride and imidazole and used for the next step without any further purification.

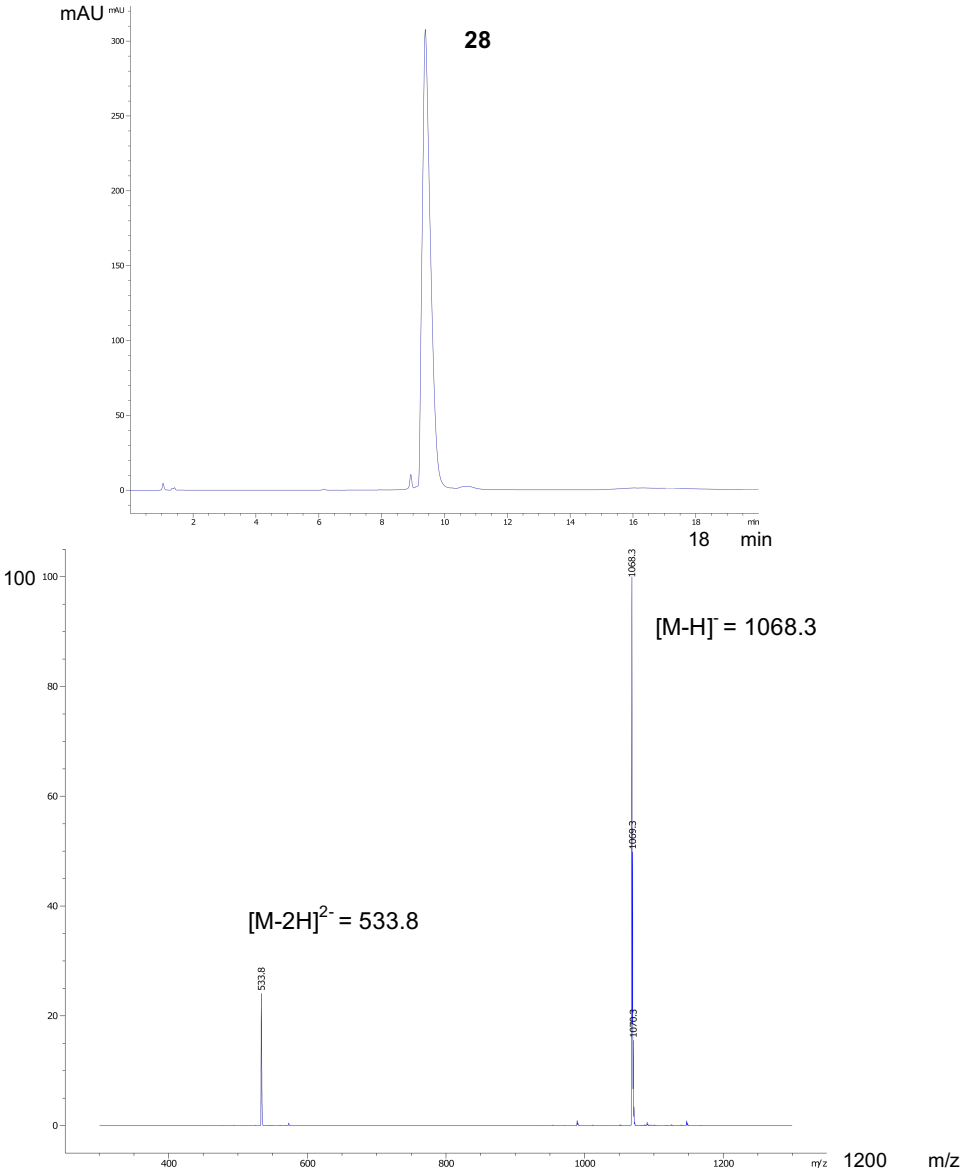

Figure S68. Analytical HPLC-MS spectra showing the production of **28** from **12** in Method A. Calculated mass $[M-H]^-$: 1068.3, observed mass $[M-H]^-$: 1068.3; Calculated mass $[M-2H]^{2-}$: 533.7, observed mass $[M-2H]^{2-}$: 533.8.

Synthesis and analytical data for model pyrophosphopeptide **44**

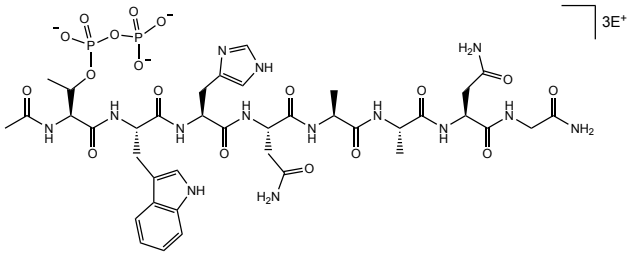

E^+ = Phosphate counter-ions (H^+, Na^+, 0.5 Mg^{2+})

Pyrophosphopeptide **44** was synthesized from **28** following the representative protocol using sodium nitrite in the same pot and then purified by preparative reverse-phase HPLC and obtained as a lyophilized solid (7.3 mg, 68%).

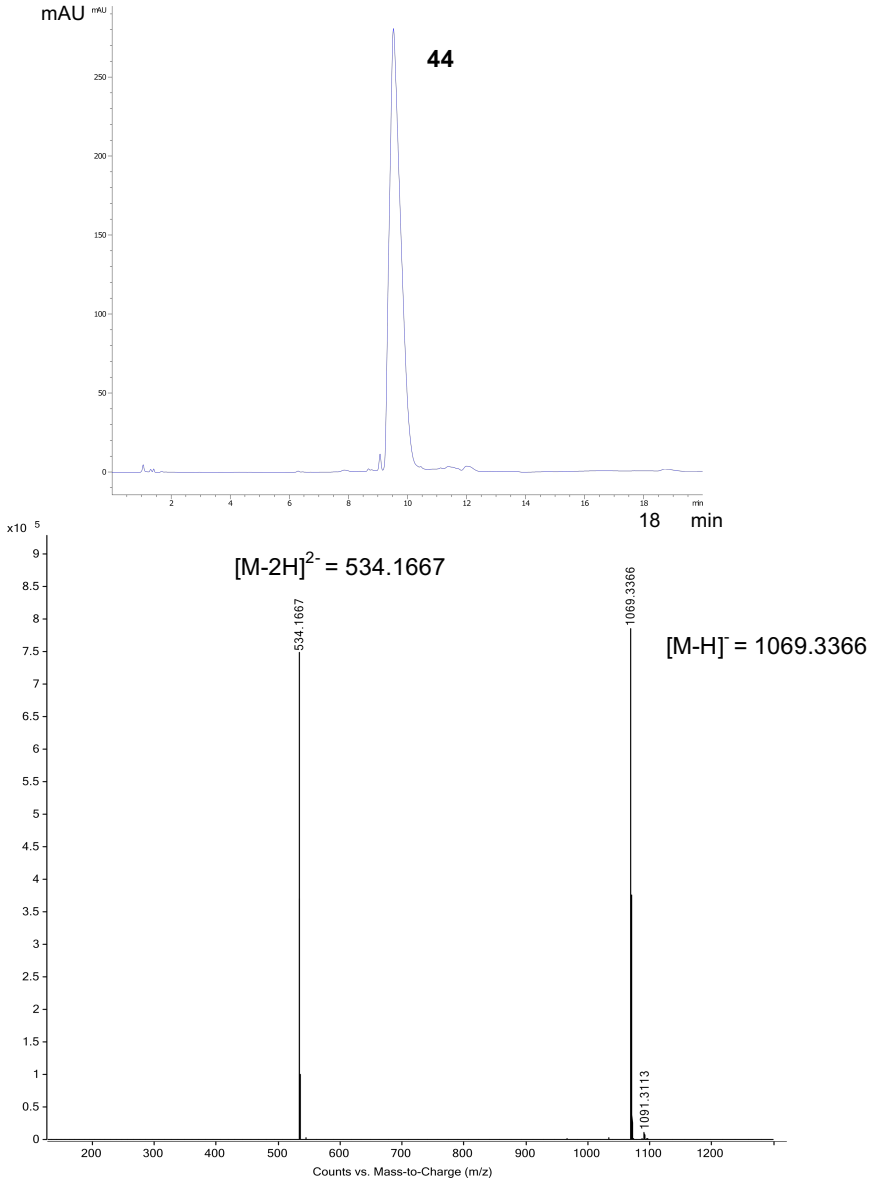

Figure S69. Analytical HPLC-MS spectra showing the production of **44** from **28** in Method A. Calculated mass $[M-H]^-$: 1069.3299, observed mass $[M-H]^-$: 1069.3366; Calculated mass $[M-2H]^{2-}$: 534.1613, observed mass $[M-2H]^{2-}$: 534.1667.

3.4.3 Standard curves of pyrophosphopeptides

The pyrophosphopeptide **41**, **43** and **44** were selected to make the standard curve for yield quantification based on the UV absorbance and integration at 280 nM. For each peptide standard curve, the concentration was set at 0.375 mM, 0.75 mM, 1.5 mM and 3.0 mM in water. 5 ul volume at each concentration was injected into the HPLC and it was run in Method A.

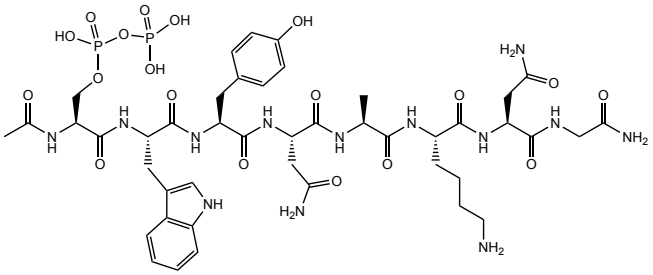

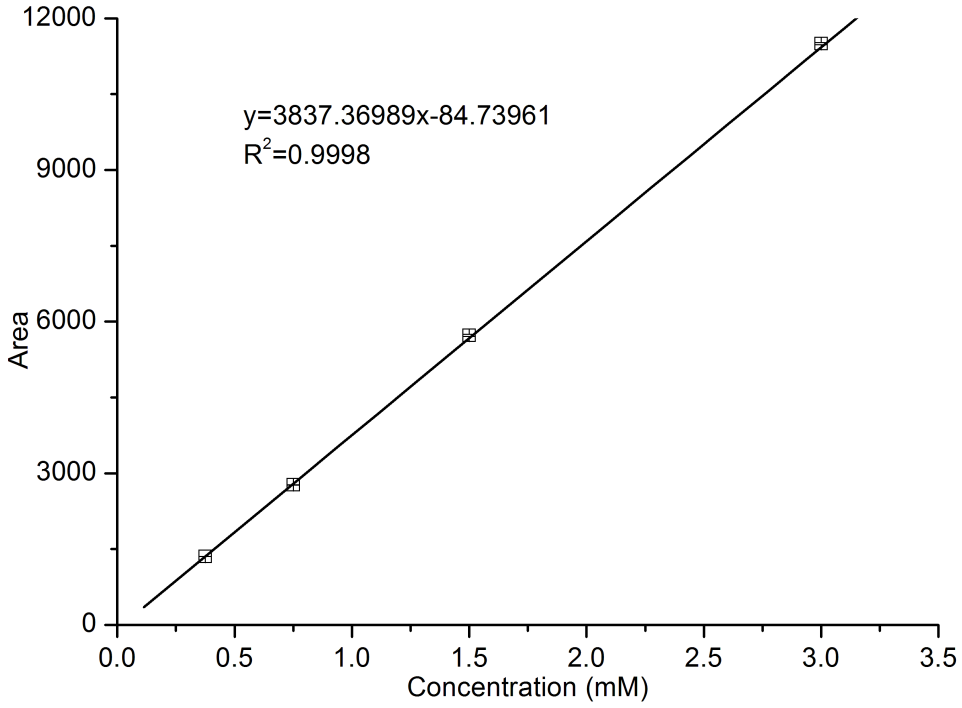

Figure S70. Standard curve of the pyrophosphopeptide **41**. The X axis represented the concentration and Y axis represented the integration area from the peak of **41** based on UV absorbance at 280 nM. Error bars were standard deviations from duplicate experiments and may be smaller than the resolution of the figure. The plot is the fit from linear regression.

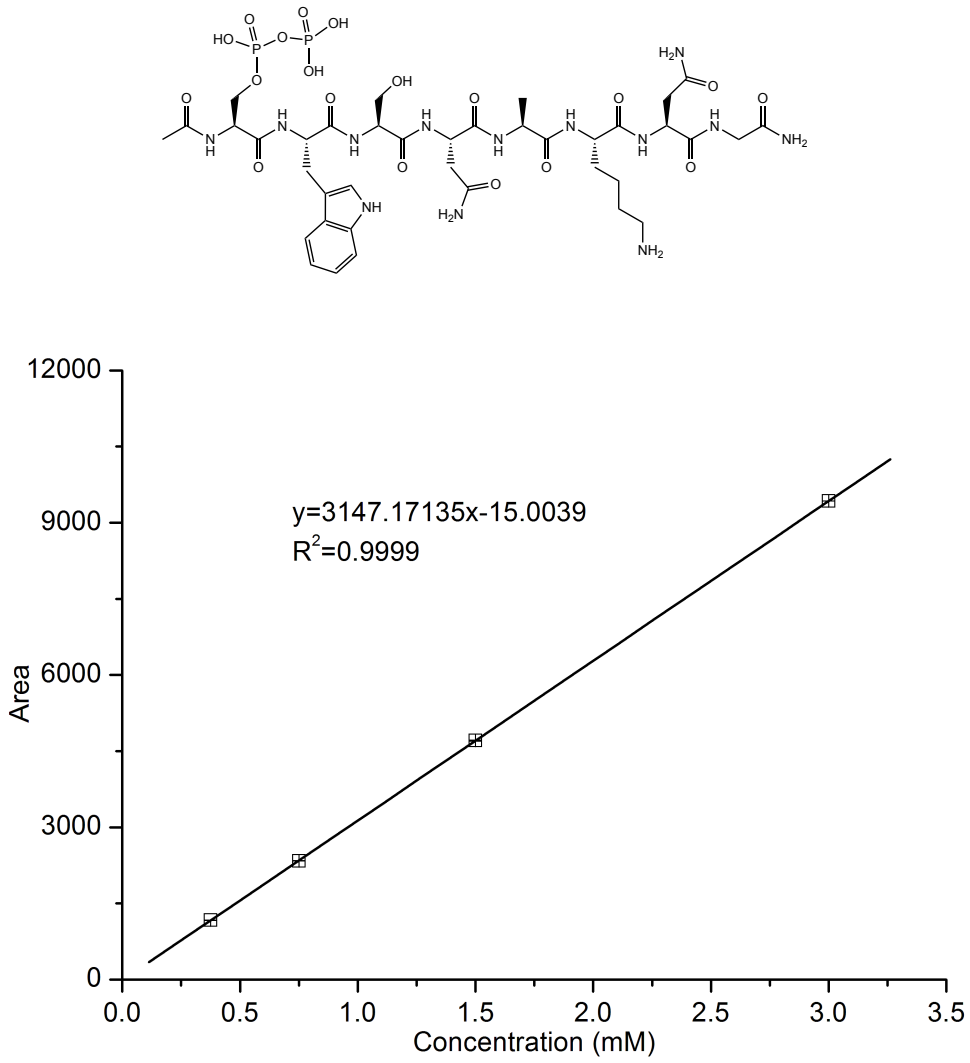

Figure S71. Standard curve of the pyrophosphopeptide **43**. The X axis represented the concentration and Y axis represented the integration area from the peak of **43** based on UV absorbance at 280 nM. Error bars were standard deviations from duplicate experiments and may be smaller than the resolution of the figure. The plot is the fit from linear regression.

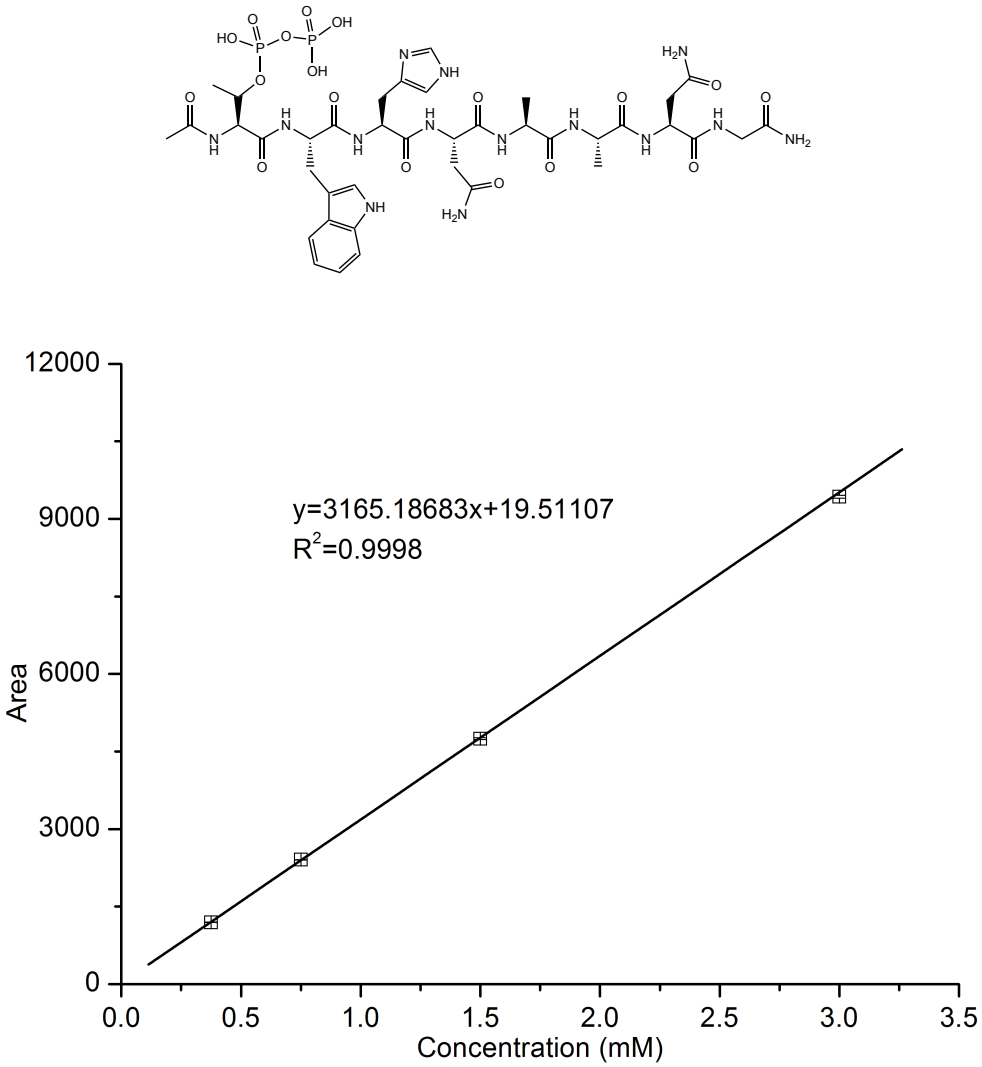

Figure S72. Standard curve of the pyrophosphopeptide **44**. The X axis represented the concentration and Y axis represented the integration area from the peak of **44** based on UV absorbance at 280 nM. Error bars were standard deviations from duplicate experiments and may be smaller than the resolution of the figure. The plot is the fit from linear regression.

3.4.4 Phosphorous nuclear magnetic resonance (^{31}P-NMR)

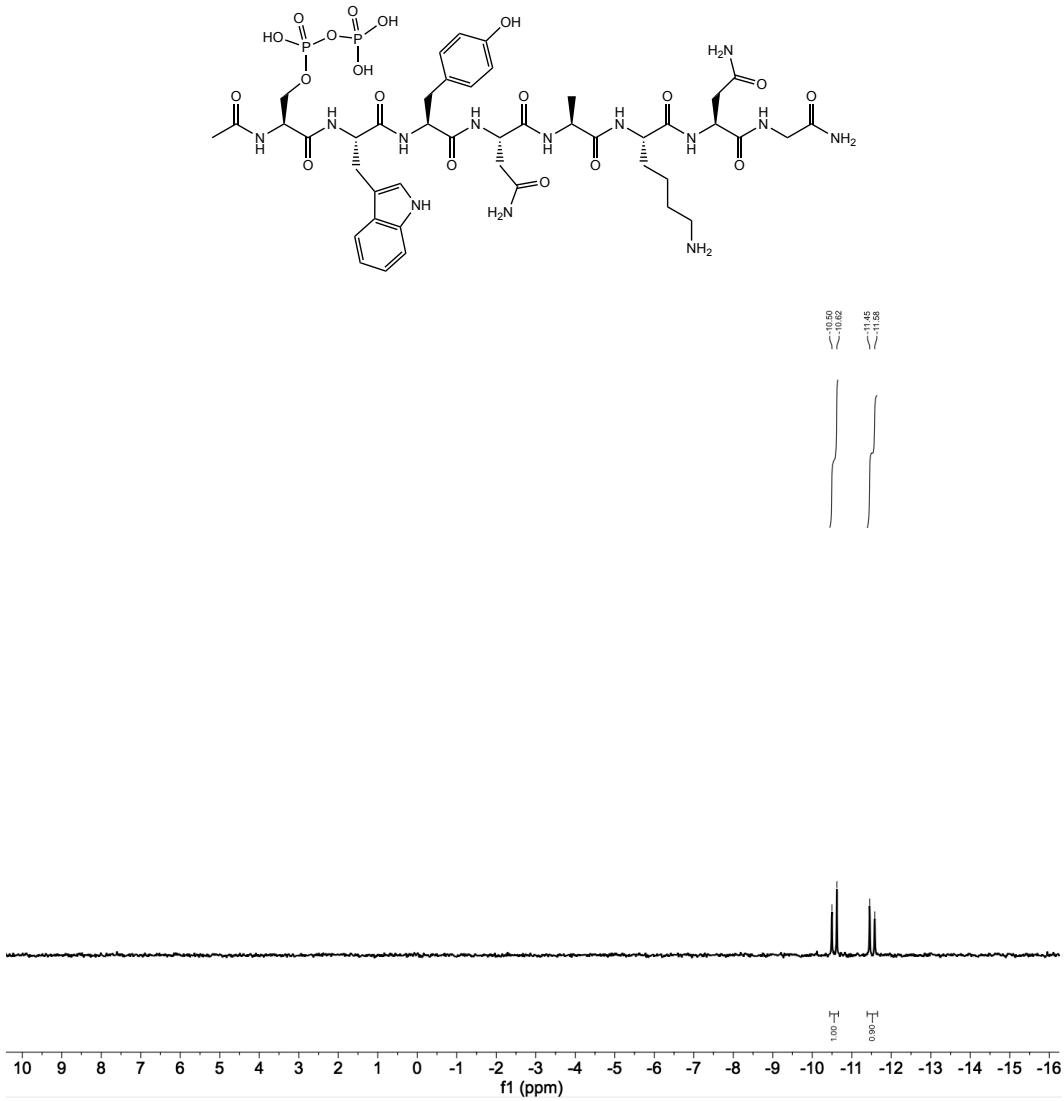

Figure S73. {H-decoupled} ^{31}P NMR spectrum of pyrophosphopeptide **41** after adding EDTA (Mg^{2+} chelation) in D_2O.

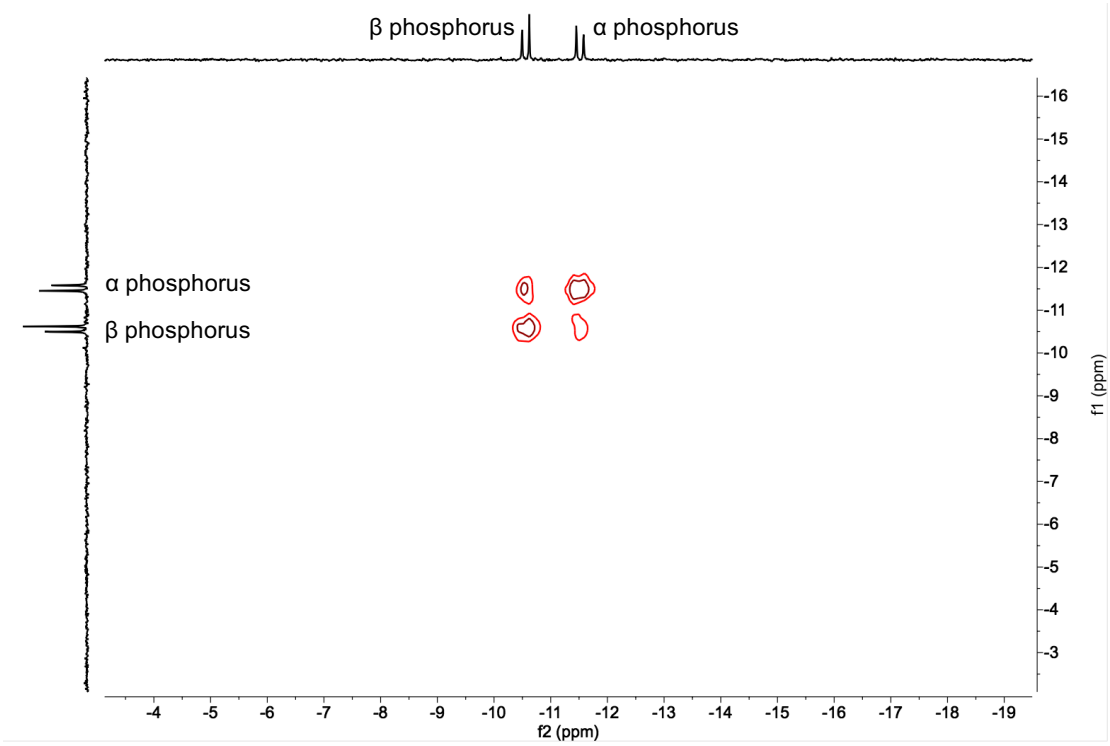

Figure S74. ^{31}P-^{31}P COSY NMR spectrum of pyrophosphopeptide **41** after adding EDTA (Mg^{2+} chelation) in D_2O.

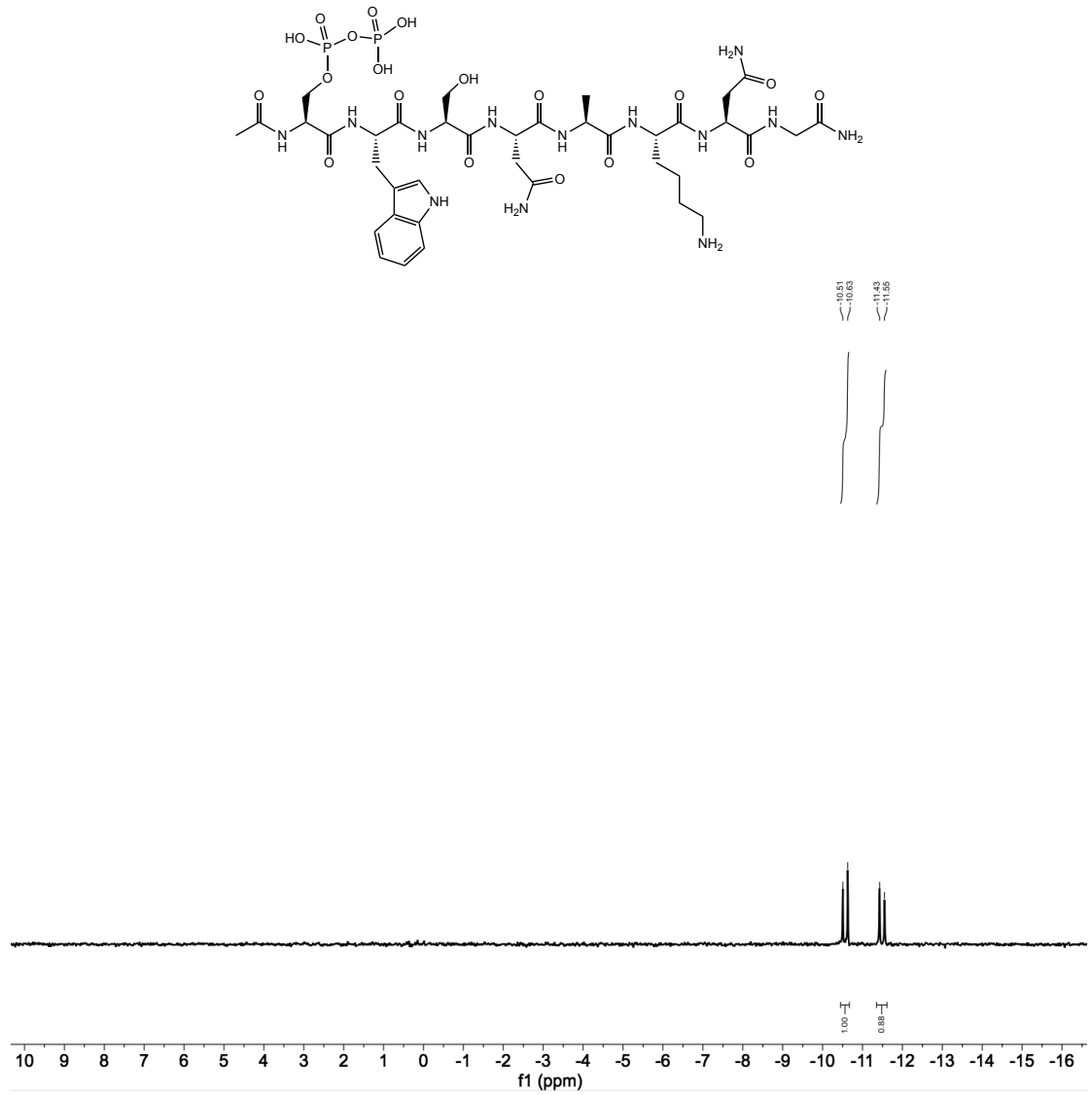

Figure S75. {H-decoupled} ^{31}P NMR spectrum of pyrophosphopeptide **43** after adding EDTA (Mg^{2+} chelation) in D_2O.

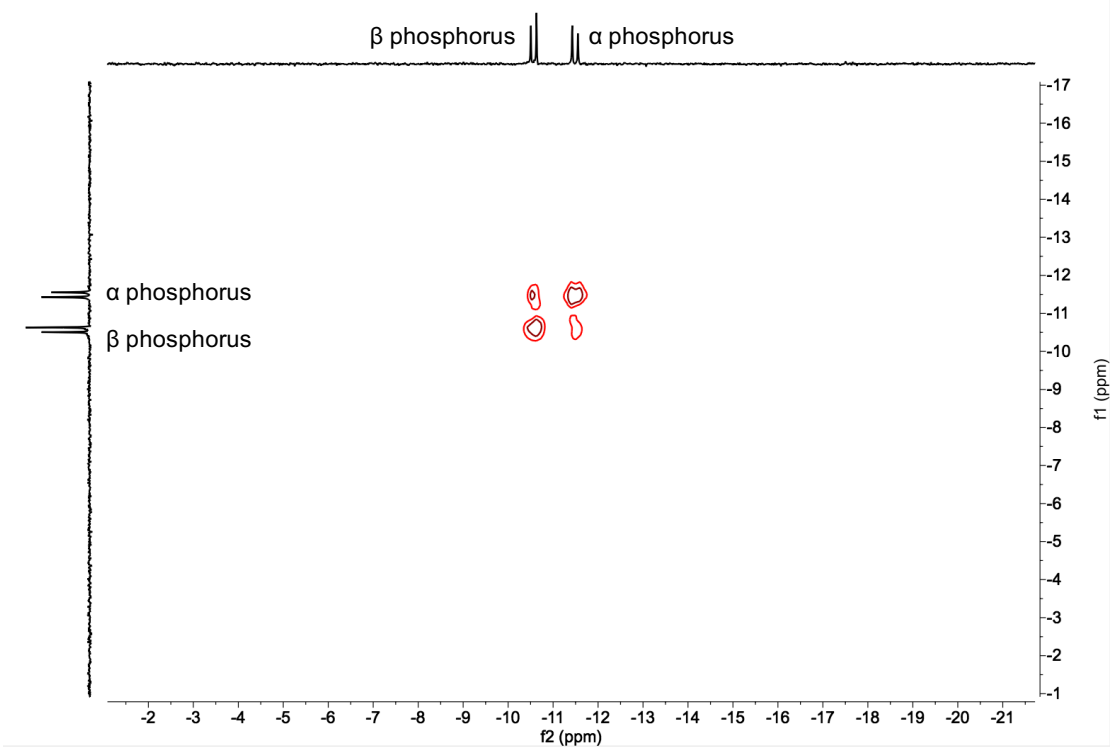

Figure S76. ^{31}P-^{31}P COSY NMR spectrum of pyrophosphopeptide **43** after adding EDTA (Mg^{2+} chelation) in D_2O.

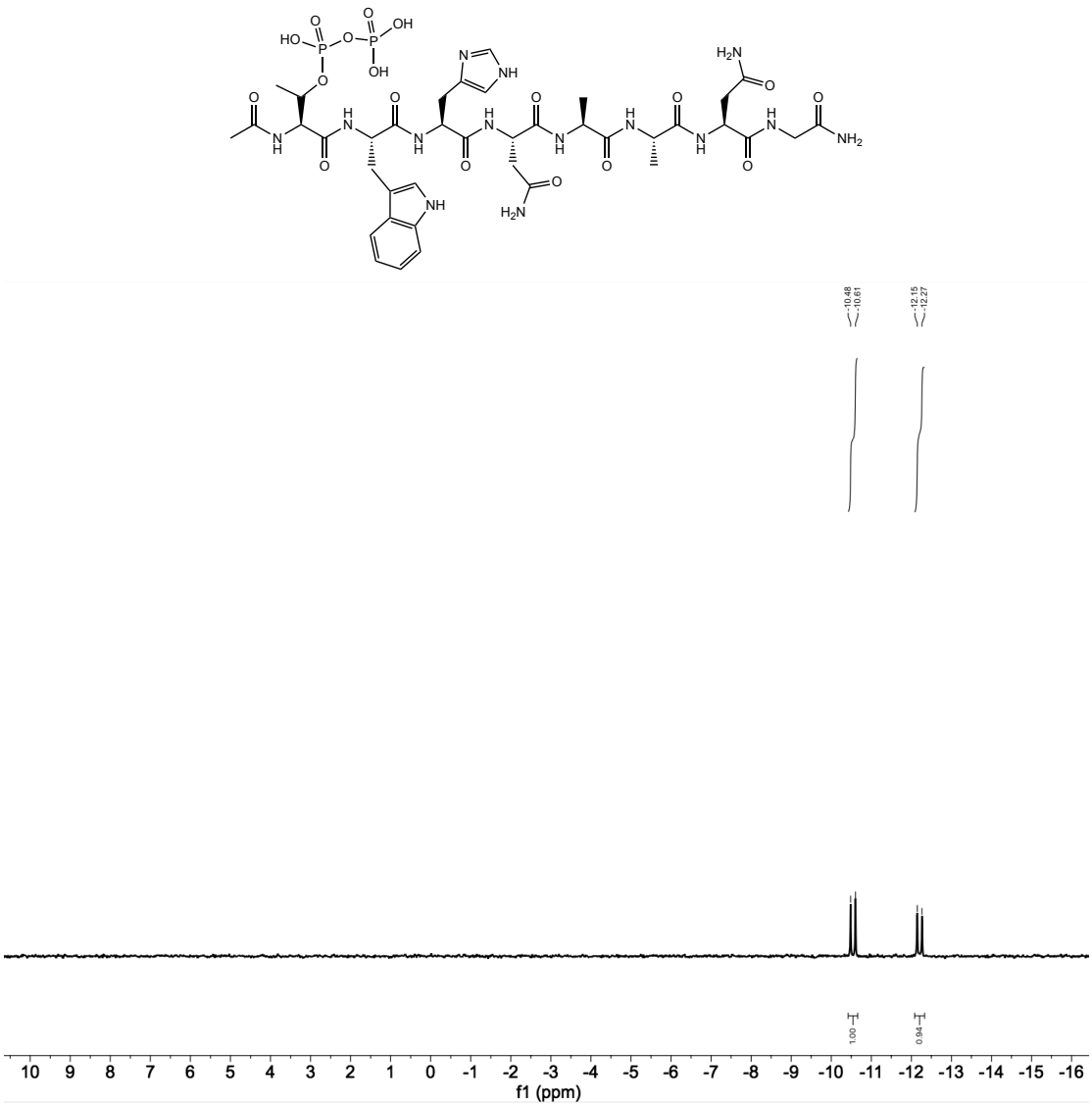

Figure S77. {H-decoupled} ^{31}P NMR spectrum of pyrophosphopeptide **44** after adding EDTA (Mg^{2+} chelation) in D_2O.

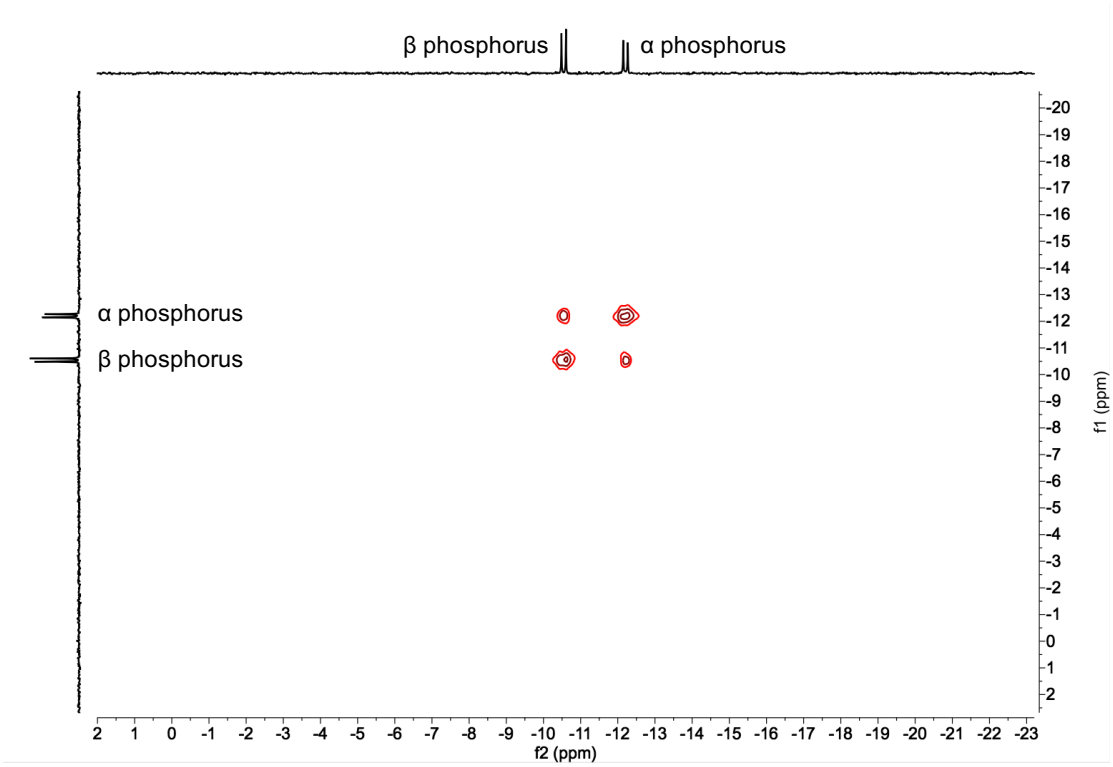

Figure S78. ^{31}P-^{31}P COSY NMR spectrum of pyrophosphopeptide **44** after adding EDTA (Mg^{2+} chelation) in D_2O.

4. Synthesis of RPA190, IC2C, Gcr1 and EIF2S2 fragment pyrophosphopeptides

4.1 Procedure of pyrophosphorylation

To a vial containing 1 mM of phosphopeptide (1 equiv.) in 400 ul H_2O, was added DAP (5 equiv.), magnesium chloride (2 equiv.) and imidazole (2 equiv.). The pH of the reaction mixture was adjusted to 5.5 with hydrochloric acid. The reactions were kept at -20°C in freezer. Progress of the amidophosphorylation was monitored by LC-MS. After 2-3 days without further purification, sodium nitrite (5 equiv.) was added into the same-pot reaction mixture. The pH of the reaction mixture was adjusted to 3.0 with hydrochloric acid. The reactions were kept at -20°C for 20 hours. Progress of the hydrolysis was monitored by LC-MS. Conversion of amidopyrophosphopeptide and final pyrophosphopeptide were determined based on the area-under-the-curve at 230 nm by analytical HPLC.

4.2 Liquid chromatography-mass spectrometry (LC-MS)

Synthesis and analytical data for RPA190 fragment amidophosphopeptide **31**

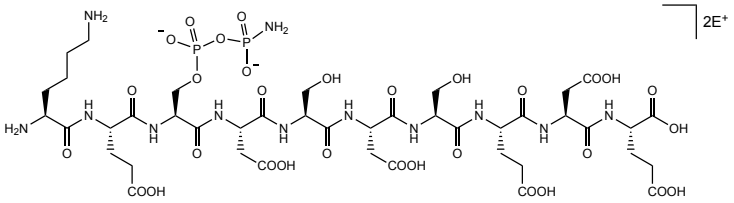

E^+ = Phosphate counter-ions (H^+, Na^+, 0.5 Mg^{2+})

Amidopyrophosphopeptide **31** was synthesized from **15** with the representative protocol using DAP, magnesium chloride and imidazole in 82% conversion indicated by HPLC and used for the next step without any further purification.

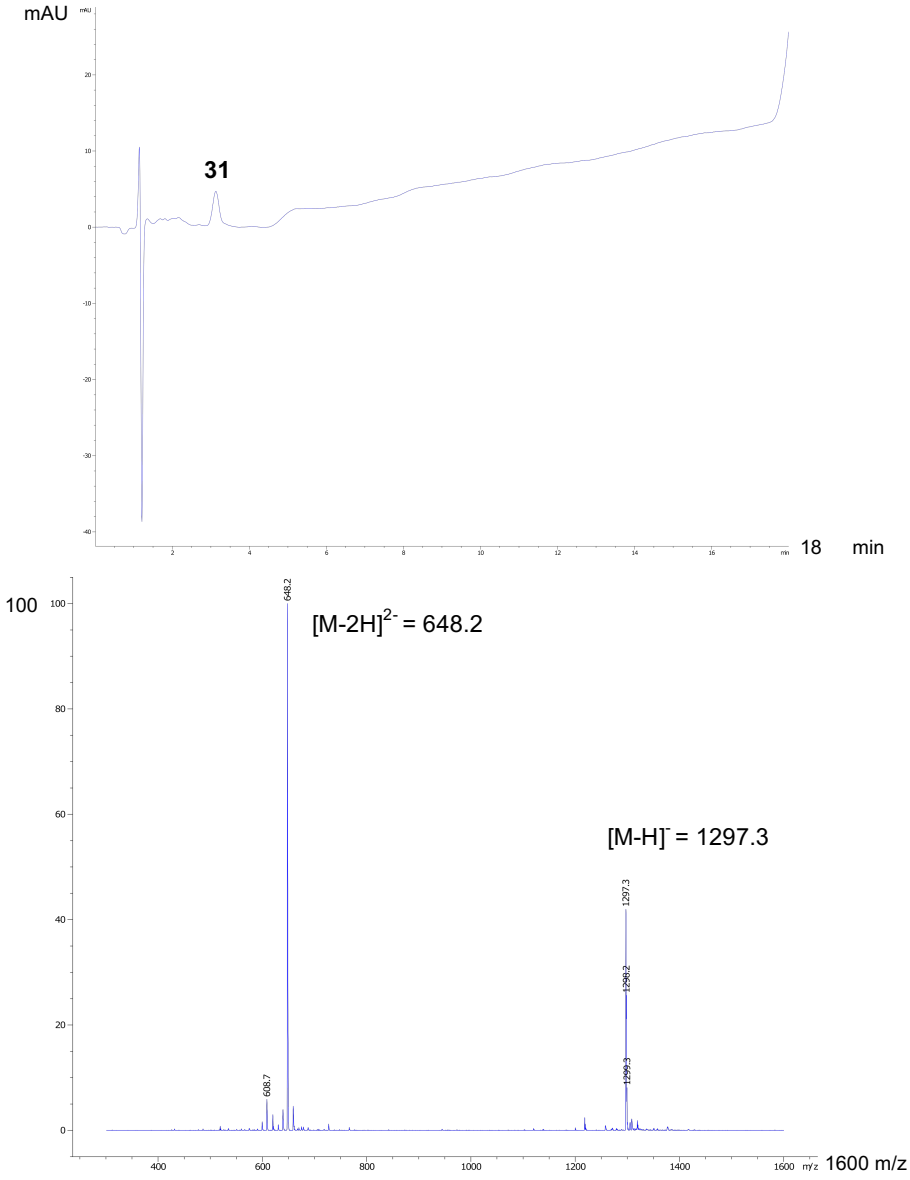

Figure S79. Analytical HPLC-MS spectra showing the production of **31** from **15** in Method F. Calculated mass $[M-H]^-$: 1297.4, observed mass $[M-H]^-$: 1297.3; Calculated mass $[M-2H]^{2-}$: 648.2, observed mass $[M-2H]^{2-}$: 648.2.

Synthesis and analytical data for RPA190 fragment pyrophosphopeptide **47**

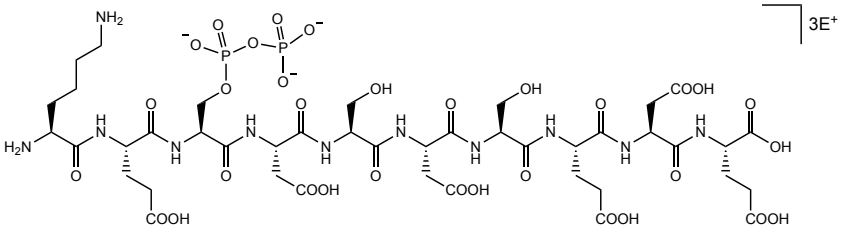

Pyrophosphopeptide **47** was synthesized from **31** following the representative protocol using sodium nitrite in the same pot in 79% conversion over two steps indicated by HPLC.

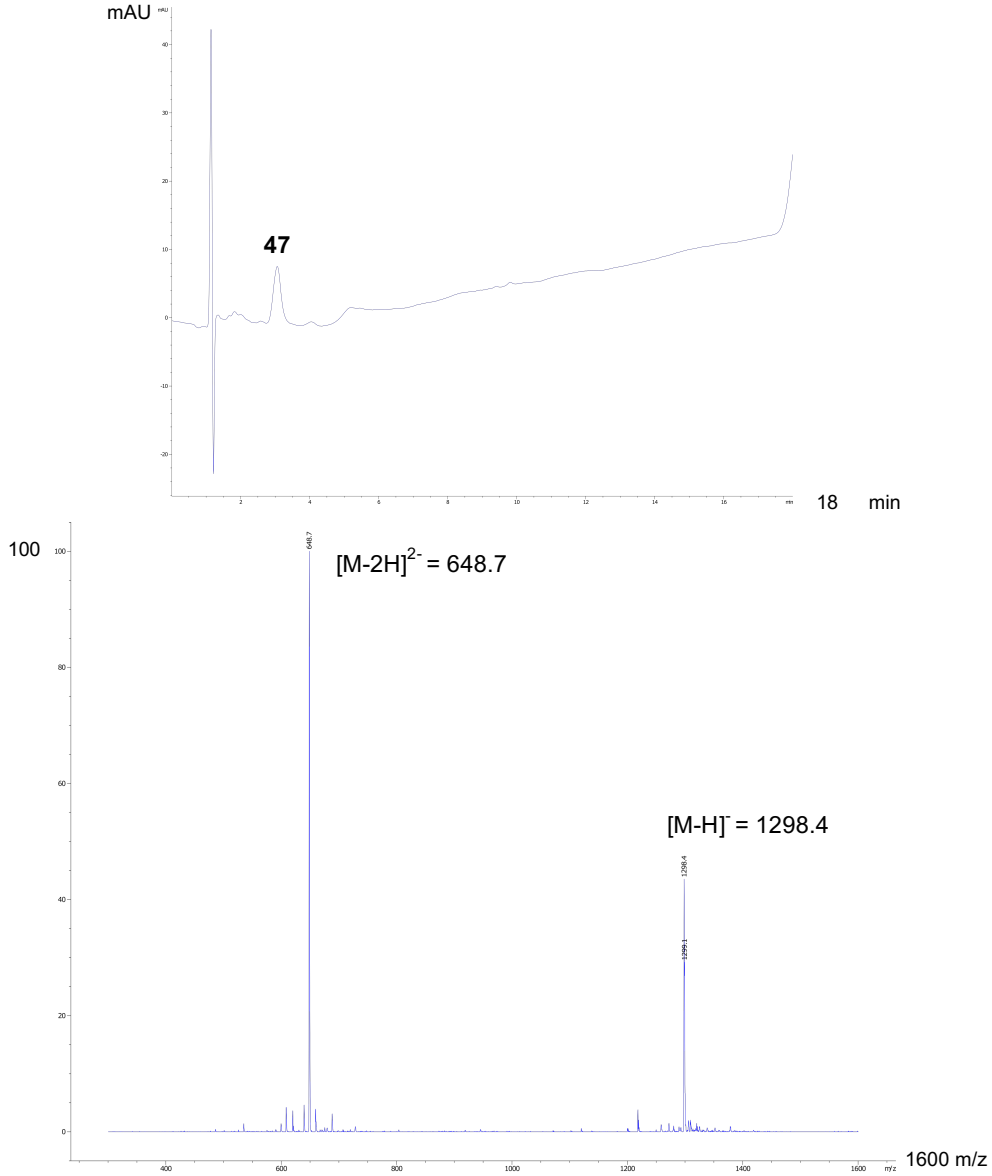

Figure S80. Analytical HPLC-MS spectra showing the production of **47** from **31** in Method F. Calculated mass $[M-H]^-$: 1298.3, observed mass $[M-H]^-$: 1298.4; Calculated mass $[M-2H]^{2-}$: 648.6, observed mass $[M-2H]^{2-}$: 648.7.

Synthesis and analytical data for IC2C fragment amidopyrophosphopeptide **32**

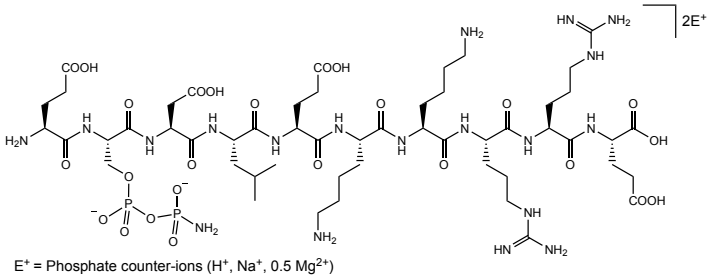

Amidopyrophosphopeptide **32** was synthesized from **16** with the representative protocol using DAP, magnesium chloride and imidazole in 63% conversion indicated by HPLC and used for the next step without any further purification.

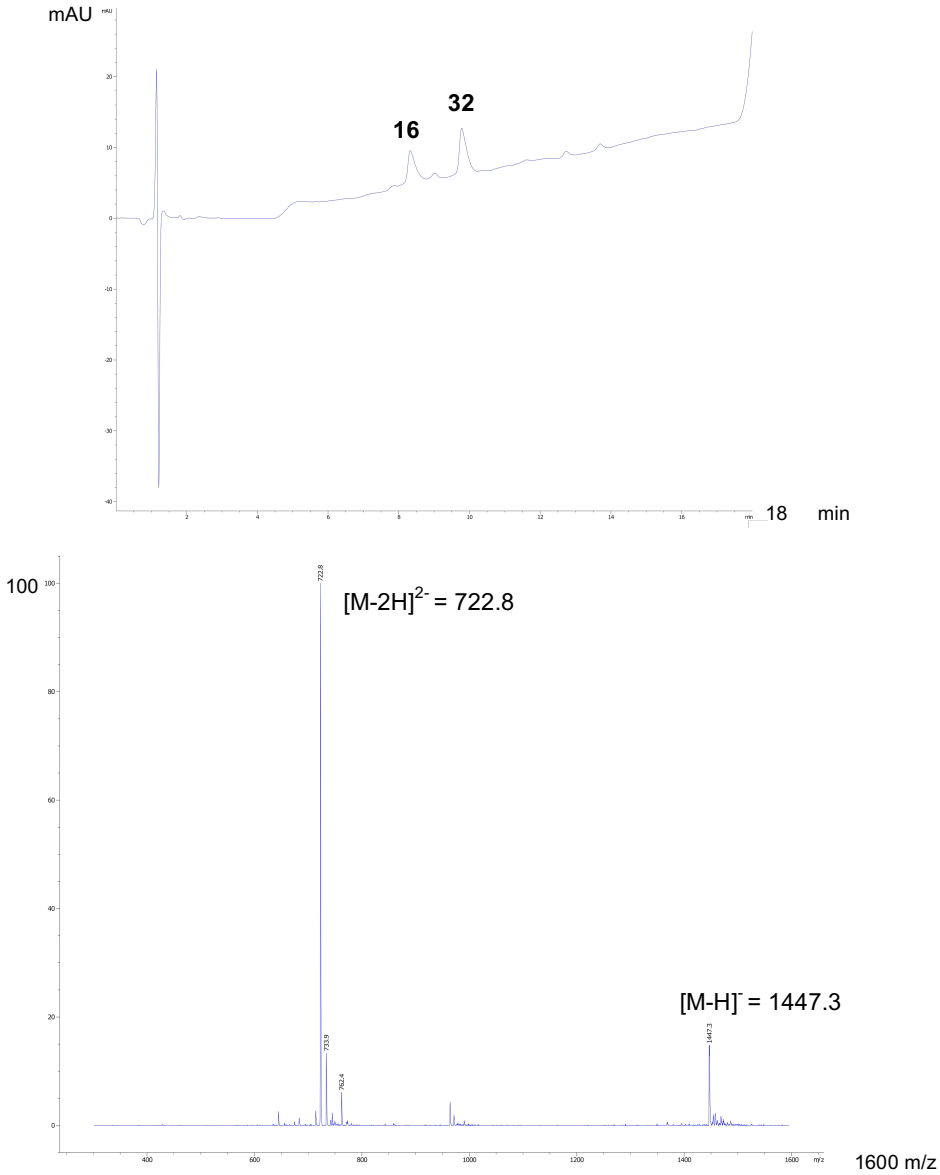

Figure S81. Analytical HPLC-MS spectra showing the production of **32** from **16** in Method F. Calculated mass $[M-H]^-$: 1447.4, observed mass $[M-H]^-$: 1447.3; Calculated mass $[M-2H]^{2-}$: 722.8, observed mass $[M-2H]^{2-}$: 722.8.

Synthesis and analytical data for IC2C fragment pyrophosphopeptide **48**

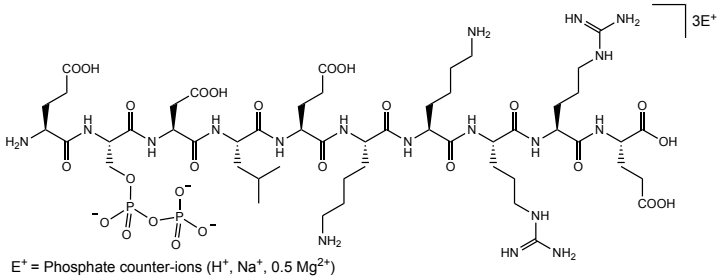

Pyrophosphopeptide **48** was synthesized from **32** following the representative protocol using sodium nitrite in the same pot in 60% conversion over two steps indicated by HPLC.

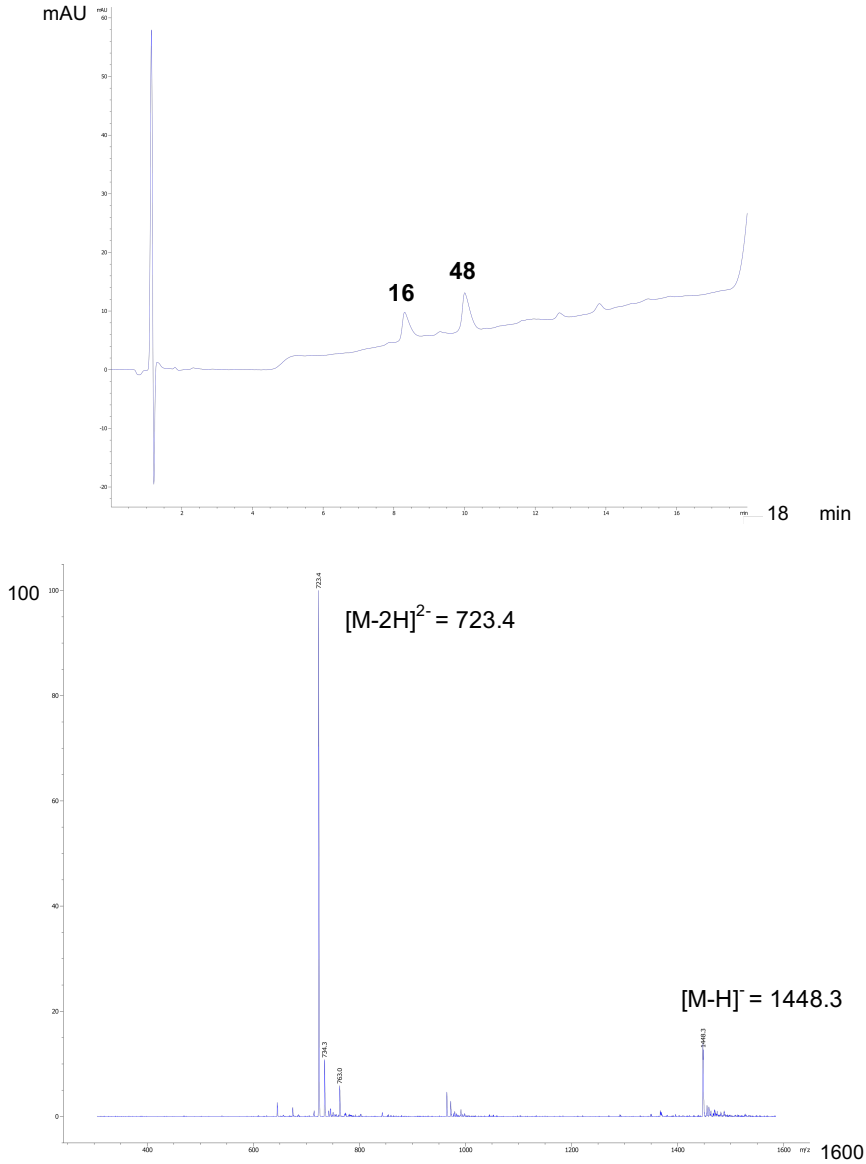

Figure S82. Analytical HPLC-MS spectra showing the production of **48** from **32** in Method F. Calculated mass $[M-H]^-$: 1448.4, observed mass $[M-H]^-$: 1448.3; Calculated mass $[M-2H]^{2-}$: 723.3, observed mass $[M-2H]^{2-}$: 723.4.

Synthesis and analytical data for Gcr1 fragment amidopyrophosphopeptide **33**

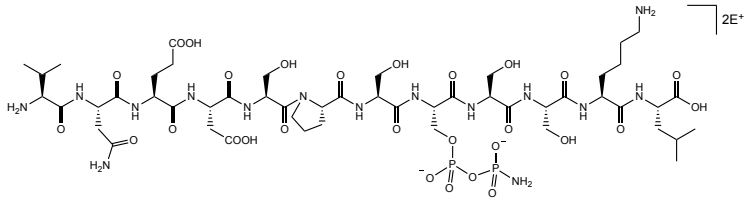

E^+ = Phosphate counter-ions (H^+, Na^+, 0.5 Mg^{2+})

Amidopyrophosphopeptide **33** was synthesized from **17** with the representative protocol using DAP, magnesium chloride and imidazole in 88% conversion indicated by HPLC and used for the next step without any further purification.

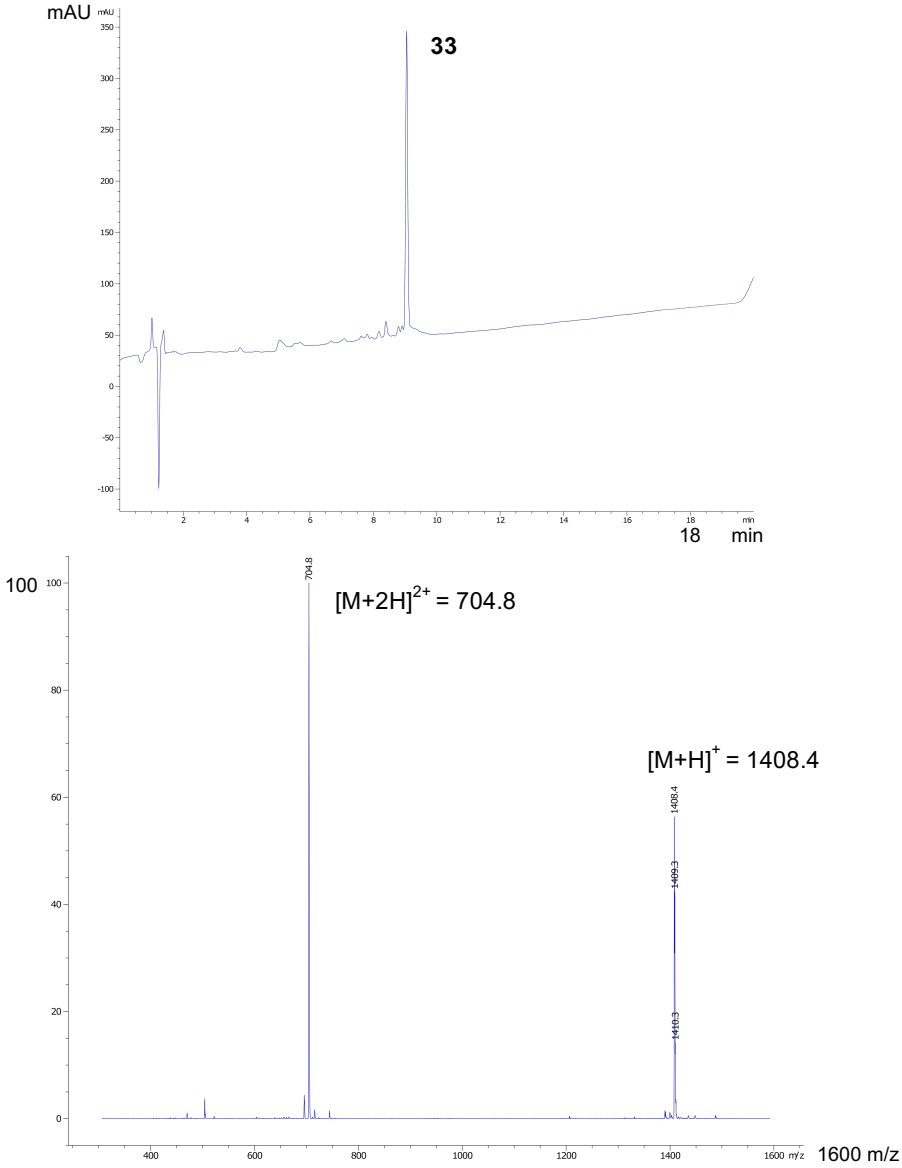

Figure S83. Analytical HPLC-MS spectra showing the production of **33** from **17** in Method B. Calculated mass $[M+H]^+$: 1408.5, observed mass $[M+H]^+$: 1408.4; Calculated mass $[M+2H]^{2+}$: 704.8, observed mass $[M+2H]^{2+}$: 704.8.

Synthesis and analytical data for Gcr1 fragment pyrophosphopeptide **49**

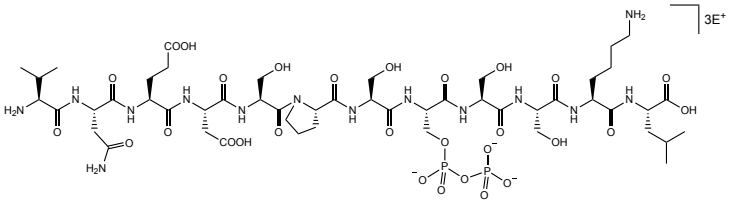

Pyrophosphopeptide **49** was synthesized from **33** following the representative protocol using sodium nitrite in the same pot in 86% conversion over two steps indicated by HPLC.

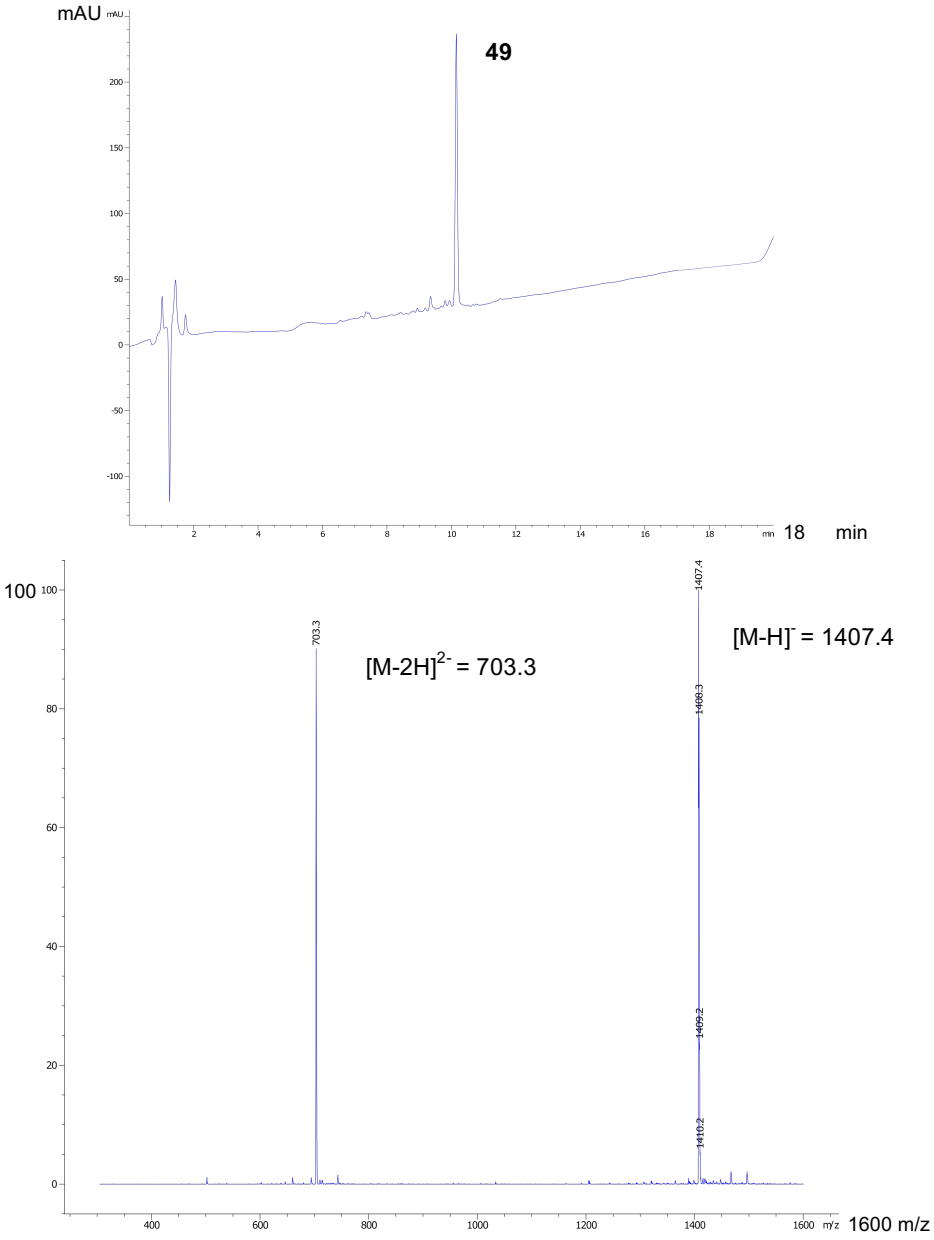

Figure S84. Analytical HPLC-MS spectra showing the production of **49** from **33** in Method B. Calculated mass $[M-H]^-$: 1407.5, observed mass $[M-H]^-$: 1407.4; Calculated mass $[M-2H]^{2-}$: 703.3, observed mass $[M-2H]^{2-}$: 703.3.

Synthesis and analytical data for EIF2S2 fragment amidophosphopeptide **34**

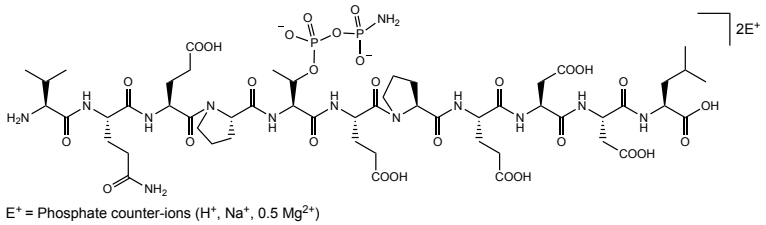

Amidopyrophosphopeptide **34** was synthesized from **18** with the representative protocol using DAP, magnesium chloride and imidazole in 70% conversion indicated by HPLC and used for the next step without any further purification.

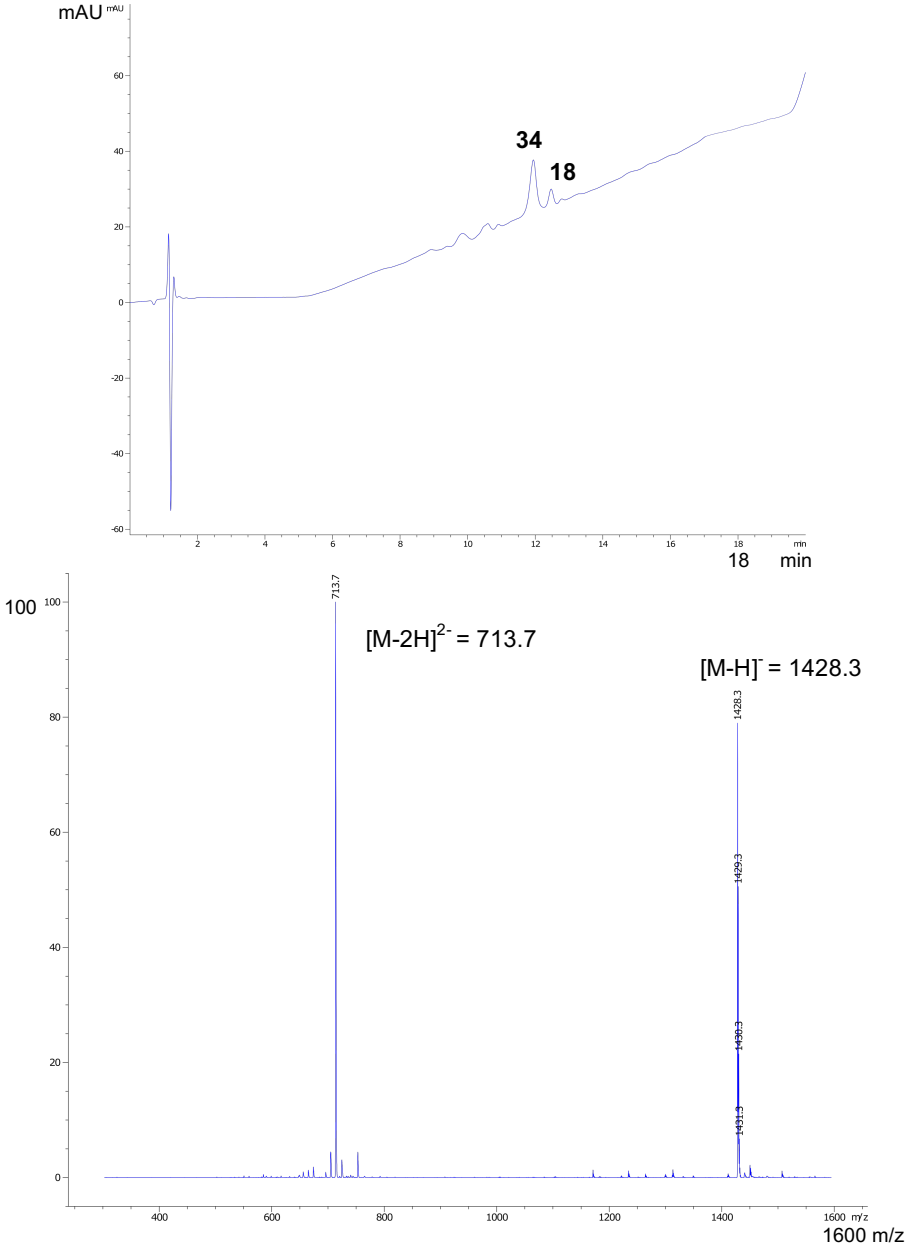

Figure S85. Analytical HPLC-MS spectra showing the production of **34** from **18** in Method C. Calculated mass $[M-H]^-$: 1428.5, observed mass $[M-H]^-$: 1428.3; Calculated mass $[M-2H]^{2-}$: 713.7, observed mass $[M-2H]^{2-}$: 713.7.

Synthesis and analytical data for EIF2S2 fragment pyrophosphopeptide **50**

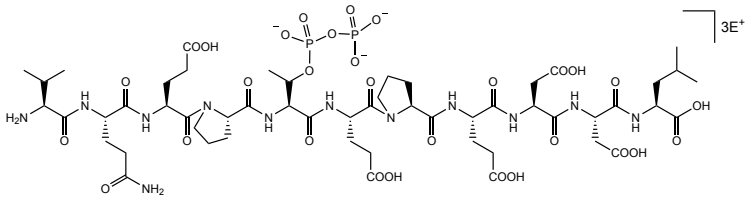

Pyrophosphopeptide **50** was synthesized from **34** following the representative protocol using sodium nitrite in the same pot in 68% conversion over two steps indicated by HPLC.

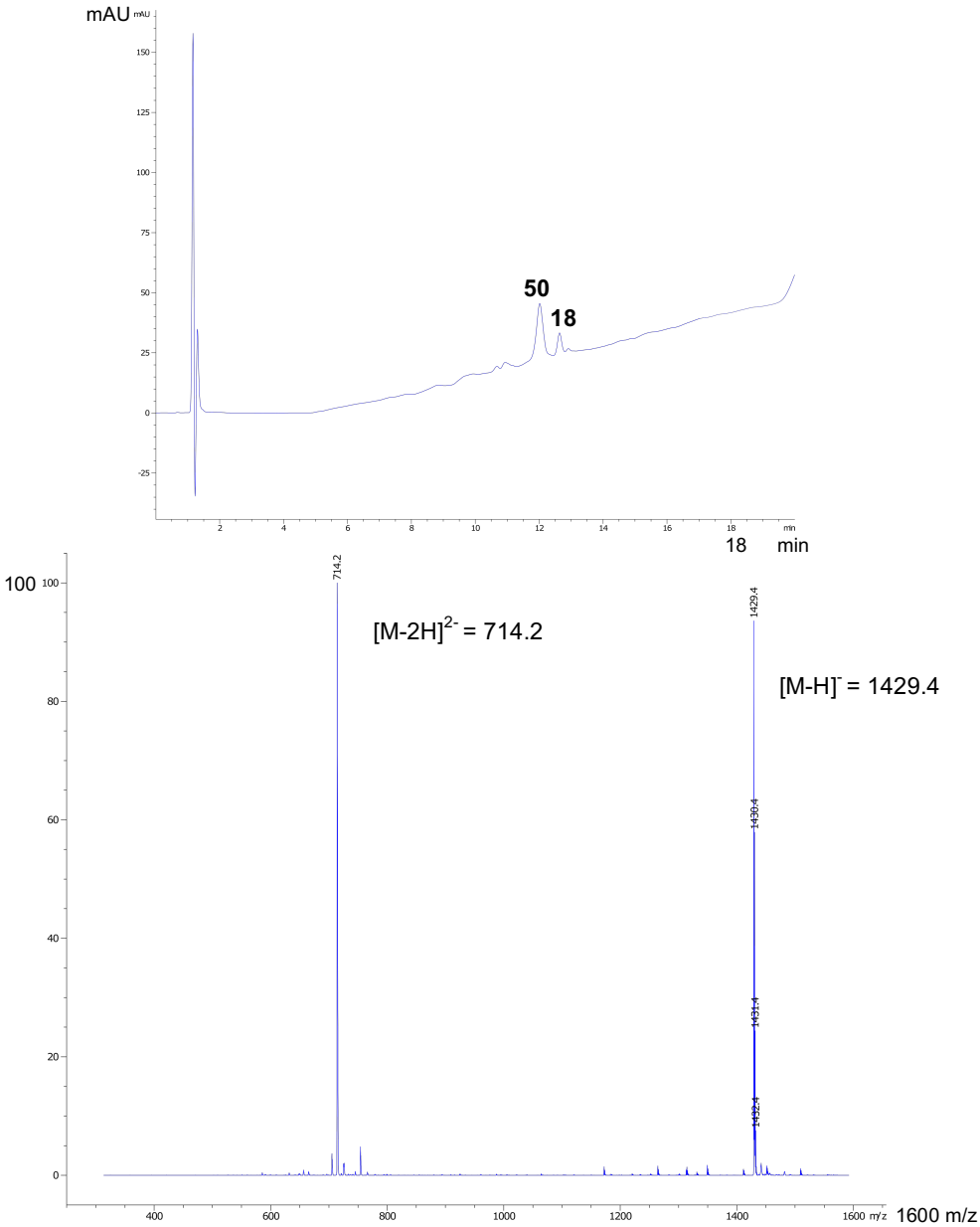

Figure S86. Analytical HPLC-MS spectra showing the production of **50** from **34** in Method C. Calculated mass $[M-H]^-$: 1429.5, observed mass $[M-H]^-$: 1429.4; Calculated mass $[M-2H]^{2-}$: 714.2, observed mass $[M-2H]^{2-}$: 714.2.

5. Tandem MS/MS spectrometry

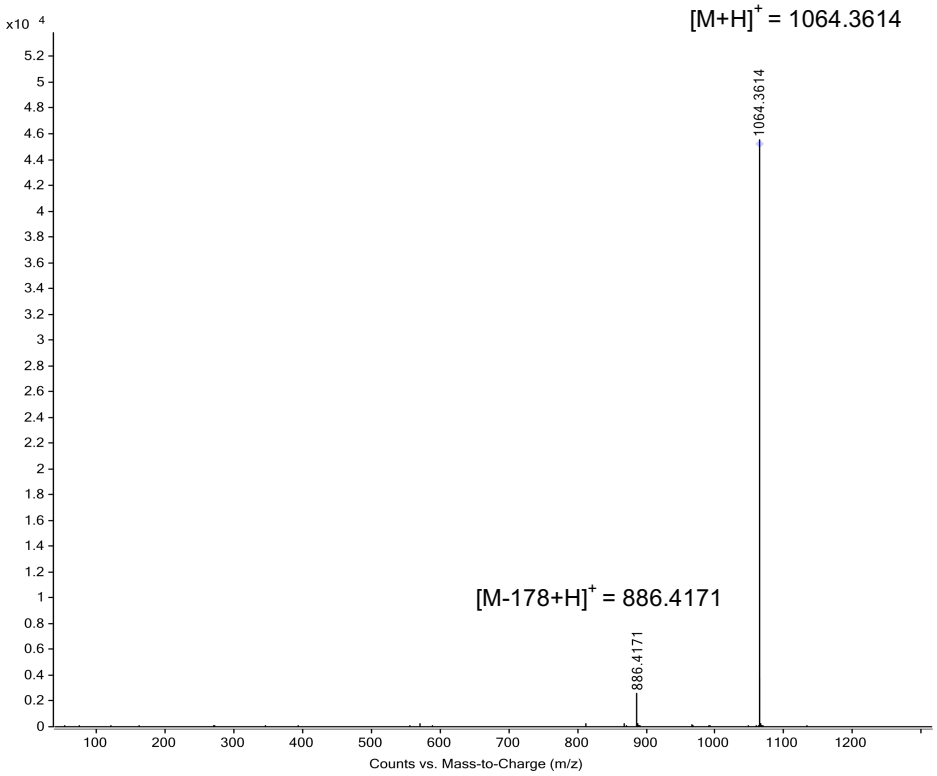

Figure S87. MS/MS spectrum of pure pyrophosphopeptide **43** in positive ion mode with a collision energy of 0 V (collision-induced dissociation). The precursor ion of **43** at 1064.3614 was prominently featured. The fragment ion of **43** losing the pyrophosphate group (M-178) was observed at 886.4171. Calculated mass $[M+H]^+$: 1064.3598, observed mass $[M+H]^+$: 1064.3614; Calculated mass $[M-178+H]^+$: 886.4166, observed mass $[M-178+H]^+$: 886.4171.

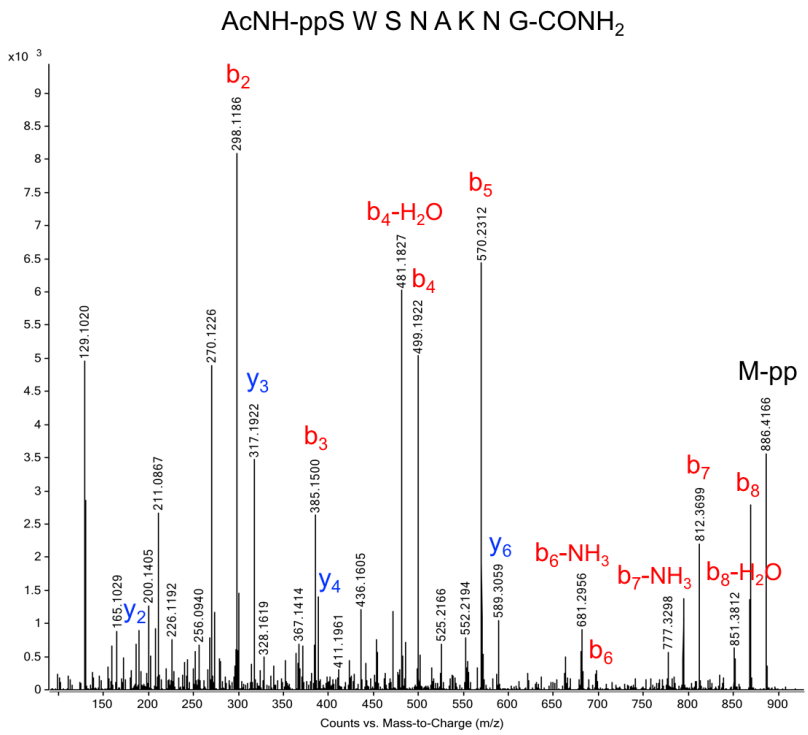

Figure S88. MS/MS spectrum of pure pyrophosphopeptide **43** in positive ion mode with a collision energy of 60 V (collision-induced dissociation). The precursor ion of **43** was not present any longer. The fragment ion of **43** losing the pyrophosphate group **43**-pp (**43**-178) and other abundant fragment ions were observed, confirming the pyrophosphorylation site in phosphoserine. The sequence of **43** as AcNH-ppSWSNAKNG-$CONH_2$ was confirmed by matching b-ions (red) and y-ions (blue) fragments. The b-ions were retained by the amino-terminal part of **43**-pp and the y-ions were retained by the carboxyl-terminal part of **43**-pp.

6. Synthesis of Nopp140 fragment pyrophosphopeptide

6.1 Procedure of pyrophosphorylation

To a vial containing 1 mM of phosphopeptide (1 equiv.) in 400 ul H_2O, was added DAP (8 equiv.), magnesium chloride (2 equiv.) and imidazole (2 equiv.). The pH of the reaction mixture was adjusted to 5.5 with hydrochloric acid. The reactions were kept at -20°C in freezer. Progress of the amidophosphorylation was monitored by LC-MS. After 20 hours without any further purification, sodium nitrite (8 equiv.) was added into the same-pot reaction mixture. The pH of the reaction mixture was adjusted to 3.0 with hydrochloric acid. The reactions were kept at -20°C for 8 hours. Progress of the hydrolysis was monitored by LC-MS. The conversion of amidopyrophosphopeptide and final pyrophosphopeptide were determined based on the area-under-the-curve at 230 nm by analytical HPLC.

6.2 Liquid chromatography-mass spectrometry (LC-MS)

Synthesis and analytical data for Nopp140 fragment amidophosphopeptide **53**

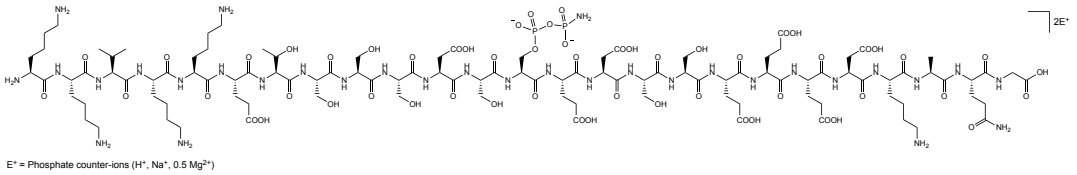

Amidopyrophosphopeptide **53** was synthesized from **52** with the representative protocol using DAP, magnesium chloride and imidazole in 75% conversion indicated by HPLC and used for the next step without any further purification.

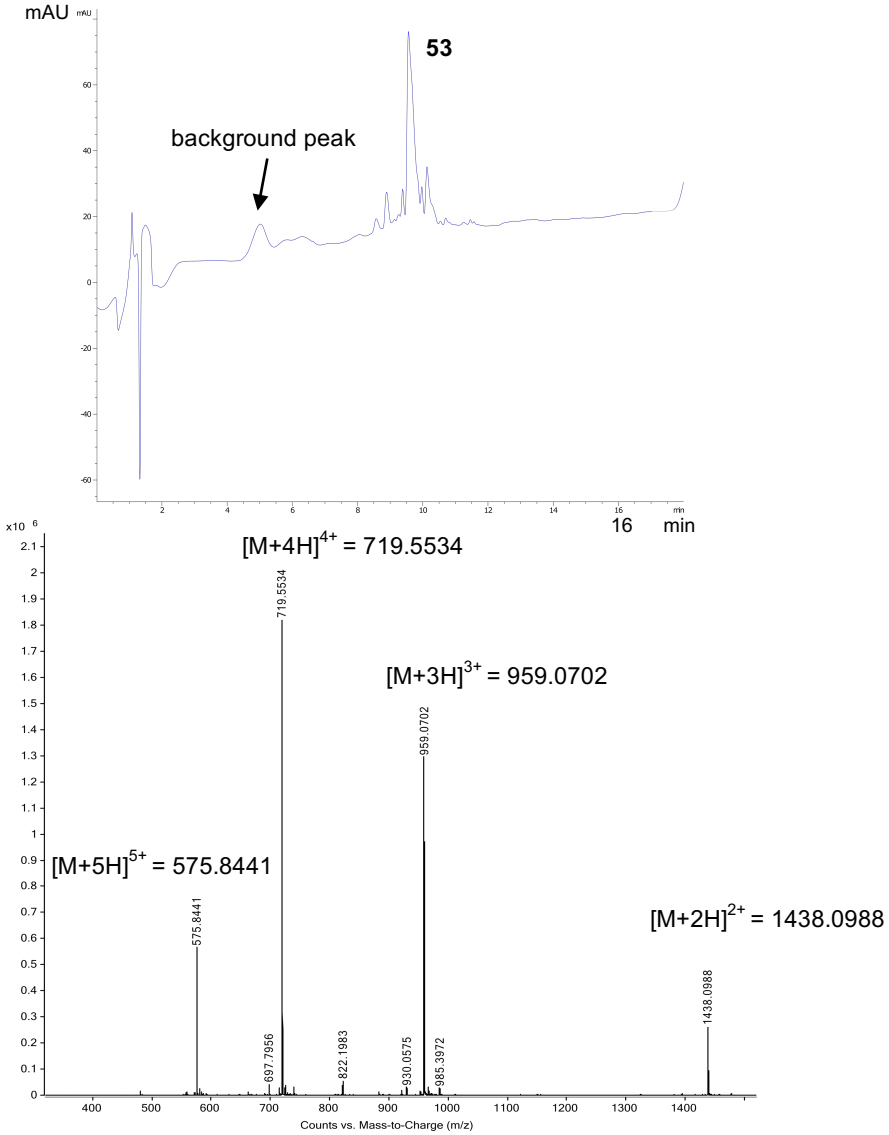

Figure S89. Analytical HPLC-MS spectra showing the production of **53** from **52** in Method D. Calculated mass $[M+2H]^{2+}$: 1438.1016, observed mass $[M+2H]^{2+}$: 1438.0988; Calculated mass $[M+3H]^{3+}$: 959.0702, observed mass $[M+3H]^{3+}$: 959.0702; Calculated mass $[M+4H]^{4+}$: 719.5544, observed mass $[M+4H]^{4+}$: 719.5534; Calculated mass $[M+5H]^{5+}$: 575.8450, observed mass $[M+5H]^{5+}$: 575.8441.

Synthesis and analytical data for Nopp140 fragment pyrophosphopeptide **54**

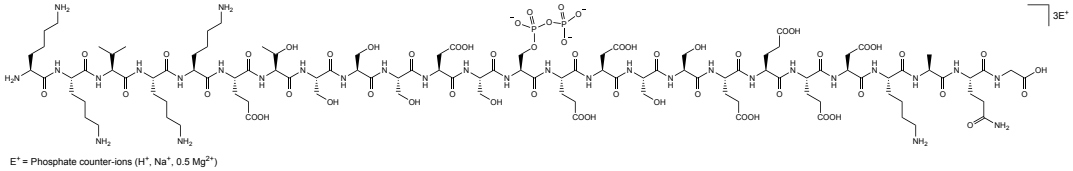

Pyrophosphopeptide **54** was synthesized from **53** following the representative protocol using sodium nitrite in the same pot in 70% conversion over two steps indicated by HPLC.

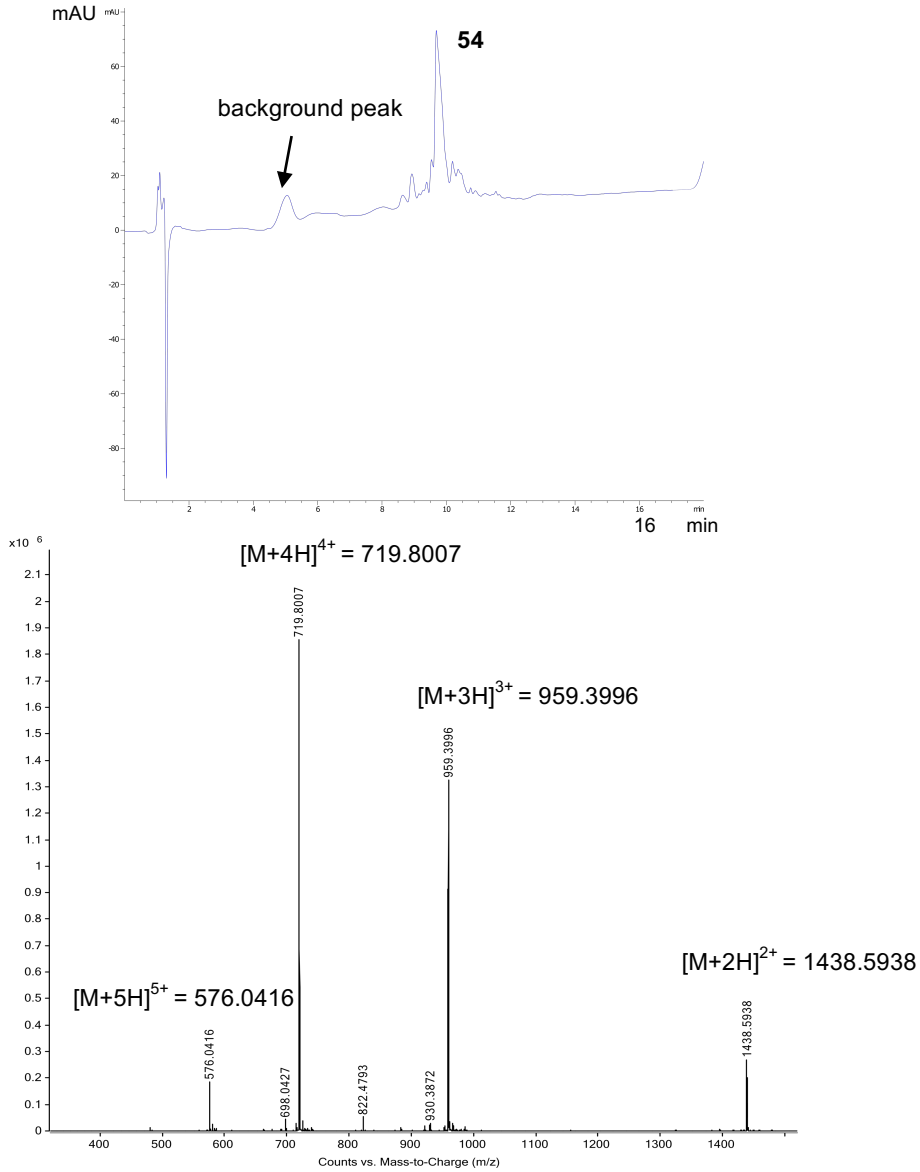

Figure S90. Analytical HPLC-MS spectra showing the production of **54** from **53** in Method D. Calculated mass $[M+2H]^{2+}$: 1438.5936, observed mass $[M+2H]^{2+}$: 1438.5938; Calculated mass $[M+3H]^{3+}$: 959.3982, observed mass $[M+3H]^{3+}$: 959.3996; Calculated mass $[M+4H]^{4+}$: 719.8004, observed mass $[M+4H]^{4+}$: 719.8007; Calculated mass $[M+5H]^{5+}$: 576.0418, observed mass $[M+5H]^{5+}$: 576.0416.

7. Synthesis of model triphosphopeptides

7.1 Procedure of triphosphorylation

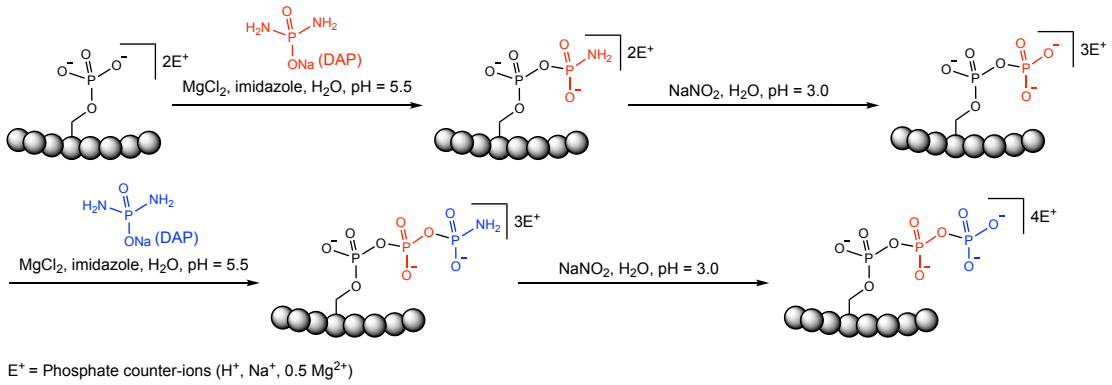

E^+ = Phosphate counter-ions (H^+, Na^+, 0.5 Mg^{2+})

Figure S91. Synthesis of triphosphopeptides from respective phosphopeptides via one-pot four step sequential amidophosphorylation-hydrolysis scenario in water.

To a vial containing 1 mM of phosphopeptide (1 equiv.) in 400 ul H_2O, was added DAP (5 equiv.), magnesium chloride (2 equiv.) and imidazole (2 equiv.). The pH of the reaction mixture was adjusted to 5.5 with hydrochloric acid. The reactions were kept at -20°C in freezer. Progress of the amidophosphorylation reaction was monitored by LC-MS. After 2 days without any further purification, sodium nitrite (5 equiv.) was added into the same-pot reaction mixture. The pH of the reaction mixture was adjusted to 3.0 with hydrochloric acid. The reactions were kept at -20°C for 20 hours. Progress of the hydrolysis was monitored by LC-MS. After pyrophosphopeptides were formed, without any further purification, amidotriphosphorylated and final triphosphorylated peptides were generated by repeating the amidophosphorylation and hydrolysis steps in the same-pot. Progress was monitored by LC-MS and anion exchange liquid chromatography. The conversion was determined based on the area-under-the-curve at 280 nm.

7.2 Liquid chromatography-mass spectrometry (LC-MS) and anion exchange chromatography

Synthesis and analytical data for model amidopyrophosphopeptide **21**

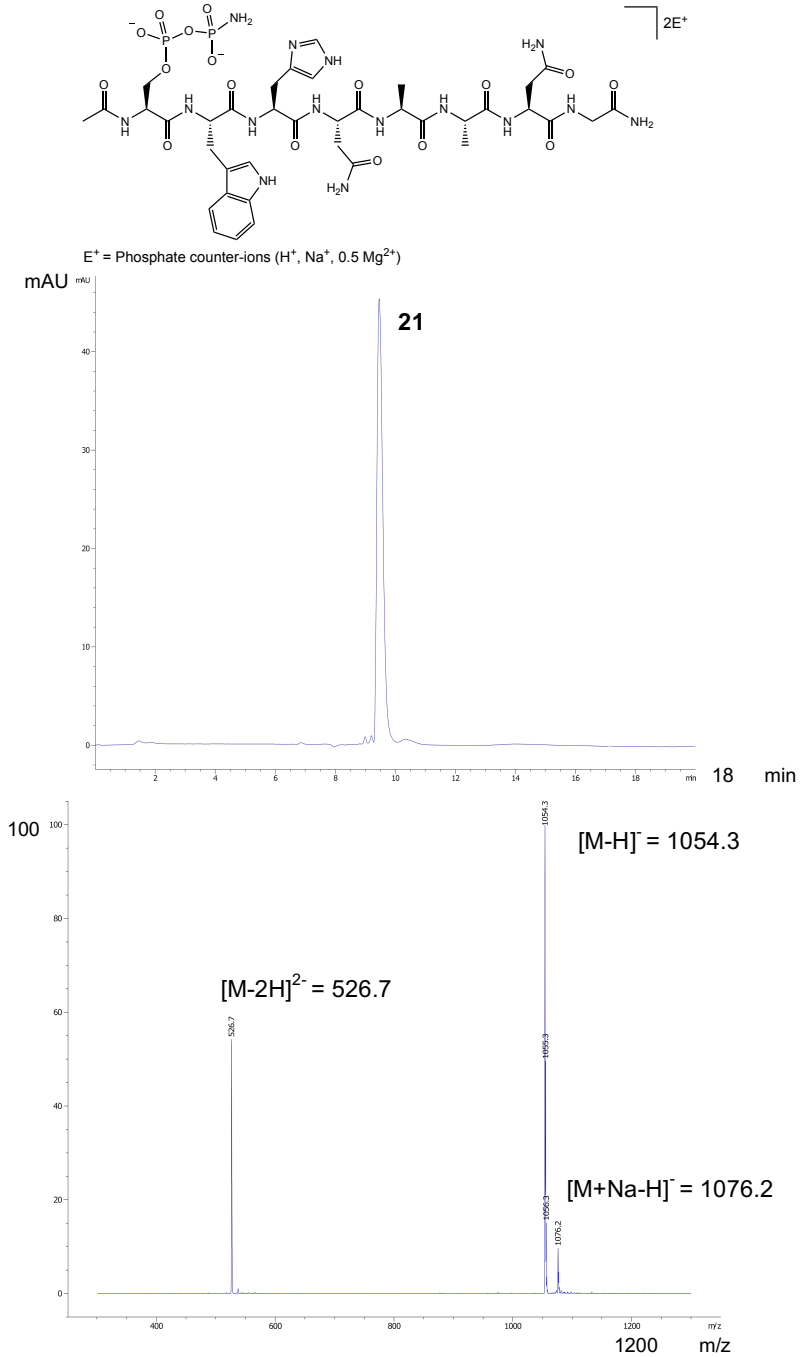

Figure S92. Analytical HPLC-MS spectra showing the production of **21** from **3** in Method A. Calculated mass $[M-H]^-$: 1054.3, observed mass $[M-H]^-$: 1054.3; Calculated mass $[M-2H]^{2-}$: 526.7, observed mass $[M-2H]^{2-}$: 526.7.

Synthesis and analytical data for model pyrophosphopeptide **37**

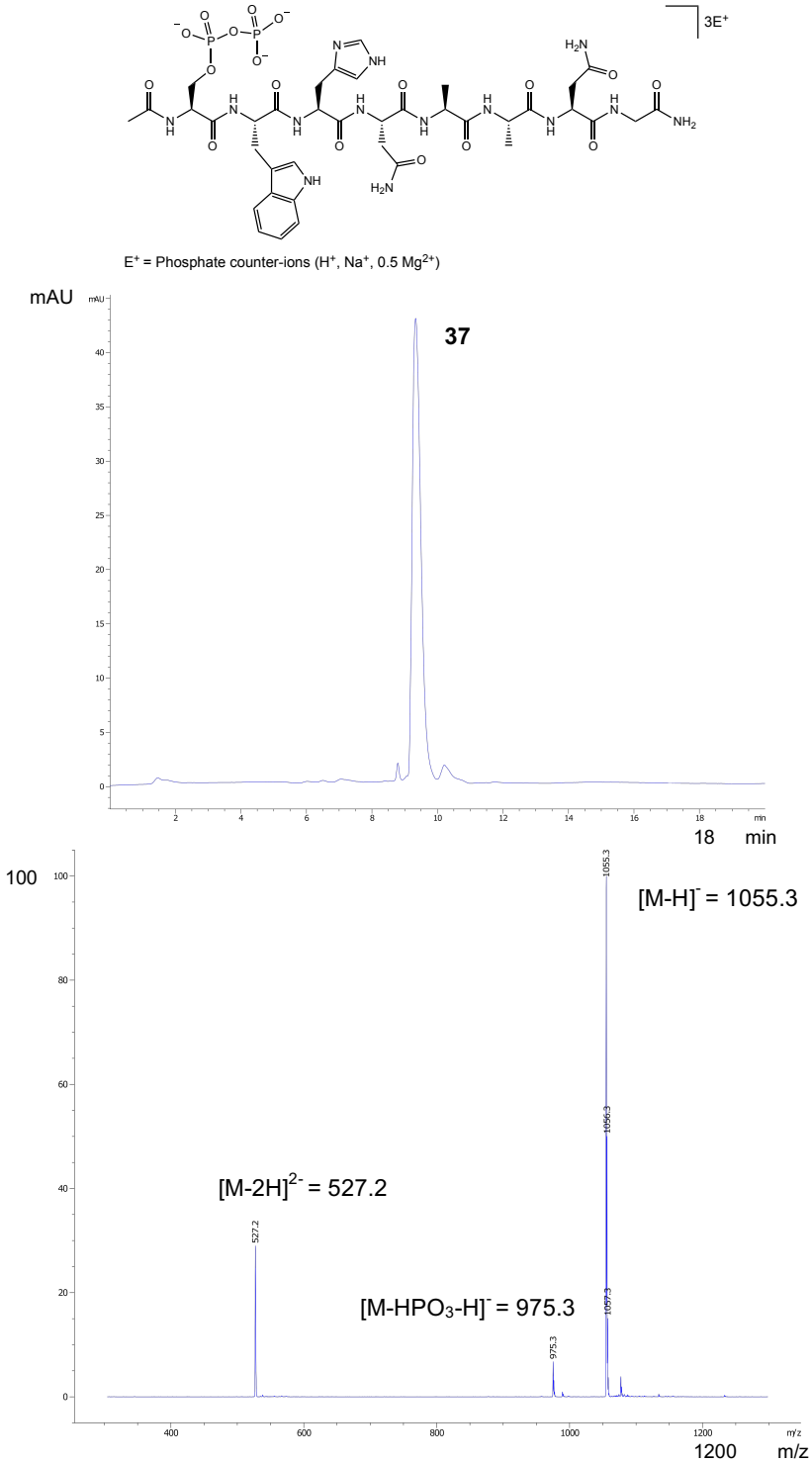

Figure S93. Analytical HPLC-MS spectra showing the production of **37** from **21** in Method A. Calculated mass $[M-H]^-$: 1055.3, observed mass $[M-H]^-$: 1055.3; Calculated mass $[M-2H]^{2-}$: 527.2, observed mass $[M-2H]^{2-}$: 527.2.

Synthesis and analytical data for model amidotriphosphopeptide **55**

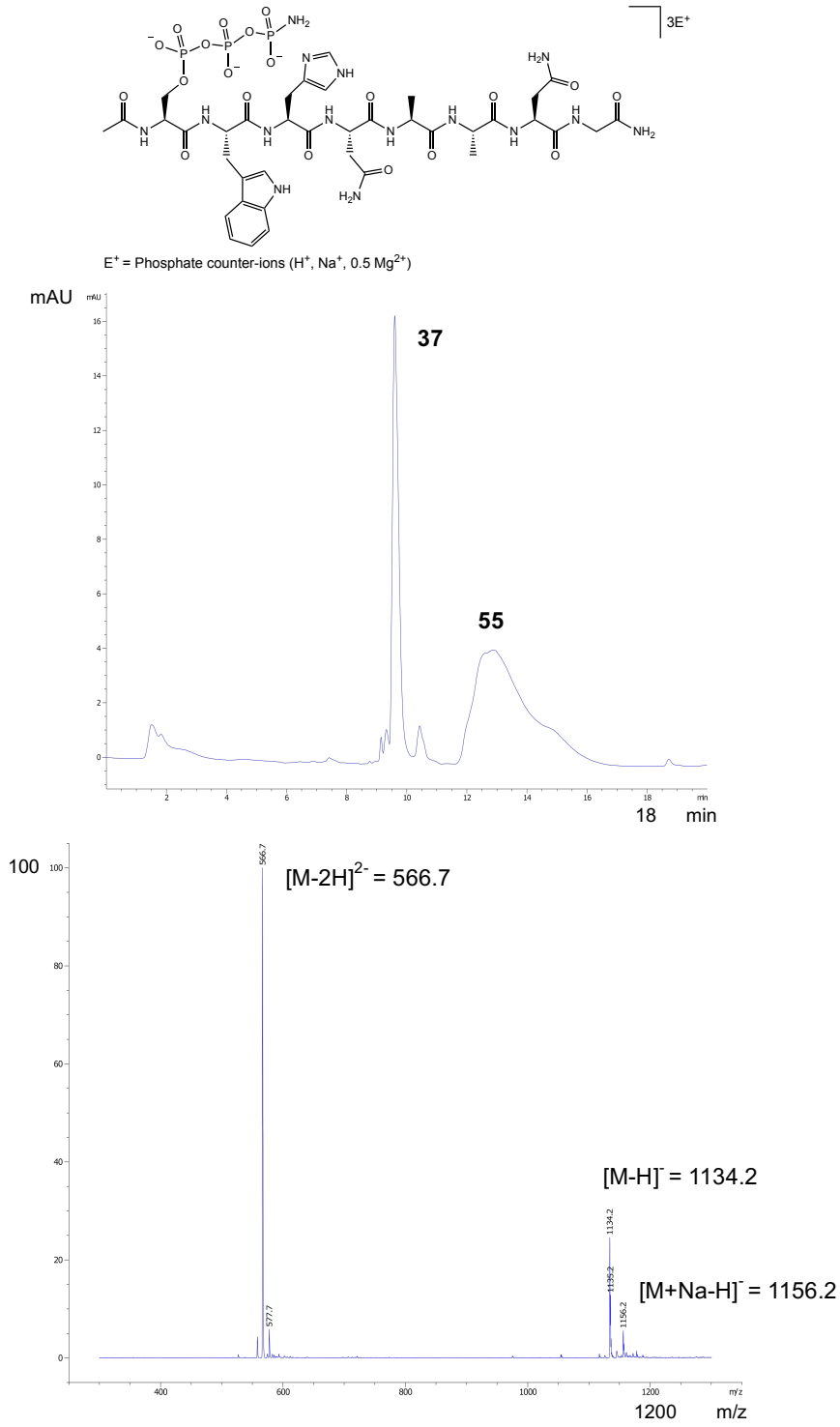

Figure S94. Analytical HPLC-MS spectra showing the production of **55** from **37** in Method A. The HPLC indicated 65% conversion. Calculated mass $[M-H]^-$: 1134.3, observed mass $[M-H]^-$: 1134.2; Calculated mass $[M-2H]^{2-}$: 566.6, observed mass $[M-2H]^{2-}$: 566.7.

Synthesis and analytical data for model triphosphopeptide **56**

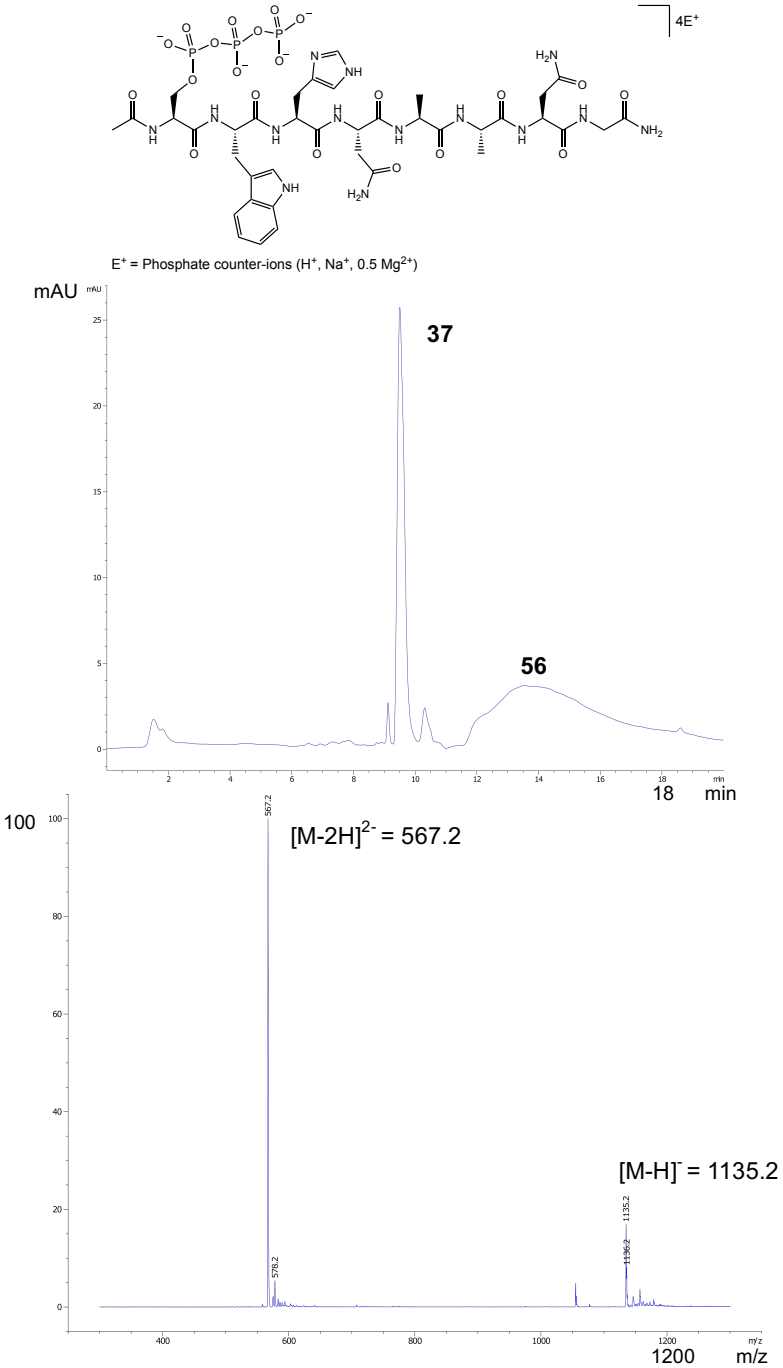

Figure S95. Analytical HPLC-MS spectra showing the production of **56** from **55** in Method A. Calculated mass $[M-H]^-$: 1135.3, observed mass $[M-H]^-$: 1135.2; Calculated mass $[M-2H]^{2-}$: 567.1, observed mass $[M-2H]^{2-}$: 567.2. Triphosphopeptide **56** was not retained well on the column, appearing as a broad peak in the chromatogram. Instead, the reaction mixture of **56** was analyzed by anion exchange chromatography (see **Figure S96**).

Synthesis and analytical data for model triphosphopeptide **56**

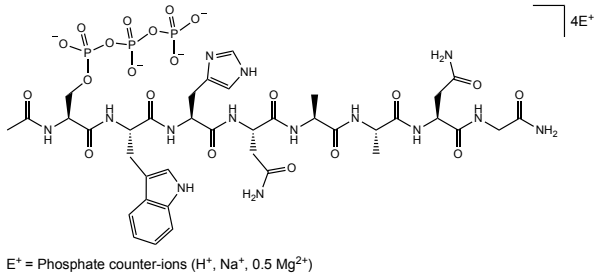

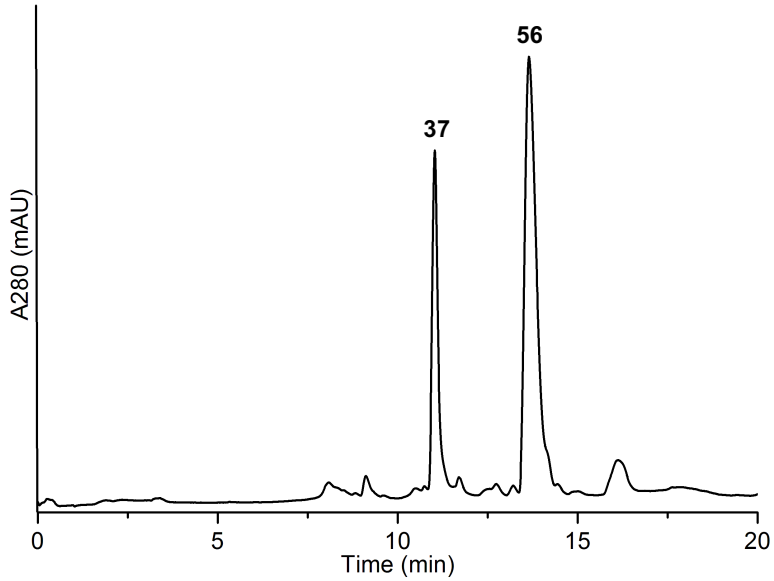

Figure S96. Anion exchange chromatogram trace showing the production of **56** from **55** with remaining **37**. The anion exchange chromatogram at 280 nm indicated the formation of pyrophosphopeptide **37** in 25% and triphosphopeptide **56** in 61% conversion, respectively, starting from phosphopeptide **3** via sequential phosphorylation-hydrolysis scenario in H_2O in one-pot four step sequence. Note: we switched to ion-exchange chromatography for analysis since the reverse phase HPLC showed a very broad peak with the correct mass (**Figure S95**). The sharp peak confirmed the clean formation of triphosphopeptide **56**.

Synthesis and analytical data for model amidopyrophosphopeptide **28**

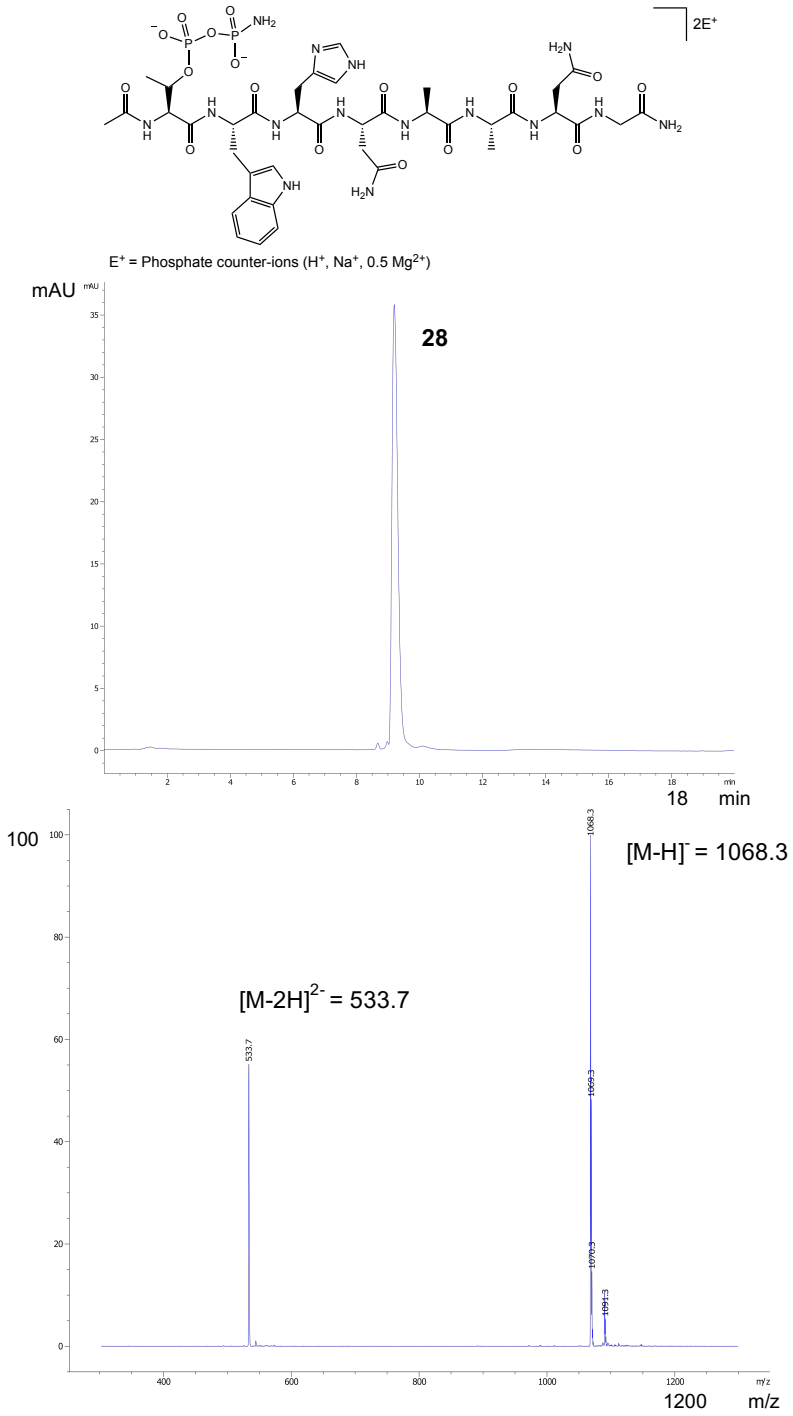

Figure S97. Analytical HPLC-MS spectra showing the production of **28** from **12** in Method A. Calculated mass $[M-H]^-$: 1068.3, observed mass $[M-H]^-$: 1068.3; Calculated mass $[M-2H]^{2-}$: 533.7, observed mass $[M-2H]^{2-}$: 533.7.

Synthesis and analytical data for model pyrophosphopeptide **44**

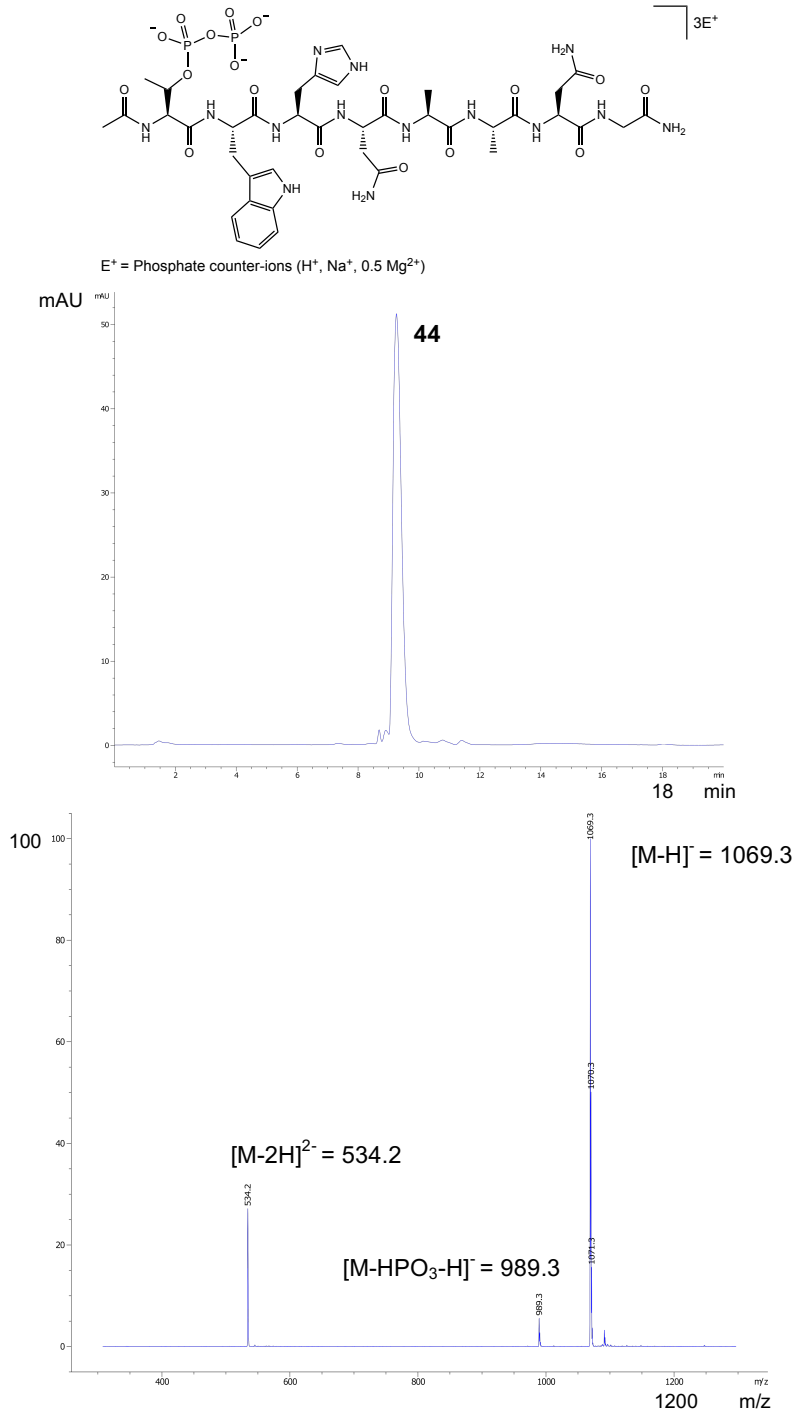

Figure S98. Analytical HPLC-MS spectra showing the production of **44** from **28** in Method A. Calculated mass $[M-H]^-$: 1069.3, observed mass $[M-H]^-$: 1069.3; Calculated mass $[M-2H]^{2-}$: 534.2, observed mass $[M-2H]^{2-}$: 534.2.

Synthesis and analytical data for model amidotriphosphopeptide **57**

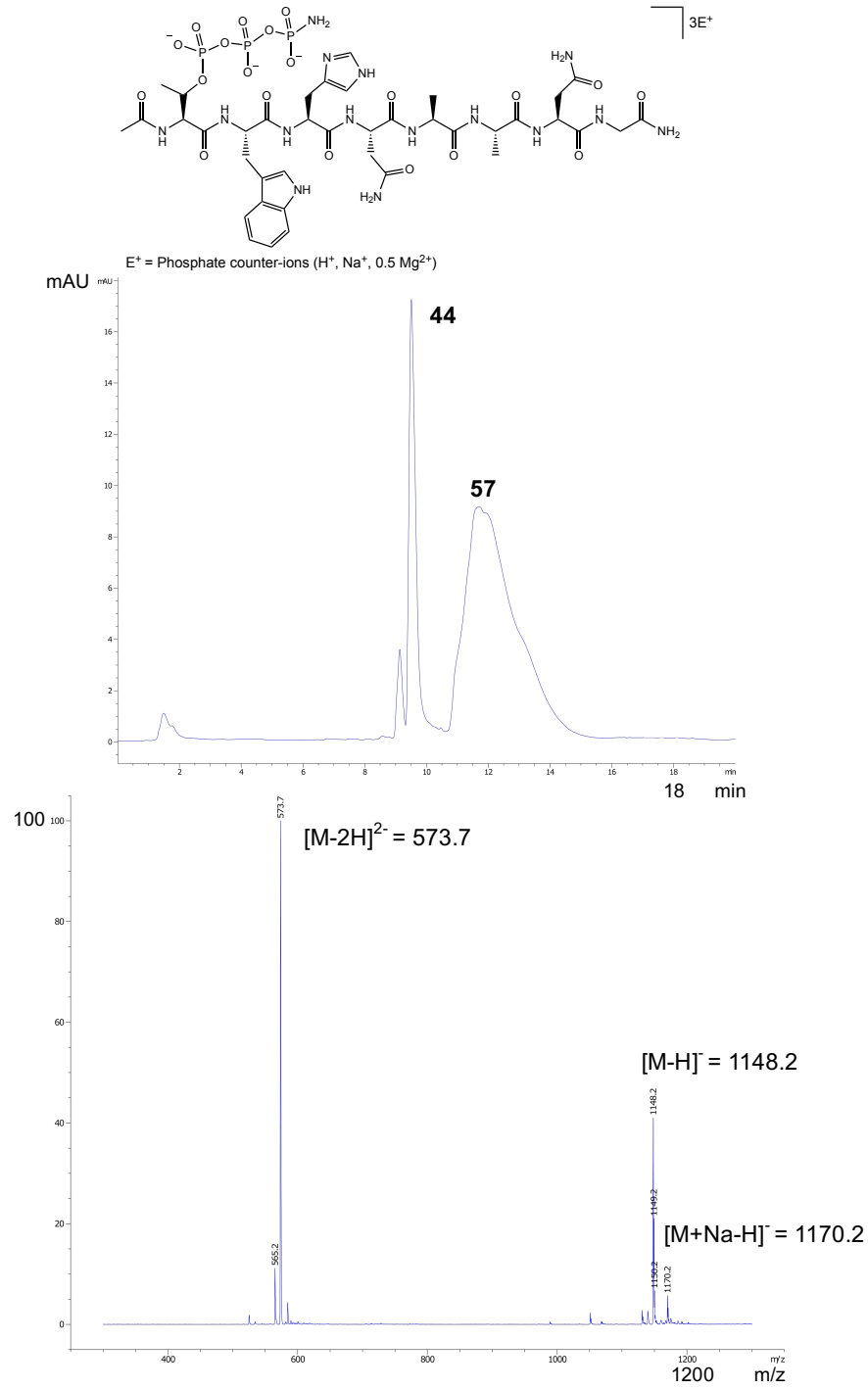

Figure S99. Analytical HPLC-MS spectra showing the production of **57** from **44** in Method A. The HPLC indicated 78% conversion. Calculated mass $[M-H]^-$: 1148.3, observed mass $[M-H]^-$: 1148.2; Calculated mass $[M-2H]^{2-}$: 573.6, observed mass $[M-2H]^{2-}$: 573.7.

Synthesis and analytical data for model triphosphopeptide **58**

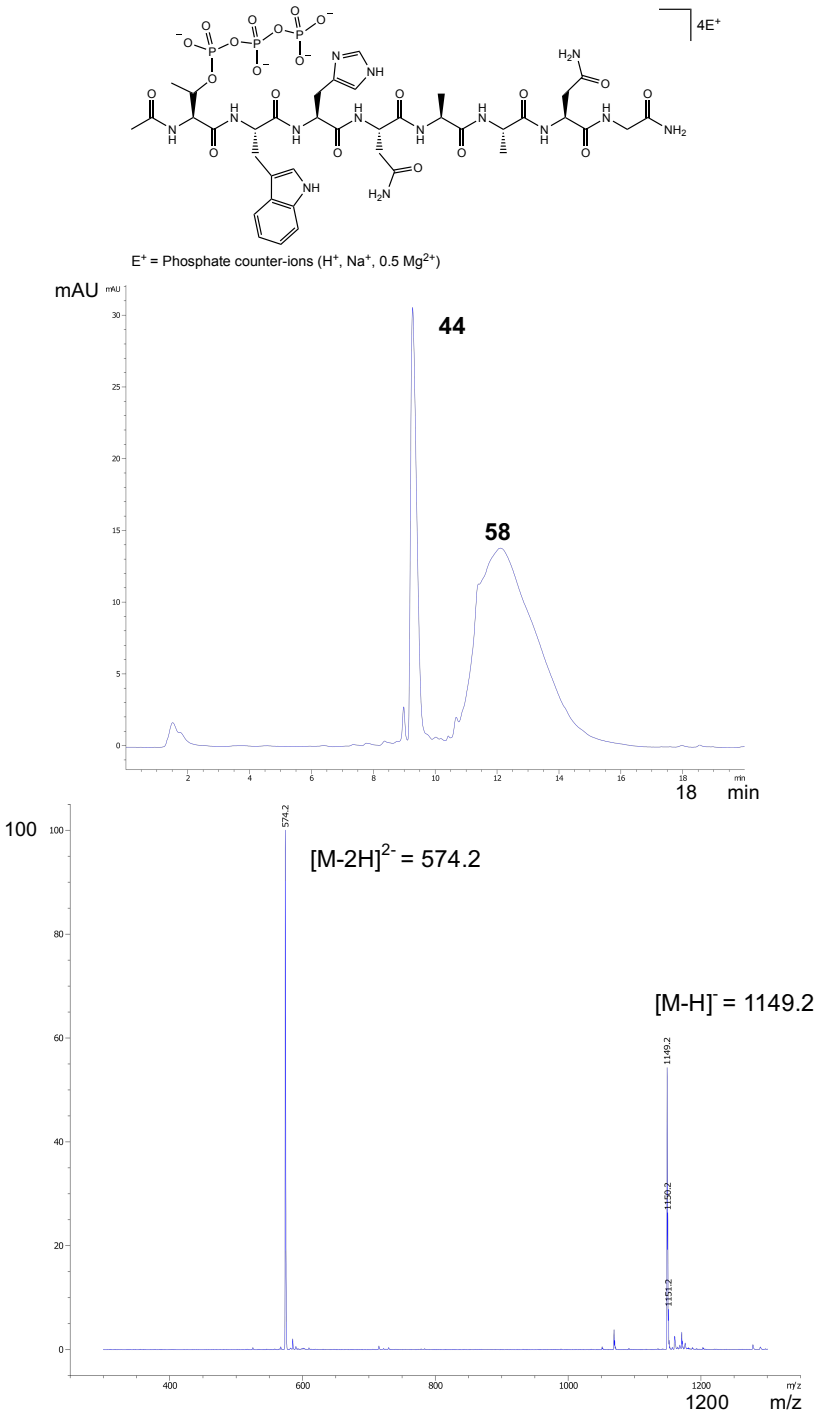

Figure S100. Analytical HPLC-MS spectra showing the production of **58** from **57** in Method A. Calculated mass $[M-H]^-$: 1149.3, observed mass $[M-H]^-$: 1149.2; Calculated mass $[M-2H]^{2-}$: 574.1, observed mass $[M-2H]^{2-}$: 574.2. Triphosphopeptide **58** was not retained well on the column, appearing as a broad peak in the chromatogram. Instead, the reaction mixture of **58** was analyzed by anion exchange chromatography (see **Figure S101**).

Synthesis and analytical data for model triphosphopeptide **58**

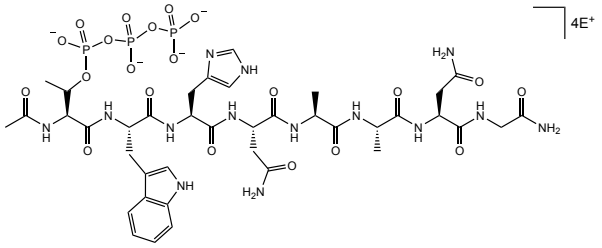

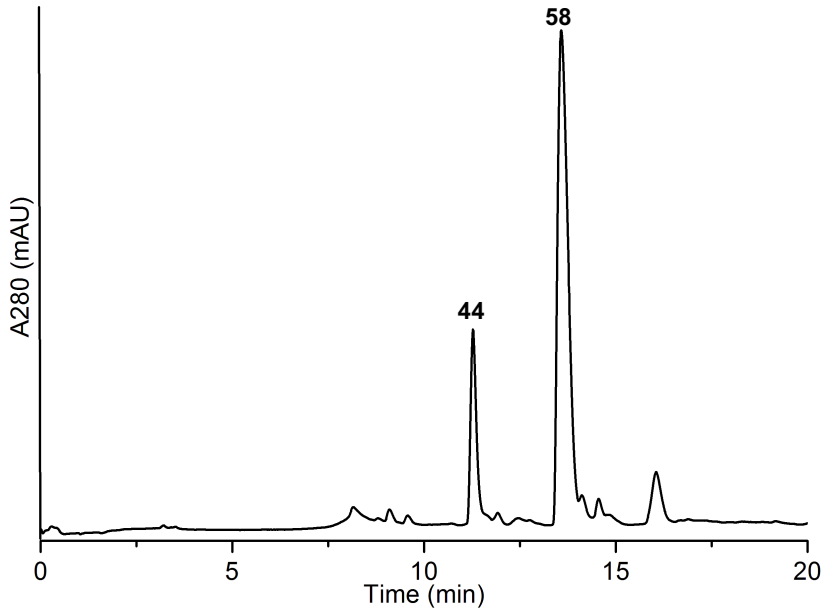

Figure S101. Anion exchange chromatogram trace showing the production of **58** from **57** with remaining **44**. The anion exchange chromatogram at 280 nm indicated the formation of pyrophosphopeptide **44** in 16% and triphosphopeptide **58** in 70% conversion, respectively, starting from phosphopeptide **12** via sequential phosphorylation-hydrolysis scenario in H_2O in one-pot four step sequence. Note: we switched to ion-exchange chromatography for analysis since the reverse phase HPLC showed a very broad peak with the correct mass (**Figure S100**). The sharp peak confirmed the clean formation of the triphosphopeptide **58**.

8. Reference

1. Gibard, C.; Bhowmik, S.; Karki, M.; Kim, E. K.; Krishnamurthy, R., Phosphorylation, Oligomerization and Self-assembly in Water under Potential Prebiotic Conditions. *Nat. Chem.* **2018**, *10*, 212-217.

2. Attard, T. J.; O'Brien-Simpson, N.; Reynolds, E. C., Synthesis of Phosphopeptides in the Fmoc Mode. *Int. J. Pept. Res. Ther.* **2007**, *13*, 447-468.

3. An, L. Y.; Dai, Z.; Di, B.; Xu, L. L., Advances in Cryochemistry: Mechanisms, Reactions and Applications. *Molecules* **2021**, *26*, 750.

4. Jencks, W. P.; Gilchrist, M., Electrophilic Catalysis. The Hydrolysis of Phosphoramidate. *J. Am. Chem. Soc.* **1964**, *86*, 1410-1417.